MARTIN MARIETTA ENERGY SYSTEMS LIBRARIES

3 4456 0269786 5

ORNL/TM-10658

ornl

OAK RIDGE NATIONAL LABORATORY

MARTIN MARIETTA

A Versatile, Highly-Efficient, High-Resolution von Hámos Bragg Crystal X-Ray Spectrometer

C. R. Vane
M. S. Smith
S. Raman

OAK RIDGE NATIONAL LABORATORY
CENTRAL RESEARCH LIBRARY
CIRCULATION SECTION
4500N ROOM 175
LIBRARY LOAN COPY
DO NOT TRANSFER TO ANOTHER PERSON
If you wish someone else to see this report, send in name with report and the library will arrange a loan.

OPERATED BY
MARTIN MARIETTA ENERGY SYSTEMS, INC.
FOR THE UNITED STATES
DEPARTMENT OF ENERGY

Printed in the United States of America. Available from
National Technical Information Service
U.S. Department of Commerce
5285 Port Royal Road, Springfield, Virginia 22161
NTIS price codes—Printed Copy: A07 Microfiche A01

This report was prepared as an account of work sponsored by an agency of the United States Government. Neither the United States Government nor any agency thereof, nor any of their employees, makes any warranty, express or implied, or assumes any legal liability or responsibility for the accuracy, completeness, or usefulness of any information, apparatus, product, or process disclosed, or represents that its use would not infringe privately owned rights. Reference herein to any specific commercial product, process, or service by trade name, trademark, manufacturer, or otherwise, does not necessarily constitute or imply its endorsement, recommendation, or favoring by the United States Government or any agency thereof. The views and opinions of authors expressed herein do not necessarily state or reflect those of the United States Government or any agency thereof.

ORNL/TM-10658

Physics Division

A VERSATILE, HIGHLY-EFFICIENT, HIGH-RESOLUTION VON HAMOS BRAGG CRYSTAL X-RAY SPECTROMETER

C. R. Vane, M. S. Smith,* and S. Raman

*Now at Yale University. Work at ORNL was supported in part by the Oak Ridge Associated Universities Summer Student Program.

Date Published - January 1988

Prepared by the
OAK RIDGE NATIONAL LABORATORY
Oak Ridge, Tennessee 37831
operated by
MARTIN MARIETTA ENERGY SYSTEMS, INC.
for the
U.S. DEPARTMENT OF ENERGY
under contract DE-AC05-84OR21400

MARTIN MARIETTA ENERGY SYSTEMS LIBRARIES

3 4456 0269786 5

CONTENTS

		PAGE
	ABSTRACT	1
I.	INTRODUCTION	1
II.	DESIGN AND CONSTRUCTION	3
	A. General Design Considerations.	3
	B. Contributions of Imaging Properties to System Energy Resolution.	7
	1. Imaging of X-ray Sources in the y = 0 Plane (Geometry 1)	7
	2. Imaging in a Tilted-Detector Geometry (Geometry 2)	13
	3. Imaging in a Rotated-Crystal, Tilted-Detector Geometry (Geometry 3)	19
	4. Comparison of Image Quality in the Three Geometries	25
	C. Construction Details.	29
III.	OPERATIONAL CHARACTERISTICS	36
	A. Calculated and Measured Performance.	36
	B. Special Operational Considerations.	41
	1. Corrections for Crystal and Detector Efficiency Variations	41
	2. Doppler Effects for X-Rays Emitted from Fast Projectiles	45
	C. Sample Data	49
IV.	ACKNOWLEDGMENTS	60
V.	REFERENCES	61

CONTENTS (continued)

APPENDICES 62

A. Calculation of Images in Geometry 1 62

B. Calculation of Images in Geometry 2 67

C. Detector Location in Geometry 3 68

D. Calculation of Images in Geometry 3 70

E. Computer Programs for Image Calculations and Analysis 73

F. Computer Program for Spectrometer Operation 122

ABSTRACT

An efficient, high-resolution, vertical-focusing, Bragg crystal x-ray spectrometer has been specifically designed and constructed for use in measurements of x rays produced in collisions of energetic heavy ions. In this report the design and resulting operational characteristics of the final instrument are fully described. A wide variety of sample data is also included to illustrate the utility of this device in several areas of research.

I. INTRODUCTION

The Nuclear Science Applications group at the Oak Ridge National Laboratory is studying the effects of chemical environment on the emission of x-rays induced by heavy ion impact.[1] Collisions involving highly energetic heavy ions ($\gtrsim$1 MeV/u) predominantly produce multiple inner-shell ionization. Resulting K_α x-ray spectra are composed of a complex series of intense, chemically sensitive satellite lines, with small energy differences between adjacent peaks (~ 17 eV for sulfur). The satellites may extend to hundreds of electron volts above the characteristic x-ray line energy. In addition, these peaks contain pronounced ~ 1 eV fine structure. Previous measurements (carried out here at ORNL and elsewhere) have usually employed commercial Bragg single-crystal spectrometers having typical energy resolutions of 6-7 eV in the 2.5 keV x-ray energy regime. A much higher resolution crystal x-ray spectrometer with high collection efficiency is needed to study the spectra of K and L x-rays from compounds and alloys of interest to us containing elements from fluorine to mercury. Unavoidable energy broadening from a number of mechanisms inherent in heavy-ion collision excitation amounts to ~ 1 eV. Therefore, the energy range of interest is 1-10 keV, with a desired total energy resolution on the order of 1 eV at 2.5 keV and 5 eV at 10 keV. Additionally, it is desirable to simultaneously collect data over a large enough energy bandwidth ($\Delta E/E > 10\%$) to fully cover the pertinent satellite structures with each positioning of the spectrometer components, and cover about 1 to 2 keV by repositioning a single crystal.

In order to obtain both high resolution and increased efficiency, a curved crystal "vertical-focusing" Bragg spectrometer was examined in detail. First proposed by Gouy,[2] and developed by von Hámos,[3] this design offers a gain in intensity of one to two orders of magnitude over conventional flat crystal spectrometers: the gain is on the order of the ratio of the crystal radius of curvature to the source height.[4,5,6] This spectrometer type differs greatly from the "horizontal-focusing" curved-crystal geometries of Johann[7] and Johannson,[8] both of which employ a crystal and detector positioned along a Rowland circle. Horizontal-focusing spectrometers concentrate x-rays in the dispersive plane and for a single point source they most effectively focus x-rays of a single energy. They require scanning of the crystal and detector in order to efficiently collect data over a substantial range of energies. The vertical-focusing types, on the other hand, focus in the non-dispersive plane, and permit, at one positioning of components, effective data collection over an energy bandwidth limited primarily by the crystal length and detector size. The imaging properties of the vertical-focusing spectrometer were examined in order to determine the aberrations affecting spectra taken by such a device. These properties have been investigated previously in refs. 5 and 6 for one specific design geometry; a more general study allowed different geometries to be evaluated on the basis of imaging quality. Based on this study and other considerations discussed in Chapter II, a versatile spectrometer has been designed and constructed. A description of the instrument, its operation, and results of initial performance tests are presented in Chapters II and III.

II. DESIGN AND CONSTRUCTION

II.A. General Design Considerations.

A schematic drawing of a vertical-focusing spectrometer, along with the coordinate system used in the following discussions, is shown in fig. 1. The spectrometer is composed of three components; an x-ray source, usually defined by a rectangular aperture, a cylindrically-curved crystal, and a position-sensitive x-ray detector. At a fixed positioning of the components, an incident x-ray location on the detector corresponds to a particular Bragg angle, and hence to a particular x-ray energy through the Bragg relation $\lambda = 2d \sin \theta_B$ (in 1st order), or

$$E(\text{keV}) = 12.398/[2d(\text{Å}) \sin \theta_B] \ . \tag{1}$$

An extended crystal diffracts x-rays having a range of energies. A quartz crystal $(10\bar{1}1)$ (2d = 6.687Å) of length 10 cm, for example, allows a large portion of our desired energy range to be reached; a one-dimensional position-sensitive proportional counter (PSPC) permits the reflected x-rays to be

ORNL-DWG 85-7000R

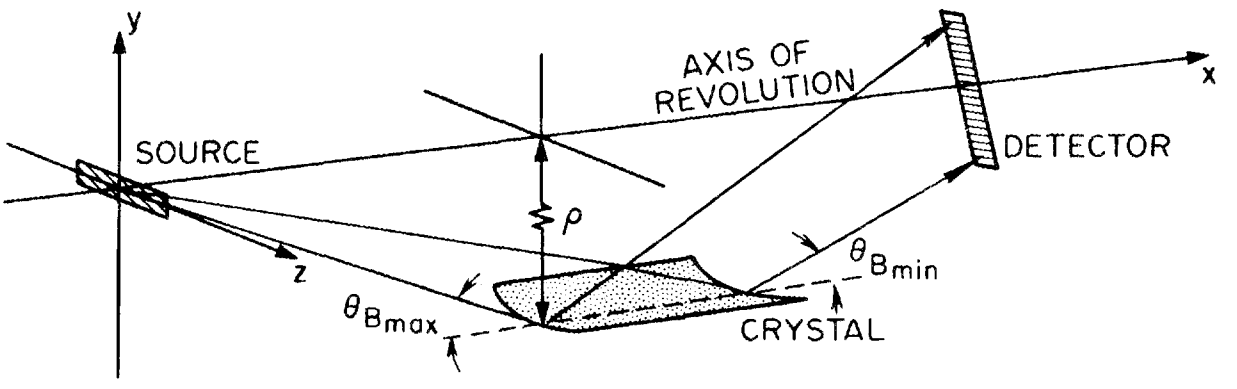

Fig. 1. Coordinate system employed in the study of imaging processes for vertical focusing crystal spectrometers. The crystal is curved in the y-z plane. The figure is not to scale.

detected with good spatial resolution. The PSPC is advantageous for our studies because of its high efficiency, real-time readout, and on-line adjustment capability. The source of x-rays is typically a solid target, impacted by a collimated heavy ion beam. Atomic systems which experience inner-shell excitation by fast heavy-ions radiatively decay with observed x-ray total line widths near ~ 1 eV. The broadening is due primarily to the ordinary natural line width (e.g., 0.6 eV for sulfur K_α) combined with the effects of recoil Doppler spreading and distributed unresolved shifts from multiple ionization of outer electron shells. Unless studies of intrinsic line shapes are anticipated, instrumental resolution significantly better than $\delta E/E \sim 1/2500$ is unnecessary for most of these ion-atom collision x-ray measurements.

The instrumental energy resolution of a single-crystal spectrometer such as the one considered here is limited by the components which contribute to the smearing of Bragg angles in the x-ray production, diffraction and focusing, and detection processes. X-ray source widths (Δy) narrower than a few hundred μm are difficult to achieve with energetic heavy-ion excitation without substantial loss of beam intensity. This extended source size produces a major component of the spectrometer resolution loss. Variation in spacing and orientation of the lattice planes in the cylindrically-bent crystal is another source of resolution loss, typically characterized by the crystal's rocking curve and resolving power. The finite detector spatial resolution also contributes to the system energy resolution. The losses due to the crystal and detector depend on the specific components employed; the loss due to a finite source size also depends on the imaging properties of the device; the loss due to imaging aberrations is related to the finite source size and can be approximated in the following manner. The differential of eq. (1) with respect to θ_B is

$$dE = E \cot\theta_B \, d\theta_B \ . \tag{2}$$

One can see from fig. 2 that the finite source width Δy allows x-rays in an energy in a range $E - dE/2$ to $E + dE/2$ to strike the same position on the detector. Optical aberrations from focusing by the curved crystal result in distorted imaging of the extended source such that detected line shapes will be broadened and possibly skewed. To evaluate dE, we assume that all the aberrations in the spectrometer are described by a factor F, such that the image width of a source slit of width Δy and height Δz in our system is equal to the image width of a slit of width $F\,\Delta y$ in a perfectly imaging system. We assume here that the ratio F is a reasonable measure of the maximum loss in spatial resolution due to optical aberrations and approximate our system by the perfectly imaging system (fig. 2) to get the angular resolution

$$d\theta_B = F\,\Delta y\,\cos\theta_B\,\sin\theta_B/2\rho\ , \tag{3}$$

ORNL-DWG 85-7001R

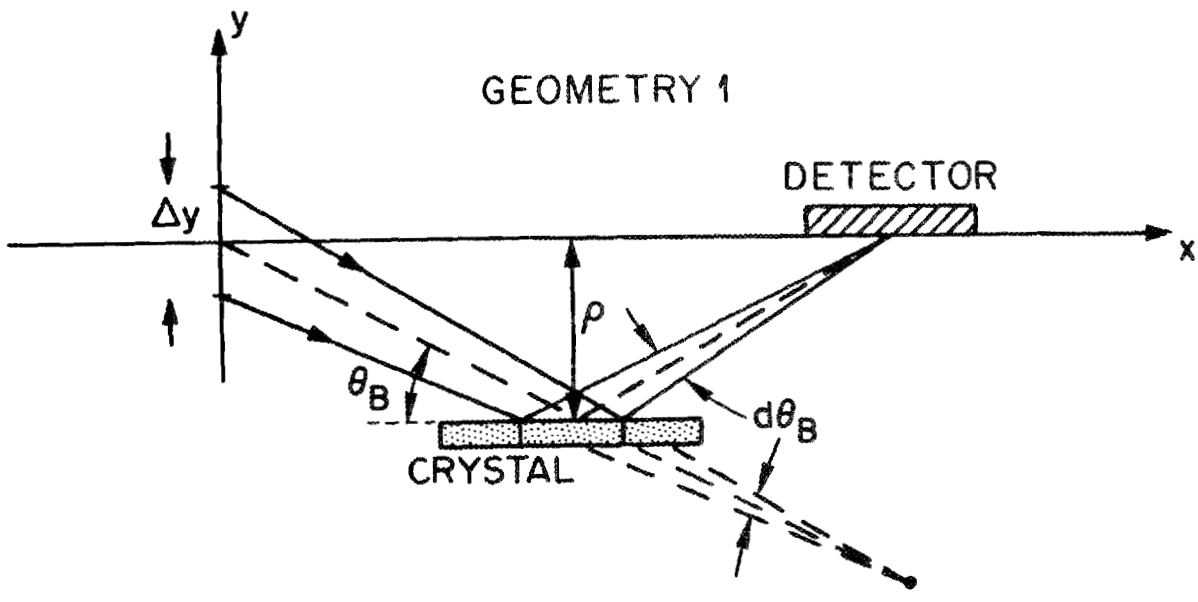

Fig. 2. Geometry 1 schematic and example rays for evaluation of resolution loss due to a finite source width Δy: x-rays with a range of Bragg angles $d\theta_B$ can strike the same position on the position sensitive detector. The figure is not to scale.

where ρ is the radius of curvature of the crystal. From (2) and (3) we conclude

$$dE/E = F\ \Delta y/2\rho\ \cos^2\theta_B\ . \tag{4}$$

The crystal radius ρ sets the scale for the physical size of the final instrument. Assuming no other broadening mechanisms, the necessarily extended source leads to a lower limit for the distance ρ for a given required energy resolution. For example, with $F = 1$, $\Delta y = 0.2$ mm, $E = 2.3$ keV, $dE \leqslant 1$ eV, and $2d = 6.687$Å, eq. (4) gives $\rho \geqslant 14$ cm. Increasing ρ leads to proportional improvement in resolution. On the other hand, for a given Bragg angle and crystal size (area = A) the total solid angle intercepted by the crystal decreases as $\sim A/\rho^2$; so that the needed high collection efficiency requires either very large crystals or compact systems (small ρ). Other considerations such as the size of the containing vacuum chamber and limited availability of extended space in most experimental areas also limit the physical size of the final design.

It is thus necessary to determine F, in terms of selected system parameters and the x-ray energy in order to evaluate the contribution to the total energy resolution. This is done in the following sections by studying the general imaging properties of the curved crystal spectrometer in several possible operating configurations, labelled geometries 1, 2, and 3.

Anticipating that F can be held to numerical values less than 2 or 3, we select as "standard" system parameters the following values: crystal radius of curvature (ρ) = 25.4 cm; crystal height (h_C) = 10.0 cm; crystal length (ℓ_C) = 10.0 cm; source half-height in z-direction = 0.5 cm; source width in y-direction (Δy) = 0.03 cm; detector active length (ℓ_D) = 10.0 cm; maximum Bragg angle range (θ_B) = 30°-70°; crystal = quartz ($10\bar{1}1$) with $2d = 6.687$Å.

II.B. Contributions of Imaging Properties to System Energy Resolution.

II.B.1. Imaging of X-ray Sources in the y = 0 Plane (Geometry 1)

Focusing by the curved crystal is optimized when the detector is placed in the y = 0 plane containing the axis of the cylindrical crystal (x-axis). We will denote this configuration Geometry 1 (see fig. 2). Film emulsion and solid state detectors may be used in this configuration. However, the spatial resolution of a position-sensitive proportional counter is seriously degraded by a conversion-depth/parallax effect when x-rays enter the detector obliquely and are converted at various depths in the working gas. Thus PSPCs may not be used effectively in Geometry 1. A study of this geometry nonetheless develops methods employed in the analysis of designs which can accommodate PSPCs. A spectrometer with Geometry 1 has been built by Yaakobi et al.[6] and used for fusion plasma diagnostics.

We wish to determine the image on a detector in the y = 0 plane of a monoenergetic x-ray source, restricted to lie in the x = 0 plane. As shown in fig. 3, we consider an arbitrary point source $S = (0, y_S, z_S)$ in the source plane. A ray from S to the crystal with a Bragg angle θ_B has a point of incidence $R(\psi) = (x_R, -\rho \cos\psi, \rho \sin\psi)$ on the crystal; the reflected ray strikes the y = 0 plane at the image point $P(\psi) = (x_P, 0, z_P)$. For any θ_B, ψ can take on values from $-\psi_0$ to ψ_0, where

$$\sin\psi_0 = h_C/2\rho \tag{5}$$

and h_C is the crystal height. Figures 4a-c show the points A, B, S, R, S', and R' used in the calculation of the image point P. First, the x-coordinate of R is calculated in Appendix A to be

$$x_R = (|BR|^2 \cot^2\theta_B - |AB|^2)^{1/2} , \tag{6}$$

ORNL-DWG 85-7004R

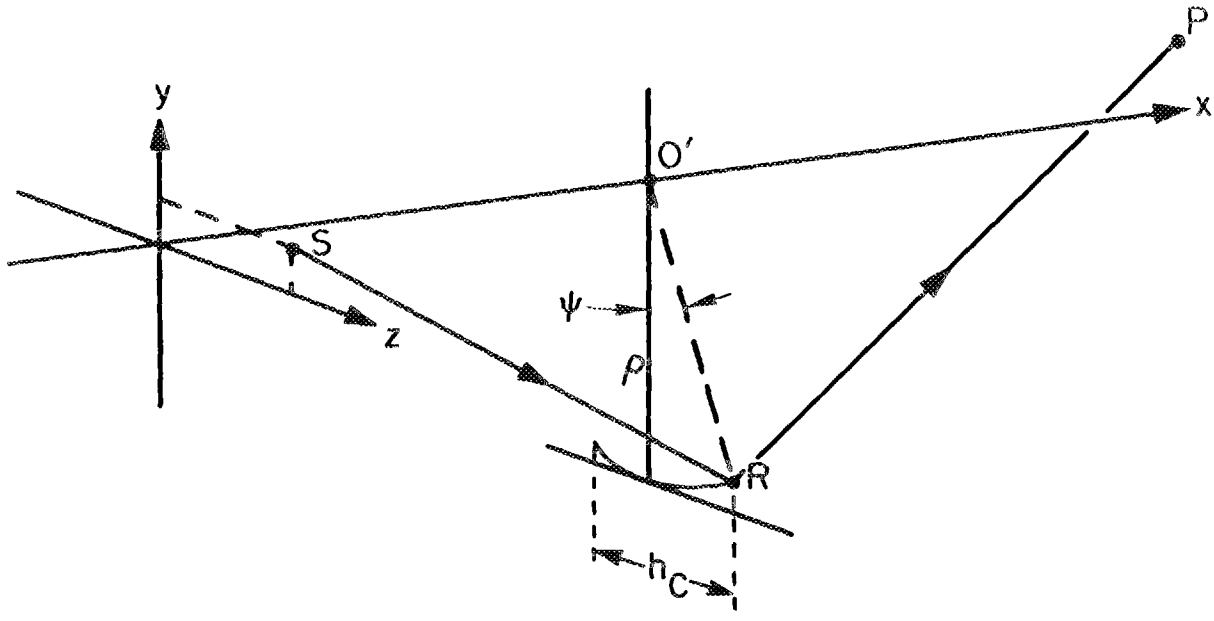

Fig. 3. The location of an arbitrary point source S in the x = 0 plane, and the point of incidence R on the crystal of height h_C.

where, for $\psi \neq 0$,

$$z_B = (z_S \tan\psi - y_S)/(\tan\psi + \cot\psi) \ , \tag{7}$$

$$|AB| = ((y_S + z_B \cot\psi)^2 + (z_S - z_B)^2)^{1/2} \ ,$$

and $$|BR| = ((\rho \cos\psi - z_B \cot\psi)^2 + (z_B - \rho \sin\psi)^2)^{1/2} \ .$$

For the point source on the axis of revolution $S_0 = (0, 0, 0)$, we have $x_R = \rho \cot\theta_B$ for all values of ψ. Thus a projection in the y = 0 plane of the locus of points of incidence $R(\psi)$, for a given θ_B, is a line parallel to the z-axis with x-coordinate x_R. For an off-axis point source, however, x_R depends on ψ, and the projection of the locus $R(\psi)$ into the y = 0 plane is a curve opening away from the source plane (fig. 5a). The shape of this locus determines the image shape in the y = 0 plane (fig. 5b). Appendix A gives the coordinates of $P = (x_P, 0, z_P)$ to be

ORNL-DWG 85-7003R

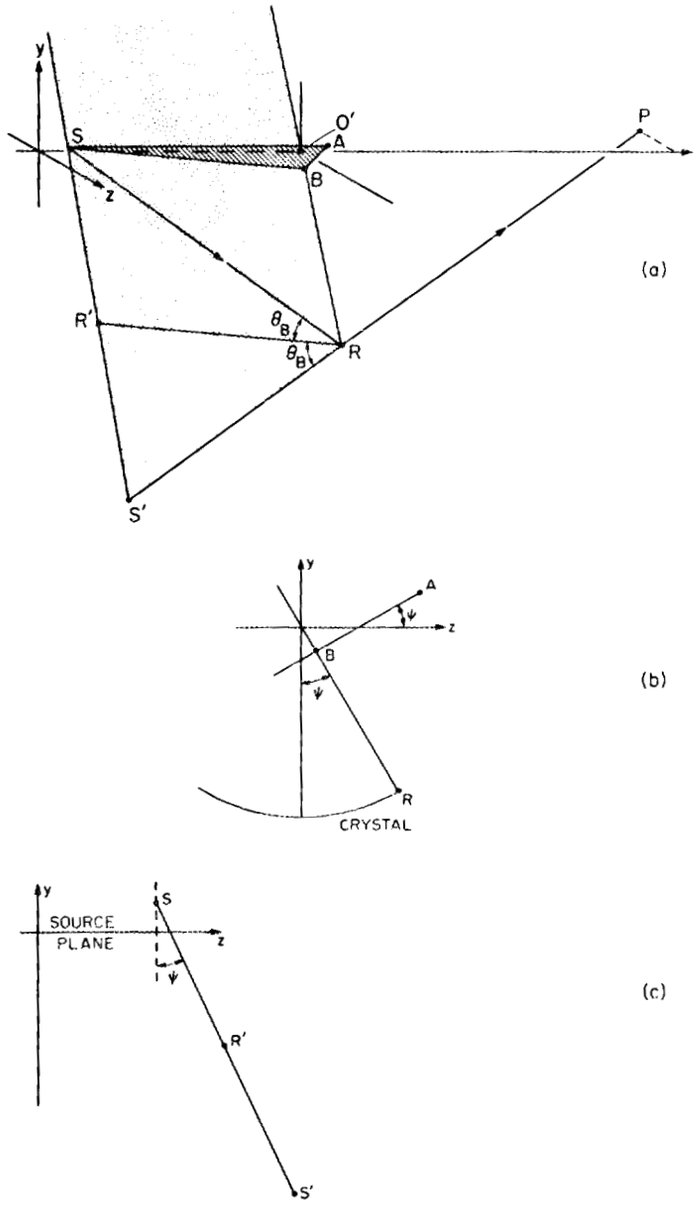

Fig. 4. Location of points and planes used to determine the coordinates of the image point $P = (x_P, y_P, z_P)$.

a. S is the point source; R is the point of incidence on the crystal; A is the projection of S into the plane $x = x_R$; $O' = (x_R, 0, 0)$; RO' is the normal to the crystal at point R; B is the projection of A onto RO'; R' is in the $x = 0$ plane such that R'R is parallel to SB; SR is the incident x-ray; RP is the reflected x-ray; S' is in the $x = 0$ plane such that S' is collinear with R and P. The plane SRO' contains the incident and reflected x-rays.

b. Location of A, B, R, and O' in the plane $x = x_R$.

c. Location of S, R', and S' in the source plane $x = 0$.

ORNL-DWG 85-7005R

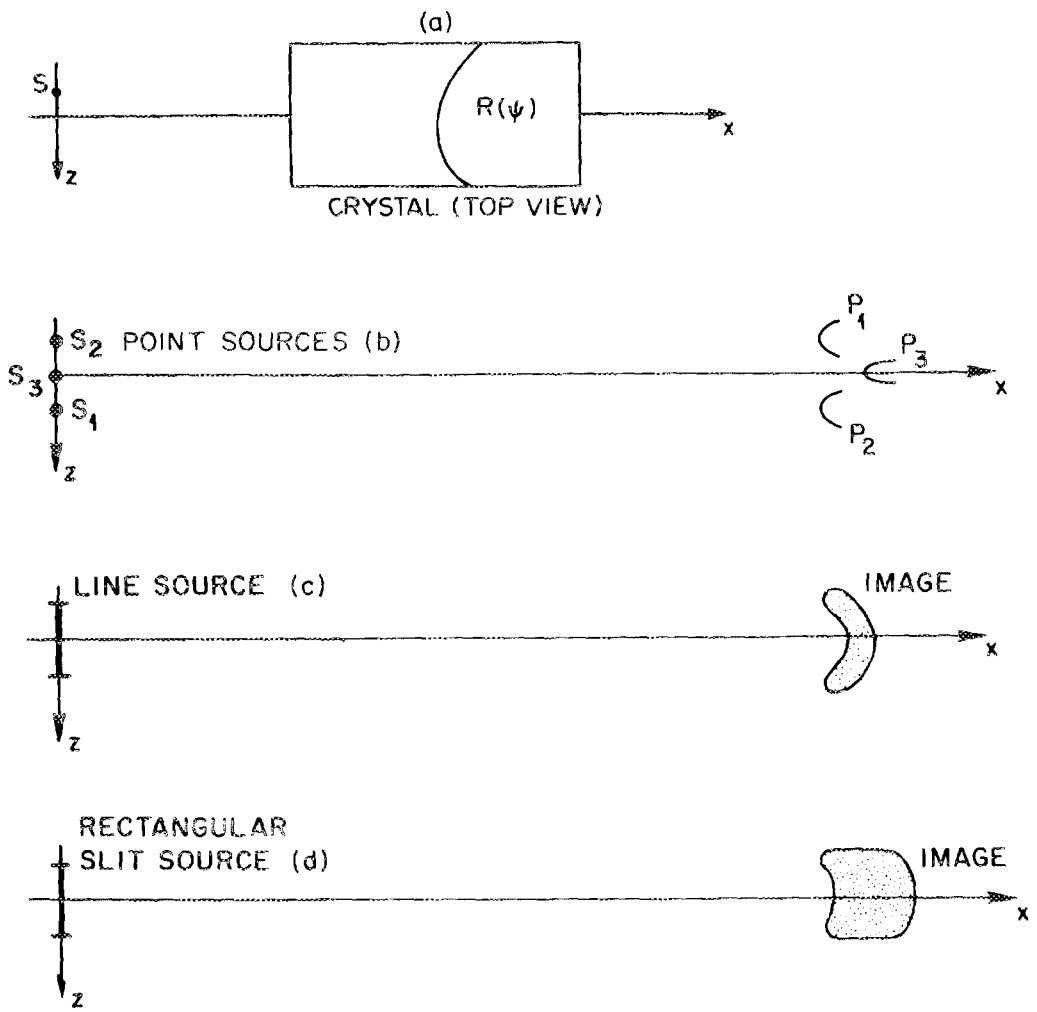

Fig. 5. Loci of points of incidence $R(\psi)$ and image points $P(\psi)$ in the $y = 0$ plane (Geometry 1) for a fixed Bragg angle. Image sizes are exaggerated.

a. $R(\psi)$ for an off-axis point source and a fixed Bragg angle.

b. Qualitative image of three point sources in the $y = 0$ plane. A reflection in the z-coordinate of the source corresponds to a reflection in the z-coordinate of the image.

c. Qualitative image of a line source parallel to the z-axis in the source plane.

d. Qualitative image of a rectangular slit source in the source plane.

$$x_P = \frac{(|BR|^2 \cot^2\theta_B - |AB|^2)^{1/2} (y_S - 2|BR|\cos\psi)}{(y_S + \rho\cos\psi - 2|BR|\cos\psi)} , \tag{8}$$

and
$$z_P = \frac{(\rho\sin\psi - 2|BR|\sin\psi - z_S)(y_S - 2|BR|\cos\psi)}{(y_S + \rho\cos\psi - 2|BR|\cos\psi)} + z_S + 2|BR|\sin\psi .$$

For the point source S_0, the image point is $P_0 = (2\rho\cot\theta_B, 0, 0)$ for all ψ: this is the only point in the source plane which images to a single point, and thus has a perfect focus on the detector. For an off-axis point source, the entire image of S is the locus $P(\psi)$, where ψ is varied from $-\psi_0$ to ψ_0. The curved shape of $R(\psi)$ on the crystal corresponds to a curved shape of $P(\psi)$ in the detector plane. By making the coordinate transformation to the detector center

$$x \to \xi = x - 2\rho\cot\theta_{BC} \quad ; \quad z \to z \tag{9}$$

where θ_{BC} is the Bragg angle from S_0 to the crystal center $C = (x_C, -\rho, 0)$, we have that S_0 images to $(\xi, y, z) = (0, 0, 0)$ when $\theta_B = \theta_{BC}$. A plot of ξ vs. z then gives a projection of the image on the detector. Figures 5b-d qualitatively illustrate the transition of the image shape as one proceeds from point sources to a line source and finally to a rectangular source.

Figure 6a gives the image of an off-axis point source generated by a computer program, where ψ is varied from $-\psi_0$ to ψ_0 in twenty-one equal increments. Expansion of the ξ-scale in this and the following figures enables the aberrations to be seen more clearly.

Symmetry requires that off-axis point sources $S_1 = (0, y_S, z_S)$ and $S_2 = (0, y_S, -z_S)$ have images which are reflections through the ξ-axis; this is in agreement with the image solutions in eq. (8). However, symmetry considerations also require that the image of $S_4 = (0, -y_S, z_S)$ should not be a reflection through the ξ-axis of the image of S_1: the contrary is reported in refs. 5 and

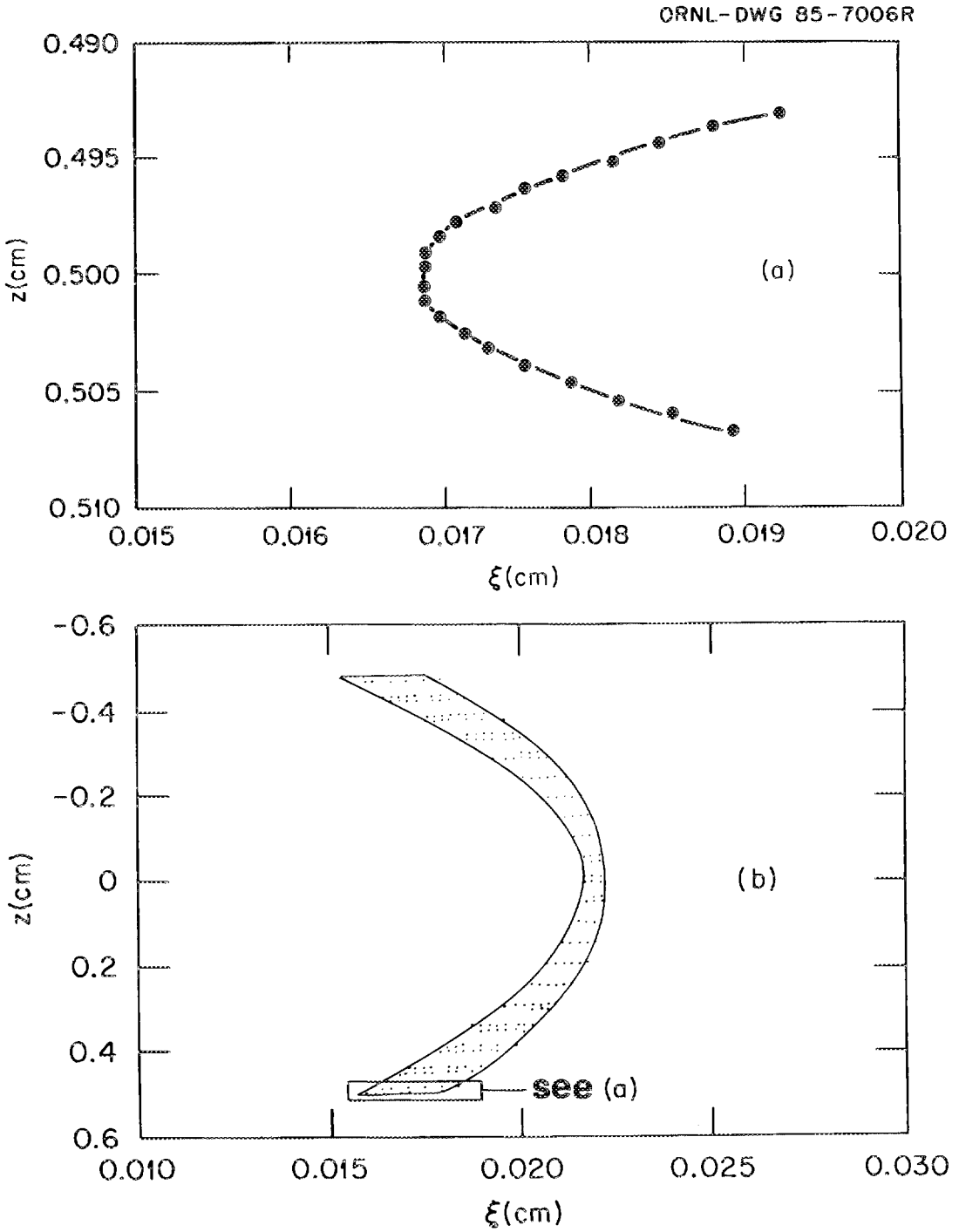

Fig. 6. Loci of points of incidence $R(\psi)$ and image points $P(\psi)$ in the $y = 0$ plane (Geometry 1) for a fixed Bragg angle.

a. $P(\psi)$ for an off-axis point source and a fixed Bragg angle. The point source has coordinates (0, 0.013 cm, -0.5 cm), and $\theta_B = 30°$; other parameters have the "standard" value.
b. Image of a line source of x-rays, with $\theta_B = 30.0°$, $y_S = 0.013$ cm, and "standard" parameter values.

6. Rather, eq. (8) shows that both images exhibit similar concave shapes opening away from the source plane, but the image of S_4 has a greater curvature than the image of S_1.

The image of a monoenergetic x-ray line source oriented parallel to the z-axis is found by calculating $P(\psi)$ as ψ and z_S are varied and y_S and θ_B are held constant. Figure 6b shows the image in the $y = 0$ plane of a line source of energy 3.7 keV ($\theta_B = 30°$) with the "standard" parameter values and $\psi_0 = 12°$.

The image of a rectangular slit source is found by computing $P(\psi)$ as ψ, y_S, and z_S are varied for constant θ_B. Listings of the programs used to generate and analyze these images are found in Appendix E.

Image quality can be assessed by determining the maximum ξ-extension $\Delta\xi$ of the image: a perfectly imaging system will produce $\Delta\xi = \Delta y$ for a slit of width Δy and a fixed Bragg angle θ_B. Defining $F_{fw} = \Delta\xi/\Delta y$, we see that this is the full width aberration factor F in eqs. (3) and (4). In Geometry 1, typical F_{fw} values are between 1 and 3; the parameters used to generate the line source image in fig. 6b produce $F_{fw} \approx 2.2$ for $\Delta y = 0.03$ cm. Additionally, it is found that a y-axis translation of the source significantly increases the ξ-extension of the image, while a z-axis translation of the source primarily results in a z-axis translation of the image in the opposite direction, with little broadening. This suggests that alignment of the source, while not very crucial in the z-direction, must be relatively precise in the y-direction. The correspondence between y-axis translation and increased aberrations also holds in the spectrometer designs studied in Sections II.B.3 and II.B.5.

II.B.2. Imaging in a Tilted-Detector Geometry (Geometry 2)

Figure 7a shows a spectrometer configuration, denoted Geometry 2, which is suitable for a PSPC. Spectrometers in this configuration, but with relatively limited bandwidths, have been built by Taylor, et al.[9] and Källne and Källne[9] and employed quite successfully for fusion plasma diagnostics. As in

ORNL-DWG 85-7011R

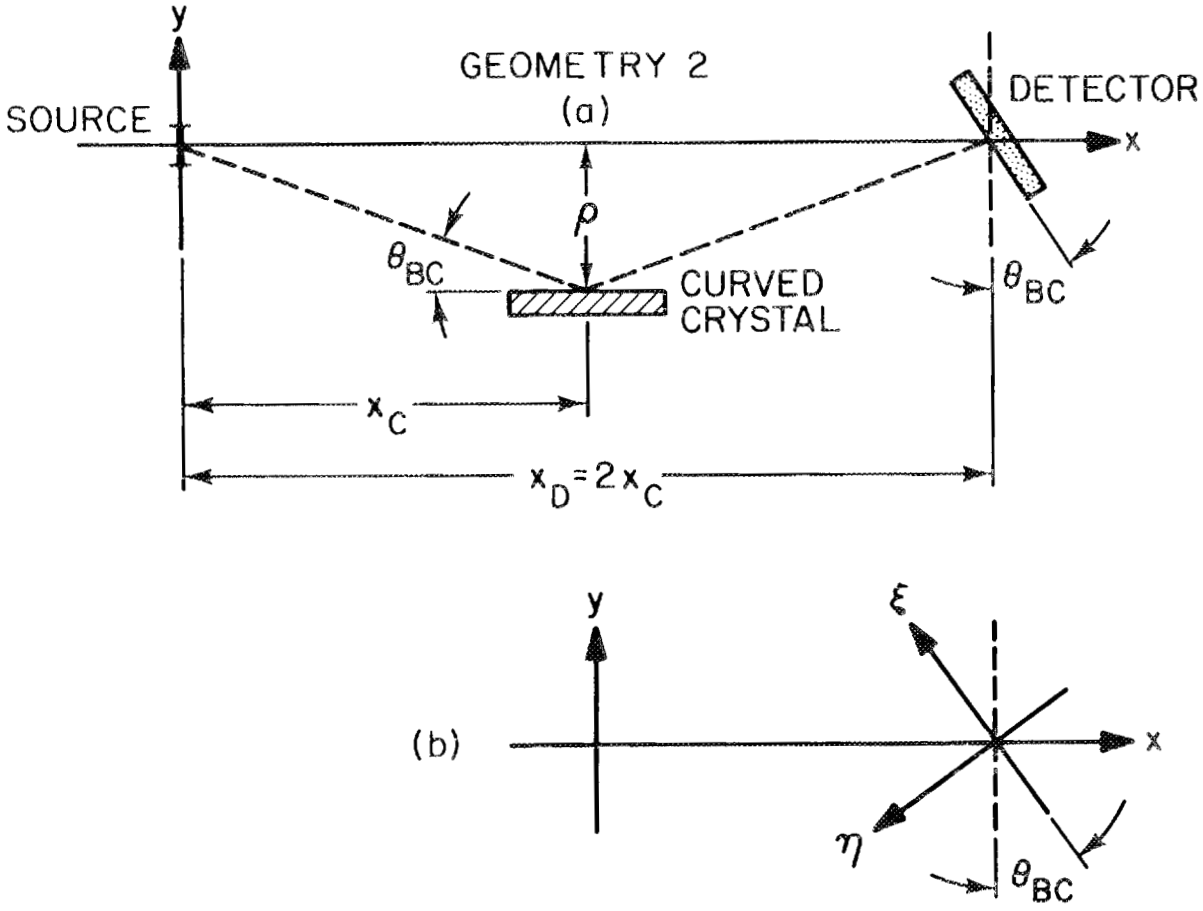

Fig. 7. a. Geometry 2, suitable for position-sensitive proportional counters. Each position on the detector ideally corresponds to a unique energy.

b. The (ξ, η, z) coordinate system attached to the detector in Geometry 2. ξ is the position sensitive coordinate; note that positive ξ will in general be toward negative x.

Geometry 1, the crystal center in Geometry 2 is equidistant from the detector center and the source. The crystal center has coordinates $C = (x_C, -\rho, 0)$ and the detector center has $D = (x_D, 0, 0)$, where

$$x_C = \rho \cot\theta_{BC} , \tag{10}$$

and $x_D = 2 \rho \cot\theta_{BC}$.

The detector, however, makes an angle θ_{BC} with the y-axis to allow x-rays from $S_0 = (0, 0, 0)$ to have normal incidence at the center of the detector. The image of an arbitrary point source $S = (0, y_S, z_S)$ is found in the same manner as in Sect. 2, employing the following equation of the detector plane:

$$y = -x \cot\theta_{BC} + 2\rho \cot^2\theta_{BC} . \tag{11}$$

Details of the calculation are found in Appendix B, with the result

$$x_R = (|BR|^2 \cot^2\theta_B - |AB|^2)^{1/2} , \tag{12}$$

$$x_P = \frac{2\rho \cot^2\theta_{BC} + 2|BR| \cos\psi - y_S}{(2|BR| \cos\psi - \rho \cos\psi - y_S)/x_R + \cot\theta_{BC}} ,$$

$$y_P = -x_P \cot\theta_{BC} + 2\rho \cot^2\theta_{BC} ,$$

and $z_P = x_P (\rho \sin\psi - 2|BR| \sin\psi - z_S)/x_R + z_S + 2|BR| \sin\psi$,

where $|AB|$, $|BR|$, and z_B are given by eq. (7). The two-dimensional image projected on the detector may be found by transforming to the ξ,η system, shown in fig. 7b:

$$x \to \xi = (x - 2\rho \cot\theta_{BC})/(-\sin\theta_{BC}) , \tag{13}$$

$$y \to \eta = 0 ,$$

and $z \to z$.

Note that images displayed in terms of ξ and η appear inverted compared to plots in x and y because of the choice of direction for positive ξ. Figure 8a gives the image of a point source in Geometry 2, and figs. 8b-d give line source images for different Bragg angles. We expect aberrations to be increased in Geometry 2 because point sources have foci on or near the plane $y = 0$: the greater the detector tilt, the larger the distance of the ends of the detector from the $y = 0$ plane and hence from the focal plane. Aberrations are minimized when θ_B is near θ_{BC}, because the image is near the detector center in the $y = 0$

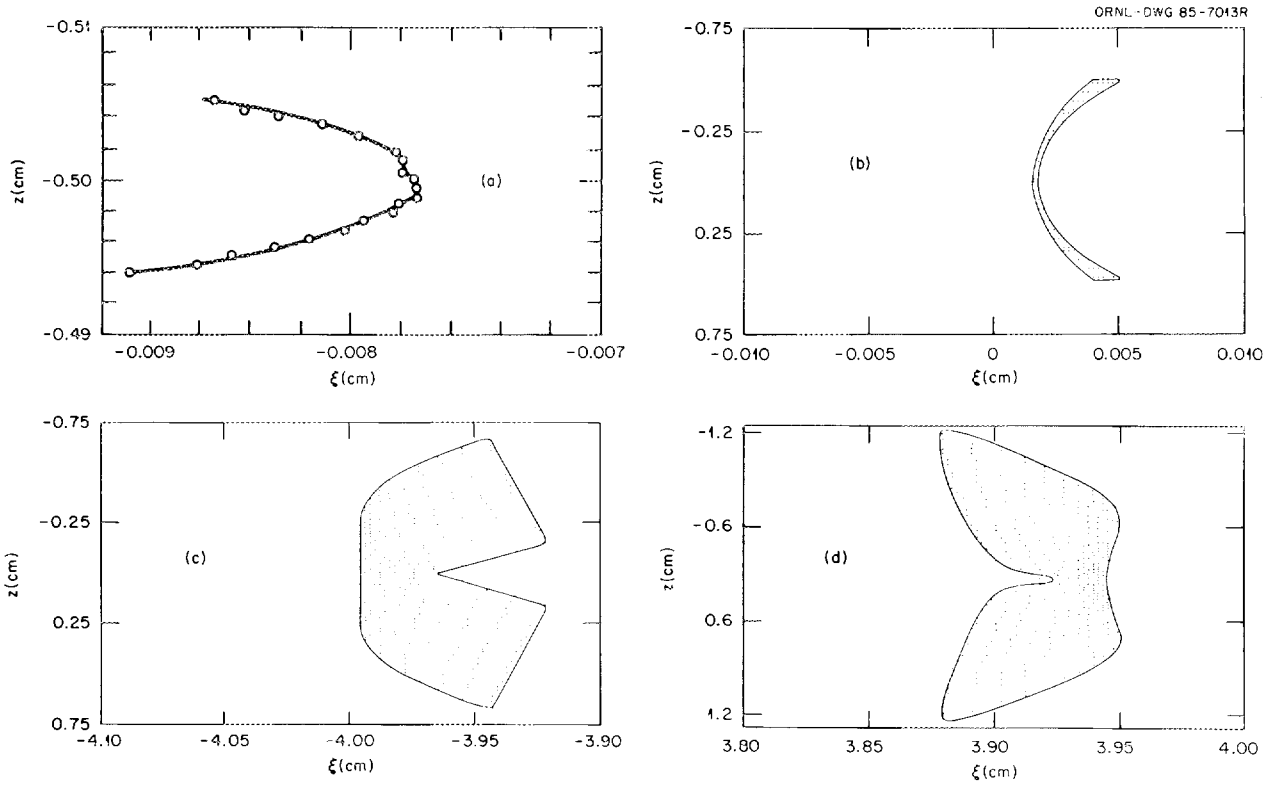

Fig. 8. Images in Geometry 2 of point and line sources. "Standard" parameter values.

a. Point source image, S = (0, 0.015 cm, 0.05 cm), with x_C = 40.0 cm, $\theta_B = \theta_{BC}$ = 32.42°.

b. Line source image, with y_S = 0.013 cm and $\theta_{BC} = \theta_B$ = 32.42°. These x-rays are reflected from the center of the crystal, and the image is very similar to 5c.

c. Line source image, with y_S = 0.013 cm, θ_B = 30.0°, and θ_{BC} = 32.42°. These rays do not strike the crystal at the center, and substantial aberrations occur.

d. Line source image, with y_S = 0.013 cm, θ_B = 34.8°, and θ_{BC} = 32.42°. These rays strike the opposite side of the crystal from those in 8c.

plane and hence near the focus. But for θ_B differing from θ_{BC}, the image moves towards the end of the detector and hence further from the focus. This expectation is verified by the solutions given in eq. (12) for Geometry 2. As an example, with the standard parameter values and with θ_{BC} = 56.2°, the factor F_{fw} has a value 1.97 for $|\theta_B - \theta_{BC}|$ = 3.2°, and a value of 2.95 for $|\theta_B - \theta_{BC}|$

= 8.0°; the total energy range is 2.05 to 2.46 keV. Figure 9 gives a plot of F_{fw} vs. θ_B in Geometry 2 employing the above parameter values over the full angular acceptance of a 10 cm long crystal. The angular acceptance width of a 10 cm long detector is smaller and is also shown in Figure 9.

The following conclusions can be made from analyses of images in Geometry 2. First, typical F_{fw} values over the detector angular acceptance range from 1 to 3, indicating that optical broadening in Geometry 2 is not significantly greater than in Geometry 1. Since this resolution loss due to aberrations in Geometry 2

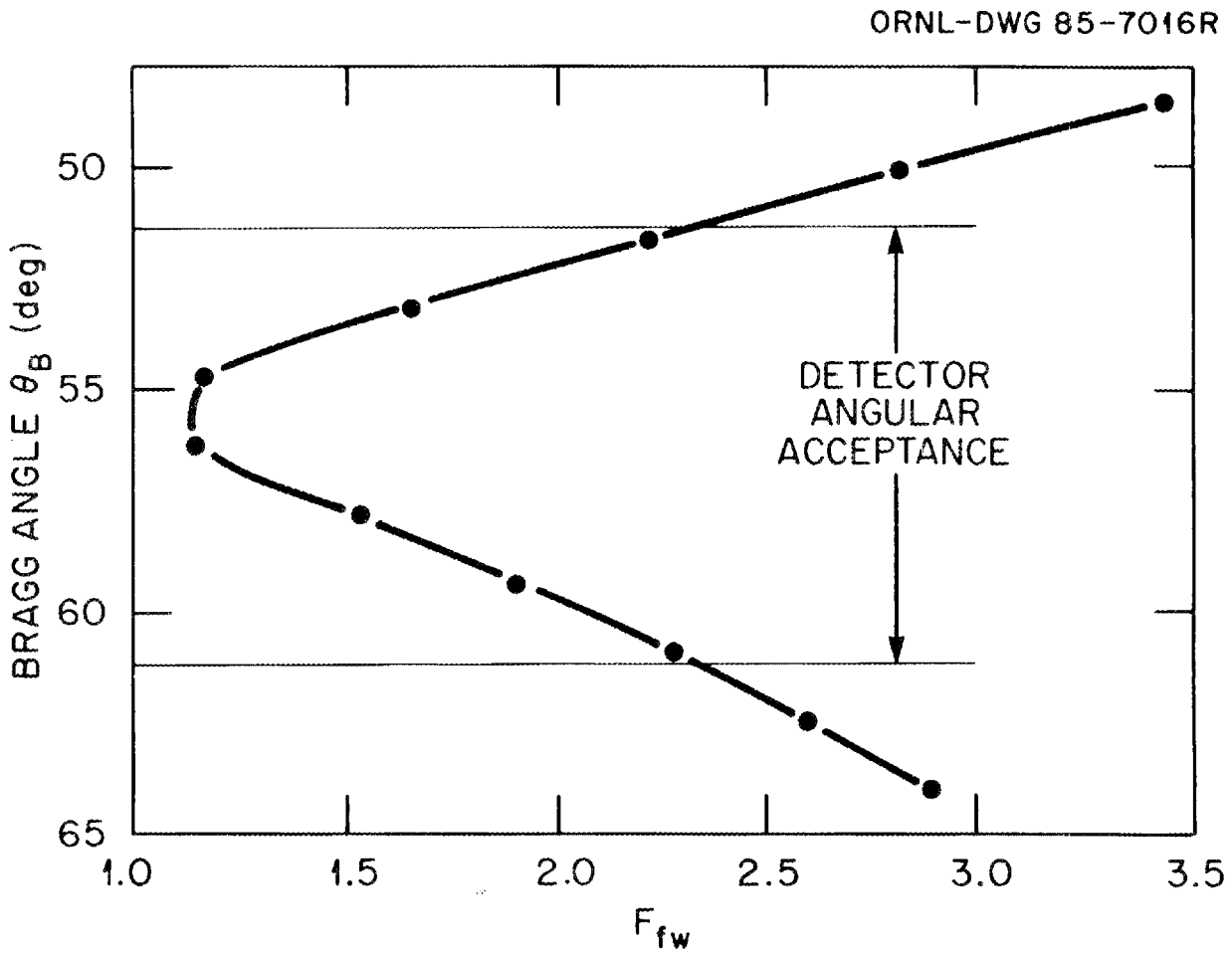

Fig. 9. A plot of F_{fw} vs. θ_B for Geometry 2, with standard parameter values and Δy = 0.03 cm, a crystal length of 10.16 cm with 2d = 6.687 Å, an energy range of 2.05 to 2.45 keV, and an angular range of 49.0 to 64.8 degrees with θ_{BC} = 56.2°.

is substantially smaller than the expected broadening from the conversion depth/parallax effect in PSPCs in Geometry 1, Geometry 2 is preferred for proportional counters. Second, the resolution loss due to aberrations may be reduced by limiting the detected z height as is evident in fig. 8: this is feasible because the loss in intensity is more than compensated by the focusing effect of the von Hamos geometry.
Additionally, the ends of the crystal (or detector) may be masked, reducing the bandwidth, so that only Bragg angles near θ_{BC} are reflected and detected. At these angles, F is minimized and resolution is optimized. These two procedures allow a portion of the x-ray spectrum to be collected at the highest possible resolution. Geometry 2 is thus a very flexible design which is well suited to our spectroscopic needs. With proper choice of crystal and detector, it can collect a large portion of the x-ray spectrum ($\Delta E/E \sim 10\%$) at each position of the components with much higher efficiency than a flat crystal spectrometer and only moderate aberrations; and when necessary, a smaller portion of the spectrum can be collected at maximum resolution.

The bandwidth of x-ray energies detected is determined by the smaller of the Bragg angle ranges that the crystal or detector subtends from the source. In order to study an energy interval larger than a few hundred eV, even with a long (~ 10 cm) detector, the central Bragg angle range must be varied. In Geometry 2, this is best achieved by a translation of the crystal and a translation and rotation of the detector (fig. 10). The intensity of x-rays at the detector is proportional to the number of x-rays reflected by the crystal, which in turn is proportional to the solid angle Ω subtended by the crystal with respect to the source. By moving the crystal away from the source to reach smaller Bragg angles and higher x-ray energies, Ω decreases rapidly. At smaller Bragg angles, and hence higher energies, the efficiency for a given crystal in Geometry 2 design falls significantly.

ORNL-DWG 85-7019R

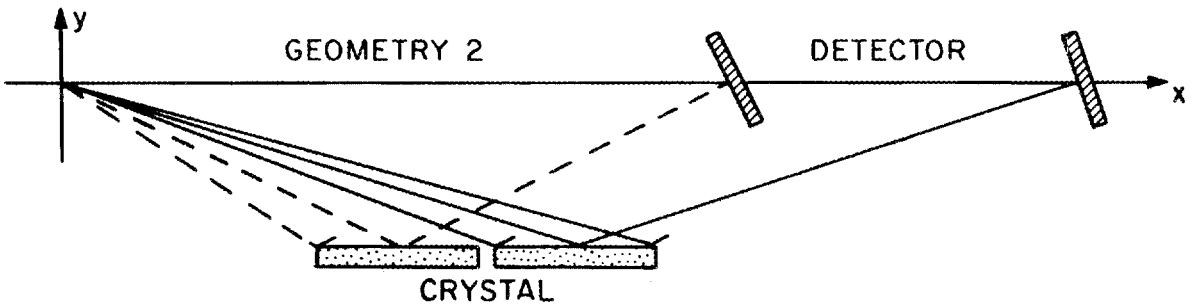

Fig. 10. Geometry 2 - crystal translation adjusts the Bragg angle range.

II.B.3. Imaging in a Rotated-Crystal, Tilted-Detector Geometry (Geometry 3)

An alternative spectrometer design denoted Geometry 3, was studied in an attempt to partially alleviate the efficiency variation problem (fig. 11a). This design utilizes crystal rotation to vary the Bragg angle range: the crystal center $C = (x_C, -\rho, 0)$ is fixed, and the rotation is about an axis through C in the z-direction. Since x_C is constant, $\Delta\Omega$ varies as the first power of $\sin\theta_{BC}$. A focus of the point source $Q = (0, y_{S0}, 0)$, the slit center, is found by placing the detector center at the intersection of the reflected ray and the ray from Q through the crystal normal a distance ρ above the crystal (fig. 11b). This geometry is also suitable for PSPCs because of near-normal incidence of the x-rays with the detector optimally oriented.

The advantage of more nearly constant collection efficiency in Geometry 3 is accompanied by a substantial increase in image distortion. Two qualitative reasons for this can immediately be given. First, recall that y-axis translation of a line source causes aberrations in both Geometries 1 and 2. Yet it is clear from figs. 12a and 12b that a line source in the x=0 source plane bears the same relationship to a rotated crystal, as a translated line source does to a non-rotated crystal. This effective translation of the source induces the

ORNL-DWG 85-7020AR

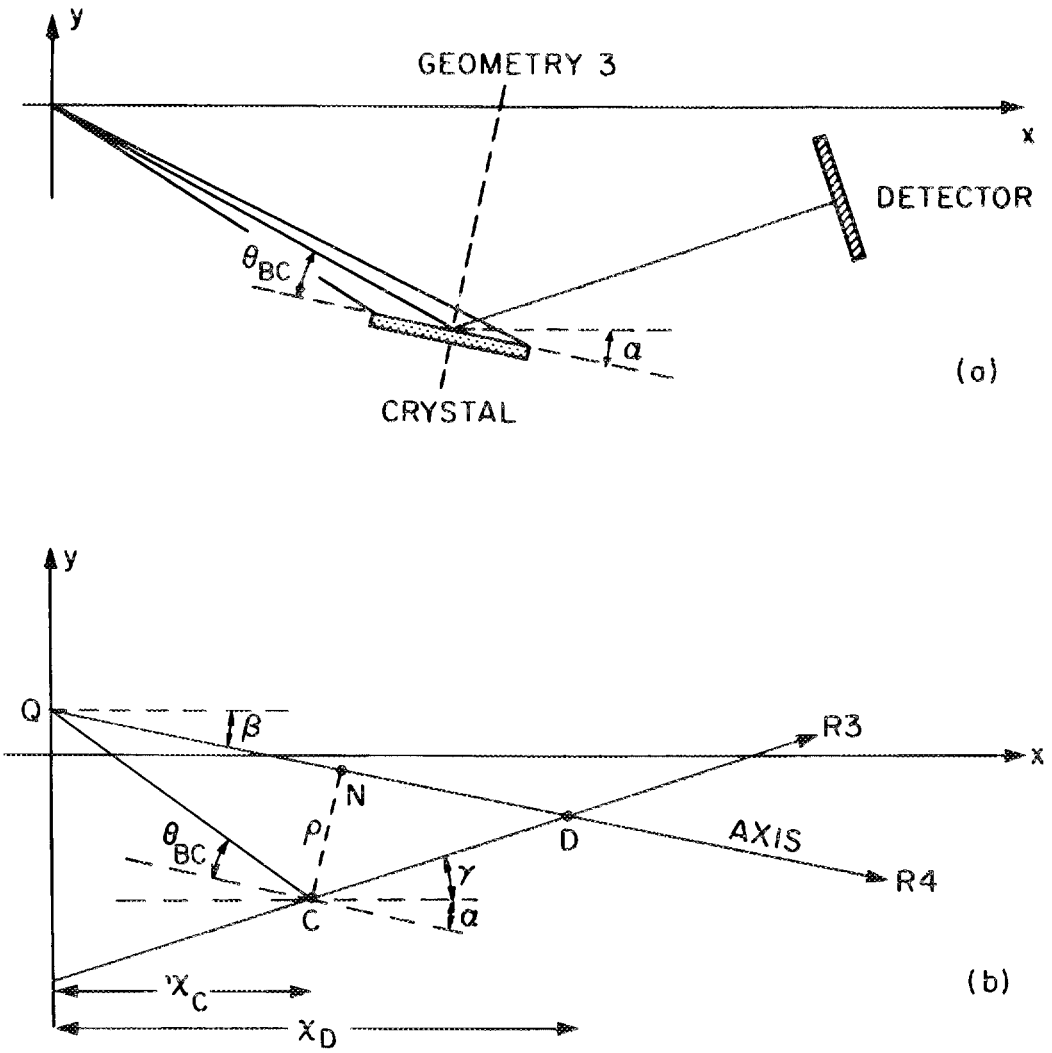

Fig. 11. a. Geometry 3 - crystal rotation adjusts the Bragg angle range. The crystal center is fixed at $C = (x_C, -\rho, 0)$.

b. The location of the detector in Geometry 3. Q is the slit center; C is the crystal center; D is the detector center; N is a distance ρ above C on the normal to the crystal at C; α is the angle of rotation of the crystal.

greater distortion. Geometry 3 cannot, however, be reduced to Geometry 2 by a simple coordinate transformation because the detector has different orientations in the two designs. Yet it does suggest a method, described below, of dealing with the complexities of a rotated crystal configuration.

ORNL-DWG 85-7023R2

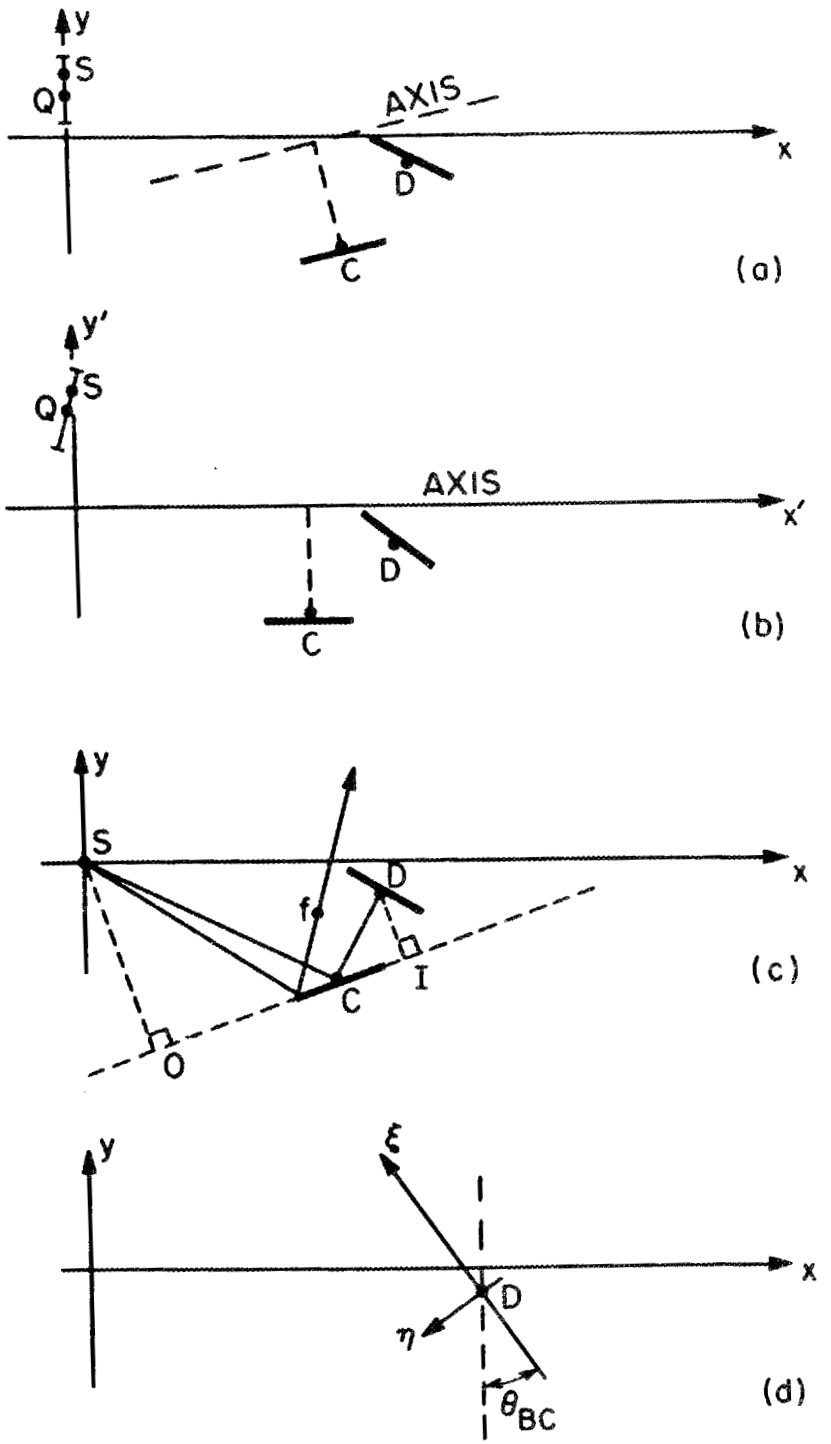

Fig. 12. The coordinate transformation in Geometry 3. A rotated-crystal geometry (a) is reduced to a non-rotated configuration, (b). Most reflected rays are not focused on the detector in Geometry 3 as shown in (c): this leads to increased aberrations. Finally, (d) shows the coordinate system attached to the detector in Geometry 3, after the coordinate transformation shown in (b).

The second qualitative argument for increased aberrations in Geometry 3 involves the detector placement. Consider two x-rays from the slit center Q, one incident at $C = (x_C, -\rho, 0)$ and the other at the edge of the crystal (fig. 12c). The detector is placed so that the ray incident at C has a focus at the detector center, given by the Lensmaker's Law for cylindrical mirrors

$$1/i + 1/o = -2/\rho \ , \tag{14}$$

where i and o are the lengths of line segments DI and SO shown in fig. 12c. However, the rays incident at the crystal edge will not have a focus on the detector. Rather, the degree of aberration in the focus worsens as the normal distance from the focus to the detector increases. Additionally, for small Bragg angles, this focus has a magnification greater than 1: thus even a perfect focus of the source would result in a substantial increase in the ξ-extension of the image.

The input parameters necessary to find images in Geometry 3 are the radius of curvature ρ, the x-coordinate of the crystal center x_C, the point source coordinates y_S and z_S, the Bragg angle θ_B, and two new parameters: the y-coordinate of the center of the slit y_{SO}, measuring misalignment; and a desired Bragg angle range (θ_1,θ_2) to be collected by the spectrometer. We then set

$$\theta_{BC} = (\theta_1+\theta_2)/2 \ , \tag{15}$$

and $$\alpha = \mathrm{atan}\,[(\rho + y_{SO})/x_C] - \theta_{BC} \ ,$$

where α is the clockwise rotation angle of the crystal from horizontal (fig. 11b). This choice of α and θ_{BC} allows the maximum portion of the desired angular (energy) range to be reached. The detector position is found in Appendix C (eq. C5) with the result that the center $D = (x_D, y_D, 0)$ is given by

$$x_D = \frac{y_{S0} + \rho + x_C \tan\gamma}{\tan\gamma + (y_{S0} - \rho \cos\alpha + \rho)/(x_C + \rho \sin\alpha)} , \tag{16}$$

$$y_D = (x_D - x_C) \tan\gamma - \rho ,$$

and $\gamma = \theta_{BC} - \alpha$.

A coordinate transformation is now made to a system in which the x-axis is the crystal's axis of revolution and the source slit is rotated and translated (fig. 12b). The method of Sect. II.3 is now employed to find the image points $P(\psi)$ on the detector plane. Finally, a transformation is made to a coordinate system attached to the detector (fig. 12d):

$$x \to \xi = (x - x_{DR})/(-\sin \theta_{BC}) , \tag{17}$$

$$y \to \eta = 0 ,$$

and $z \to z$.

where x_{DR} is the x-coordinate of D in the new coordinate system. The image solutions are found in Appendix D to be

$$x_P = \frac{x_{DR} - y_{SR} + 2|BR| \cos\psi + x_{DR} \cot\theta_{BC}}{(y_S - y_{SR} + 2|BR| \cos\psi)/x_R + \cot\theta_{BC}} , \tag{18}$$

and $z_P = x_P (\rho \sin\psi - z_S - 2|BR| \sin\psi)/x_R + z_S + 2|BR| \sin\psi$,

with (ξ, η, z) given by eq. (18), and x_{DR}, y_{DR}, y_{SR}, x_R, and $|BR|$ given by eqs. (D3), (D5), and (D6) in Appendix D.

Figures 13a-d show images of line sources in Geometry 3. Note that y-axis translation and the shift of θ_B from θ_{BC} results in substantial increase in the ξ-extension of the image. The third, and dominating, factor causing aberrations is the angle of crystal rotation α. Even a small angle of rotation can greatly distort the image at any Bragg angle, even those equal to or deviating only slightly from θ_{BC}. Figure 14 shows plots of F_{fw} vs. θ_B for Geometry 3, analogous to fig. 9 for Geometry 2. Here X_C = 30.0 cm and α = 15.23° to achieve

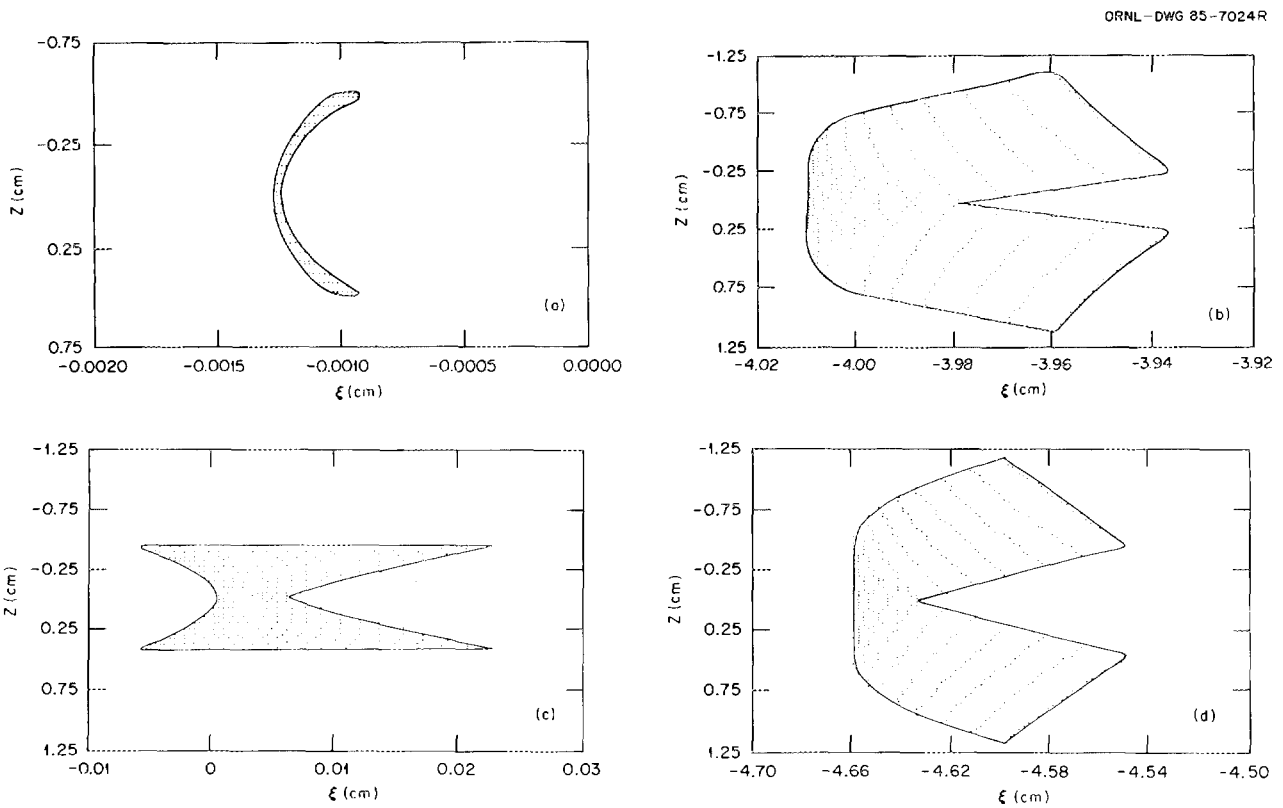

Fig. 13. Images of line sources in Geometry 3 with standard parameter values $y_{S0} = 0$, $x_C = 40.0$ cm.

a. $y_S = 0.015$ cm, $\theta_B = \theta_{BC} = 32.42°$, similar to fig. 8b. $\alpha = 0.0°$: there is no crystal rotation.

b. $y_S = 0.015$ cm, $\theta_B = 30.0°$, $\theta_{BC} = 32.42°$, $\alpha = 0.0°$, as in fig. 8c.

c. $y_S = 0.0$ cm, $\theta_B = 35.0°$, $\theta_{BC} = 35.0°$, $\alpha = -2.58°$. Small rotation of crystal causes large aberrations.

d. $y_S = 0.0$ cm, $\theta_B = 32.0°$, $\theta_{BC} = 35.0°$, $\alpha = -2.58°$. Both the effect of crystal rotation and of a shift of θ_B from θ_{BC} are evident in large aberrations.

$\theta_{BC} = 55.92°$ which for quartz$(10\bar{1}1)$ gives a central-ray Bragg energy of 2.24 keV. The F_{fw} are 2 to 5 times those found for Geometry 2 (see fig. 9). As another example to show the strong α dependence, a crystal rotation of 2.43° gives F_{fw} values from 1.99 to 4.79 depending on θ_B, with $x_C = 40$ cm, $\rho = 25.4$ cm, $\Delta y = 0.03$ cm, and an energy range of 2.12-2.40 keV. If α is increased to 10.65° to reach 4.5-5.5 keV, F_{fw} dramatically increases to a range of 15.35 to 18.29.

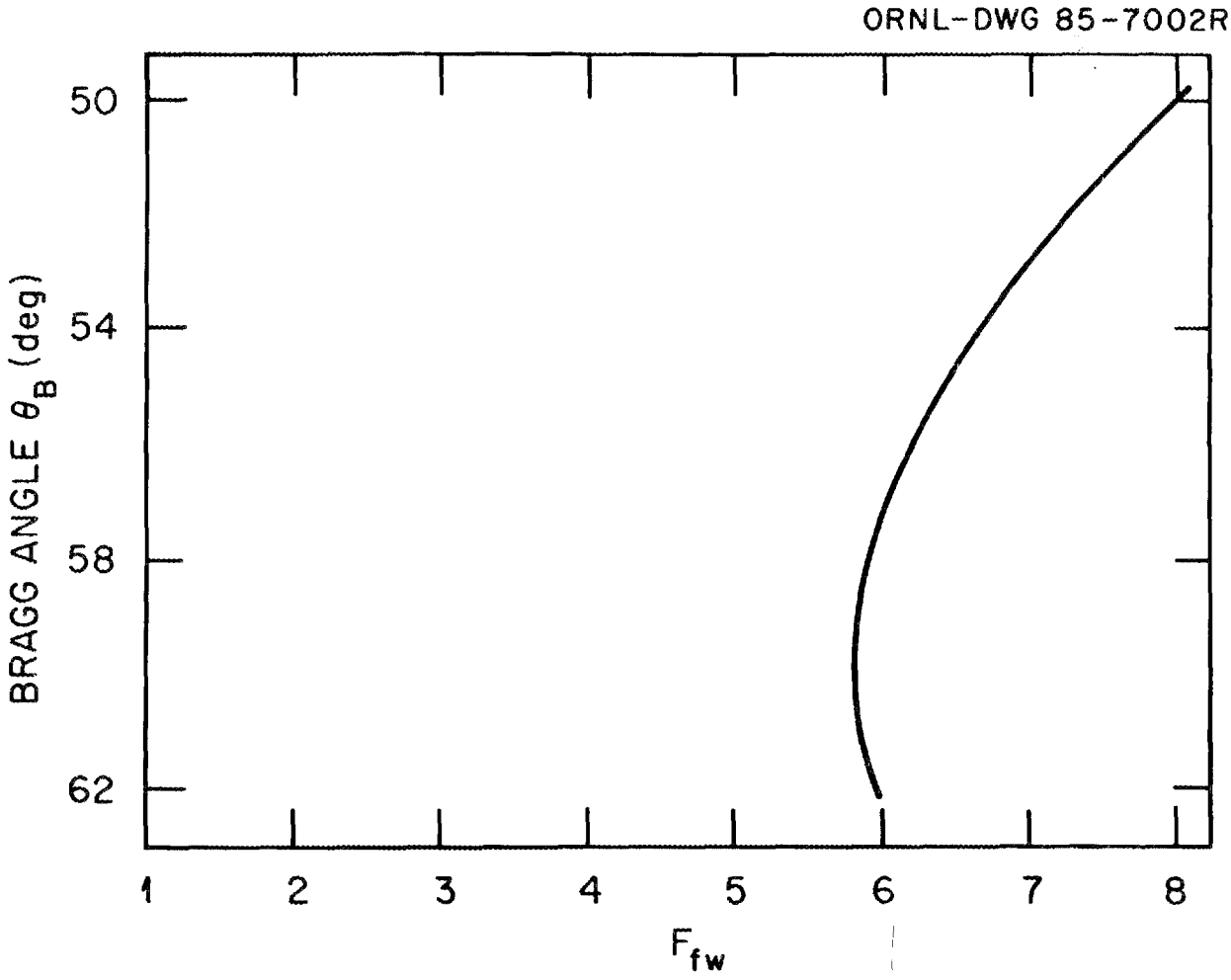

Fig. 14. A plot of F_{fw} vs. θ_B for Geometry 3, with standard parameter values and with Δy = 0.03 cm, x_C = 30.0 cm, α = 15.23°, θ_{BC} = 55.92°. The energy range is 2.09 to 2.43 keV, similar to the situation shown in Fig. 9 for Geometry 2. The rotation of the crystal has caused F_{fw} to have values as high as 8.17.

Thus with the above set of parameter values, the full width ξ-extension of the image is 15 times the source width (the fwhm ξ-extension is approximately 10 times larger than the source width.)

II.B.4. Comparison of Image Quality in the Three Geometries.

The values of the aberration factor F_{fw} (Figs. 9 and 14) clearly show the imaging superiority of Geometry 2 over Geometry 3. Another comparison of image quality can be made by examining the signals generated by the PSPC in the two

geometries. The proportional counters suitable for use in Geometries 2 or 3 may be position-sensitive in either one or two dimensions. One dimensional counters are useful to our studies when they are aligned along the ξ-direction, integrating signals in the z-direction: all signals with a ξ-coordinate in a particular interval are counted in the same data channel. This integration can be simulated by employing the ξ vs. z image plots, as long as two assumptions are made. First, we assume that a rectangular source slit is uniformly illuminated. This allows the source to be approximated by an array of point sources evenly spaced in the y- and z-directions, each isotropically emitting x-rays with the same intensity. Secondly, assume $\rho >> z_S$ for all point sources S approximating the slit. Then each unit of surface area ΔA on the crystal subtends the same solid angle for any angle ψ with respect any source point S. Now it can be seen that each x-ray from S to $R(\psi)$ reflected to $P(\psi)$, for all S and all ψ, represents an equal amount of intensity when ψ, y_S, and z_S are evenly incremented. This follows from the above assumptions: for any one S, incrementing ψ marks off equal areas of the crystal ΔA, which subtend equal solid angles $\Delta\Omega$ with respect to S as shown above. The number of x-rays striking ΔA is proportional to $\Delta\Omega$, and this is equal to the number of x-rays reflected from ΔA to the neighborhood of $P(\psi)$. Since all point sources S emit similarly, each image point represents the same amount of intensity. So by integrating the image points in the z-direction and plotting against the ξ-coordinate, we simulate the integration physically performed by the one-dimensional PSPC and generate a plot of counting intensity vs. ξ. Figures 15 and 16 give sample plots of relative intensity vs. ξ for Geometries 2 and 3, respectively, given a source height $\Delta y = 0.03$ cm, standard parameter values, and various Bragg angles and slit alignments. Once again, the imaging quality of Geometry 2 is seen to be superior to Geometry 3: the fwhm of the intensity plots are greatly increased by any rotation of the crystal.

To summarize, we have studied the imaging properties of the von Hamos-type curved-crystal x-ray spectrometer for three different design geometries. The

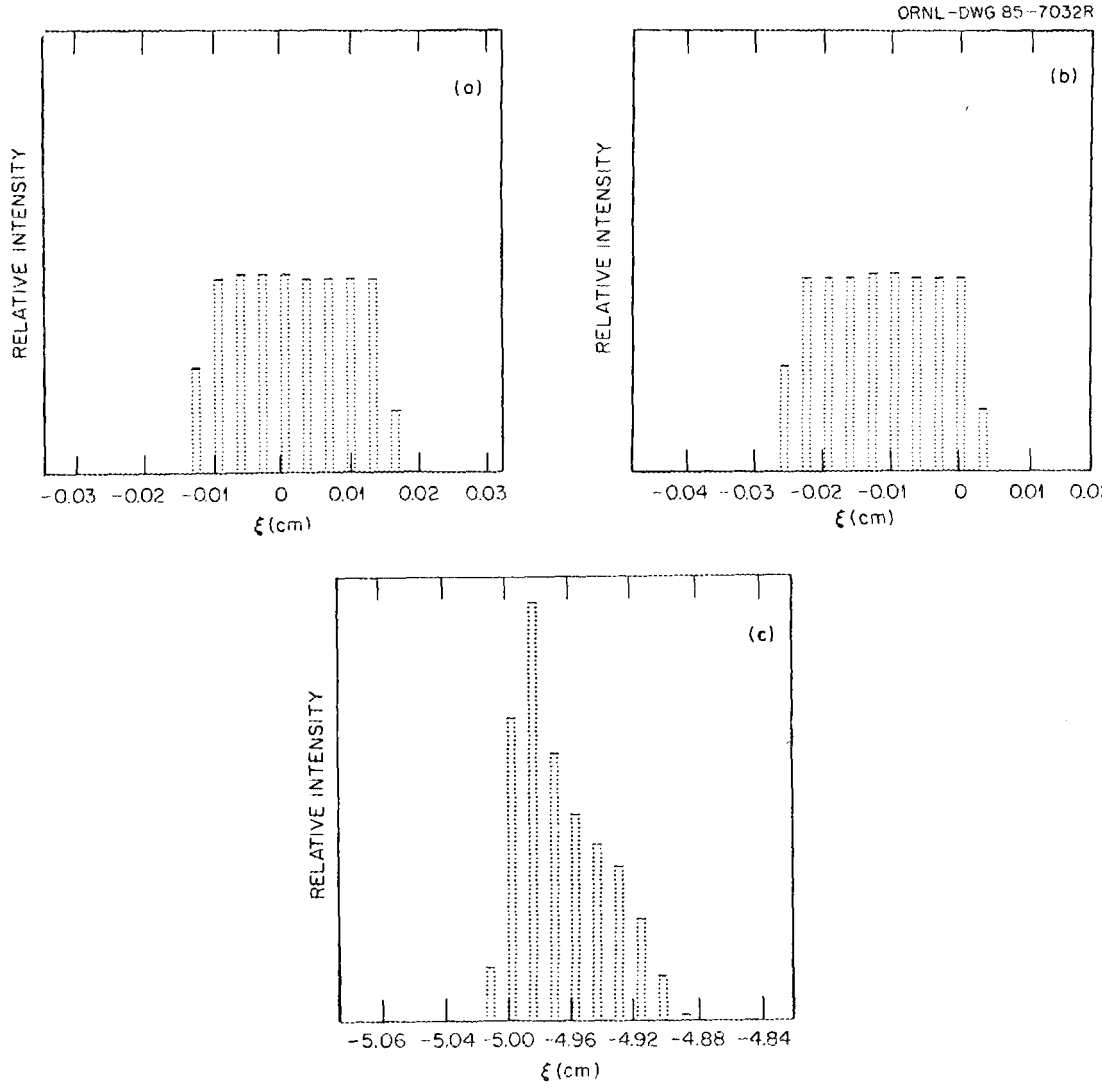

Fig. 15. Plots of intensity vs. position on detector (ξ) in Geometry 2 for input parameters identical to those in fig. 8.

a. The Bragg angle θ_B = 32.42°, and these rays thus strike the crystal center. The intensity pattern has a width slightly larger than the slit width ($F_{fw} \approx 1$).

b. A translation of the source slit along the y-axis by an amount 0.015 cm, with the same parameters and with θ_B = 32.42°. The pattern is shifted along the detector, but is not broadened.

c. Changing the Bragg angle to θ_B = 29.94° leads to a coma effect; these rays strike the edge of the crystal. F_{fw} increases to approximately 4. ($F_{fwhm} \approx 1.7$)

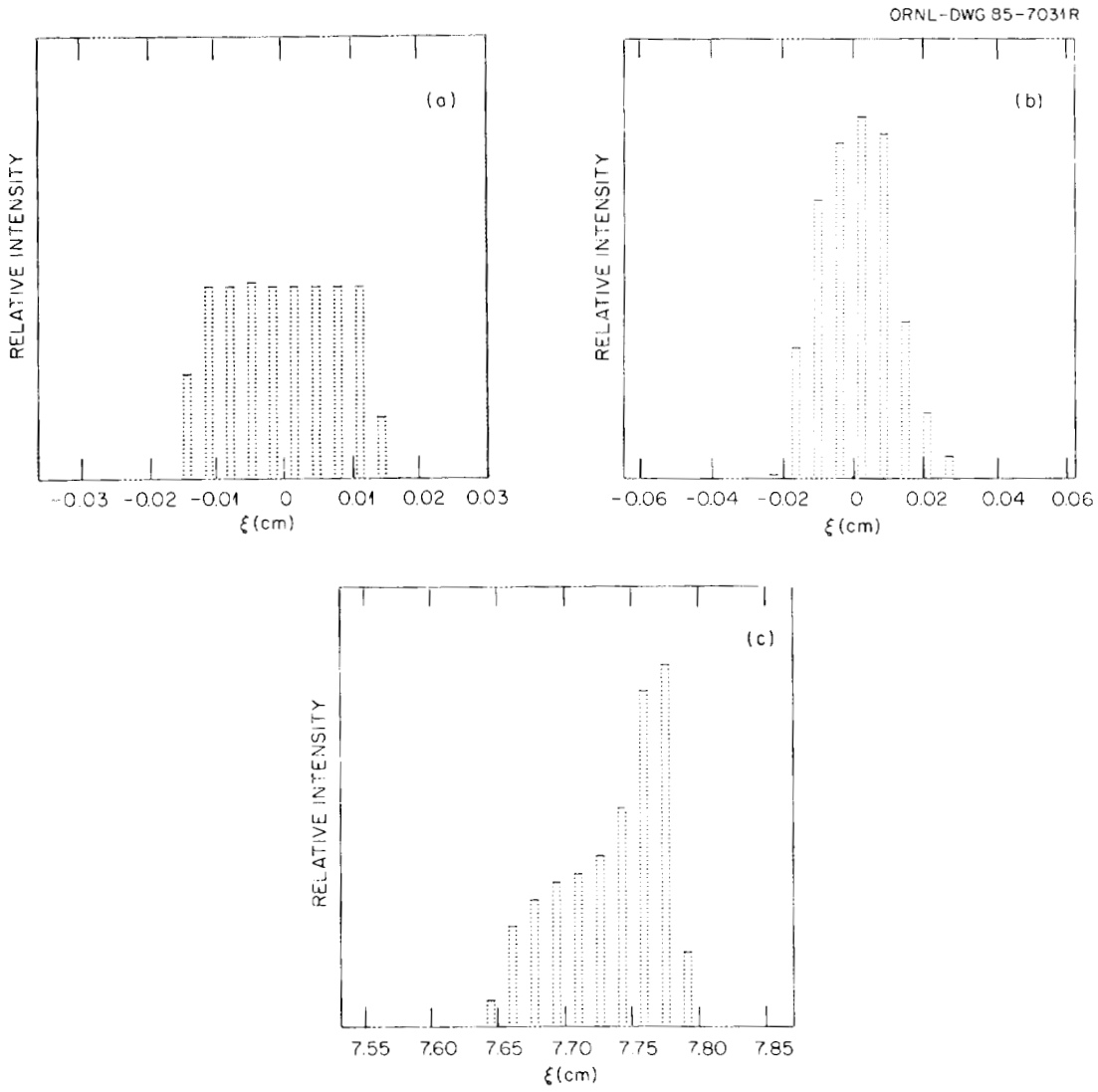

Fig. 16. Plots of intensity vs. ξ for Geometry 3 with input parameters as in fig. 15 and x_C = 40.0 cm.

a. θ_B = 32.42°, α = 0.0°. This is identical to fig. 15a (no crystal rotation).

b. θ_B = 35.0°, α = -2.58°. Here $F_{fw} \approx 2.5$, and the intensity pattern is that of the image shown in fig. 13c. Notice the low energy tail in the pattern. These rays do strike the center of the crystal.

c. θ_B = 40.0°, α = -2.58°. This has both effects of crystal rotation and shift of θ_B. F_{fw} has grown to approximately 5.

first design involves placing a detector along the crystal's axis of revolution: this design, ideal for solid state or film emulsion detectors, offers superior image quality. A second design involves tilting the detector towards the crystal to allow near-normal x-ray incidence. The crystal and the detector are translated to vary the Bragg angle range. This design is ideal for position-sensitive proportional counters, and has only slightly greater aberrations than the first configuration. The main disadvantage for both of these designs is that they suffer from strong collection efficiency variation with central Bragg angle for a given crystal. A third design involves fixing the source-to-crystal distance and rotating the crystal about its center to vary the Bragg angle range. This design offers greater collection efficiency over the detected bandwidth, especially at high energies, than the previous designs. However, a severe increase in image distortion, even at small crystal rotations, makes this design unsuitable for most high resolution needs.

All three designs offer advantages over flat-crystal and curved-crystal horizontal-focusing spectrometers. First, the von Hamos geometry gives a large gain in intensity of x-rays at the detector over flat-crystal types: the tilted-detector design does this with only moderate aberrations. Second, a large portion of the x-ray spectrum may be collected at each positioning of the crystal and detector: horizontal-focusing spectrometers using point or slit sources require scanning of the crystal and detector to collect a sizeable energy range. With a moderate-size crystal, the tilted-detector design can collect $\Delta E/E \geqslant 10\%$ without scanning, and by masking the ends of the crystal, a smaller range can be collected with the highest energy resolution possible in the von Hamos geometry.

II.C. Construction Details.

Based on the above considerations and on the availability of commercial components, we decided to construct a Geometry 2 type von Hamos spectrometer (as displayed schematically in fig.17) according to the following system para-

ORNL-DWG 84-14559R

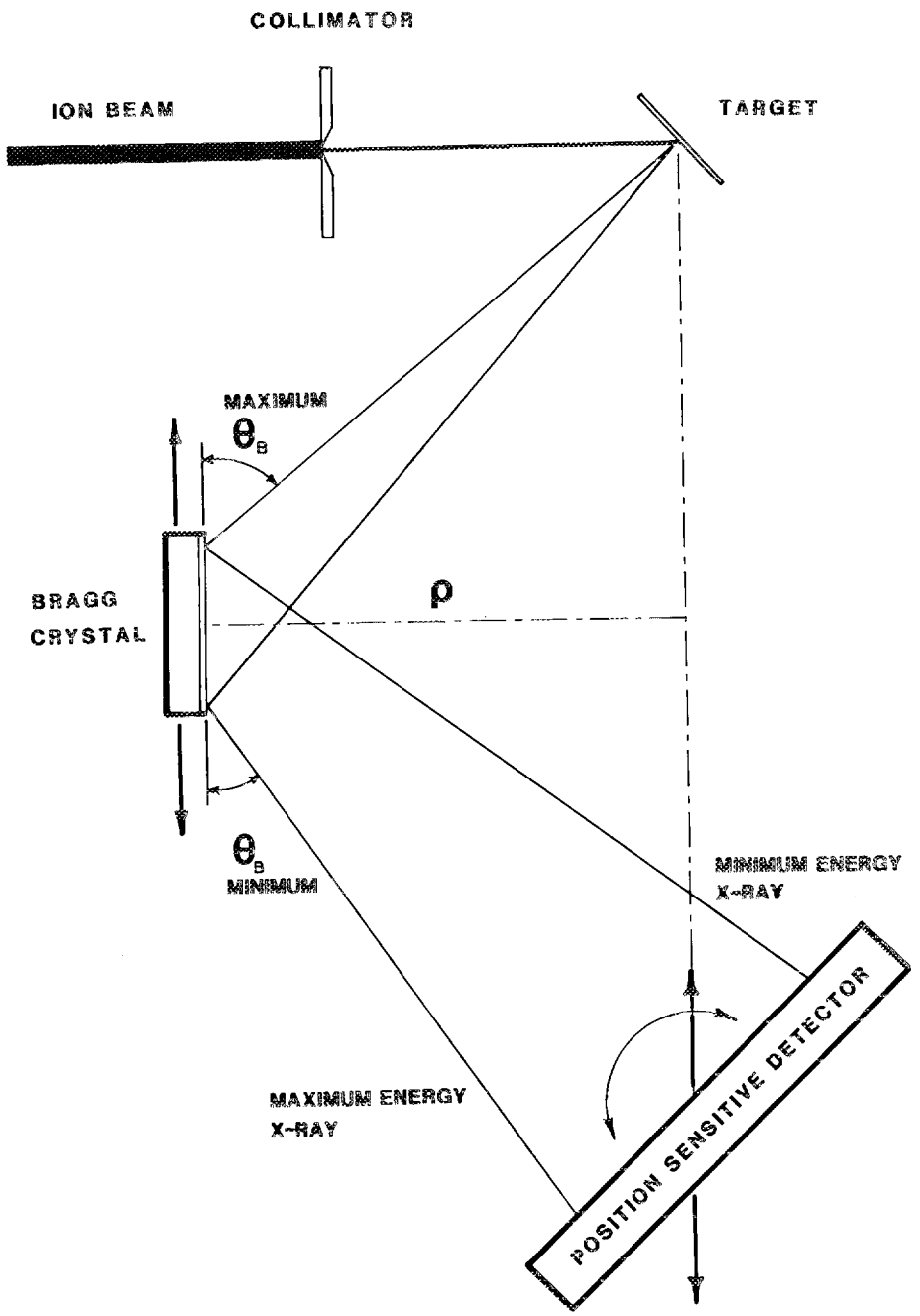

Fig. 17. Schematic of von Hamos spectrometer as constructed. View is of plane containing the ion beam and the crystal axes. Remotely controlled adjustment motions of crystal and detector are indicated by arrows.

meters: (1) The crystal radius is set at $\rho \leq 25.4$ cm. As noted previously, a required energy resolution of $\delta E/E \leq 1/2500$ together with realistic source width of $w_S \geq 0.2$ mm essentially dictates that the crystal radius be $\rho \geq F \cdot 14$ cm. With F held to ≤ 2, $\rho = 25.4$ cm permits the required energy resolution to be achieved. For measurements not requiring such high resolution, use of crystals with smaller ρ is also possible. (2) The adjustment of crystal and detector relative positions allows the central Bragg angle (Θ_{BC}) to be varied from 30 to 70 degrees which gives full coverage of x-ray energies from 1 to 10 keV using only a few different crystals. This angular range together with ρ = 25.4 cm determines the scale for the size of the instrument (and the containing vacuum vessel) to approximately 60 x 120 x 15 cm^3. (3) The crystal and detector lengths are set at 10 cm to achieve a detected energy bandwidth $\Delta E/E \geq 10\%$. Consultation with various crystal preparation experts[10] led us to 10 x 10 cm^2 as the maximum crystal size (for ρ = 25.4 cm). The thin crystals are permanently glued in place on aluminum blocks machined to a precise concave cylindrical surface. We have ordered and received two crystals (Interactive Radiation, Inc.; Northvale, NJ). One is quartz($10\bar{1}1$) with 2d spacing of 6.687 Å particularly suited for study of sulfur K_α satellites; The other is ADP(101) with 2d spacing of 10.648 Å.

The detector is a commercial (TEC, Knoxville, Model 210F) position-sensitive proportional counter. It is a gas-flow type with a thin(12 μm) aluminized mylar window allowing optimization of efficiency and spatial resolution for x-rays of various energies by appropriate choices of working-gas, pressure, and bias. Initially, at 2.3 keV, we are using P10 gas(90% Ar, 10% CH_4) at a pressure of 1 atmosphere. Position of detected x-rays is determined by timing of from the two ends of the quartz-fiber anode.[11] The full-width-half-maximum position resolution is measured to be 150 μm at a bias of +1385 volts. The detection efficiency at 8 keV is $\geq 80\%$. The detector and preamplifiers operate wholly within the vacuum chamber.

The x-ray source consists of a spatially well-defined, ion (or electron)-target interaction region. Collisions of either electrons or high-energy ions generate x-rays in the target cell shown in fig. 18. The ion beam is collimated by two sets of 4-jaw slits situated 200 and 60 cm upstream of the target. A beam skimmer mounted immediately in front of the target on the target cell outer

ORNL-DWG 85-10021

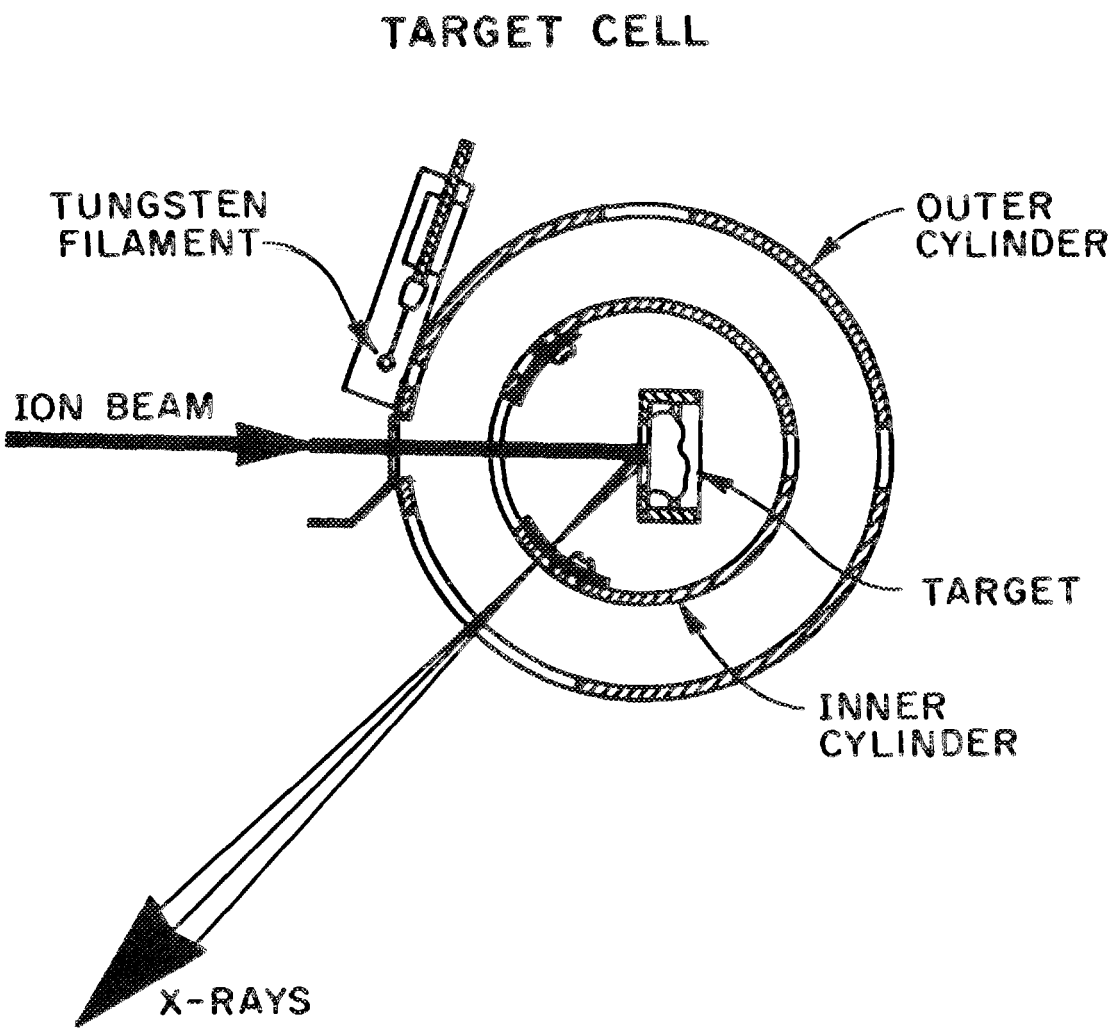

Fig. 18. Target cell x-ray source assembly. Target x-rays are generated by either electron or ion impact. Source size is determined by (1) ion spot size or (2) x-ray limiting slits mounted on the inner cylinder.

cylinder reduces the extended spray of slit-scattered ions and guarantees that the ion beam position on the target is stably located. Typical beam-on-target widths, measured from beam spots observed after lengthy bombardments, amount to ~ 0.3 mm. For solids, the targets are mounted on an electrically isolated ladder oriented perpendicular to the plane of fig. 18. The target ladder position is rigidly maintained by a guide track fixed within the target cell, so that exact repositioning of the x-ray source region may be achieved when targets are changed. This is an important feature which is discussed in more detail in Chapter III. The two cylinders shown surrounding the target are also electrically isolated so that, with appropriate biasing, beam current may be taken from thick targets for normalization and/or beam monitoring. The inner cylinder contains the x-ray defining slits which may be externally rotated with respect to the cylinder axis. The fixed outer cylinder is an x-ray shield used to reduce detected background by limiting departing x-rays to those that fall on the crystal directly. A tungsten filament for electron impact x-ray production is also mounted on this cylinder, as indicated.

The crystal, detector and target cell are all contained in a stainless steel vacuum chamber as shown in fig. 19. The chamber is pumped to $\sim 1 \times 10^{-7}$ torr static pressure by a 350 ℓ/s cryopump. Two large rectangular ports on the chamber side permit access for crystal and detector adjustment and replacement. The crystal and detector are mounted on carriages supported by dove-tail tracks with precision lead screw drives which are controlled and monitored externally. Similarly, the rotational orientation of the detector with respect to the crystal axis is externally adjustable. The crystal and detector mounting tracks are aligned parallel by using a laser beam reflected from a mirrored target to the crystal and onto the detector center at all positions along its track. Once aligned, the tracks are locked in place.

The thin mylar detector window permits a small leak rate of detecting gas into the vacuum chamber so that the spectrometer operating pressure is typically $\sim 10^{-6}$

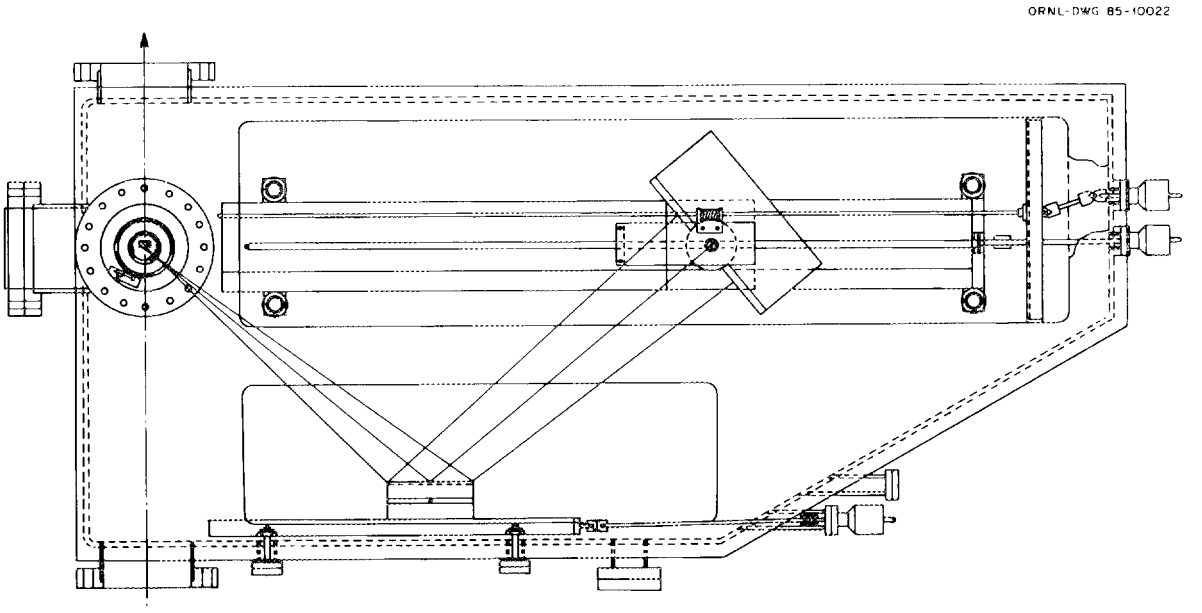

Fig. 19. Drawing of spectrometer vacuum chamber showing mechanical assembly of crystal and detector, their mounting tracks, and motion controls.

torr. At the Holifield Heavy Ion Research Facility (HHIRF) tandem accelerator, beamline pressures are ~ 10^{-8} torr. To accommodate the large pressure differential, a liquid nitrogen trapped vacuum isolator is placed at the entrance to the spectrometer.

The spectrometer chamber is mounted vertically on a mobile stand which has jacking screws for leveling and height adjustment. A typical operating configuration for the entire instrument attached to a HHIRF tandem beamline is shown in fig. 20.

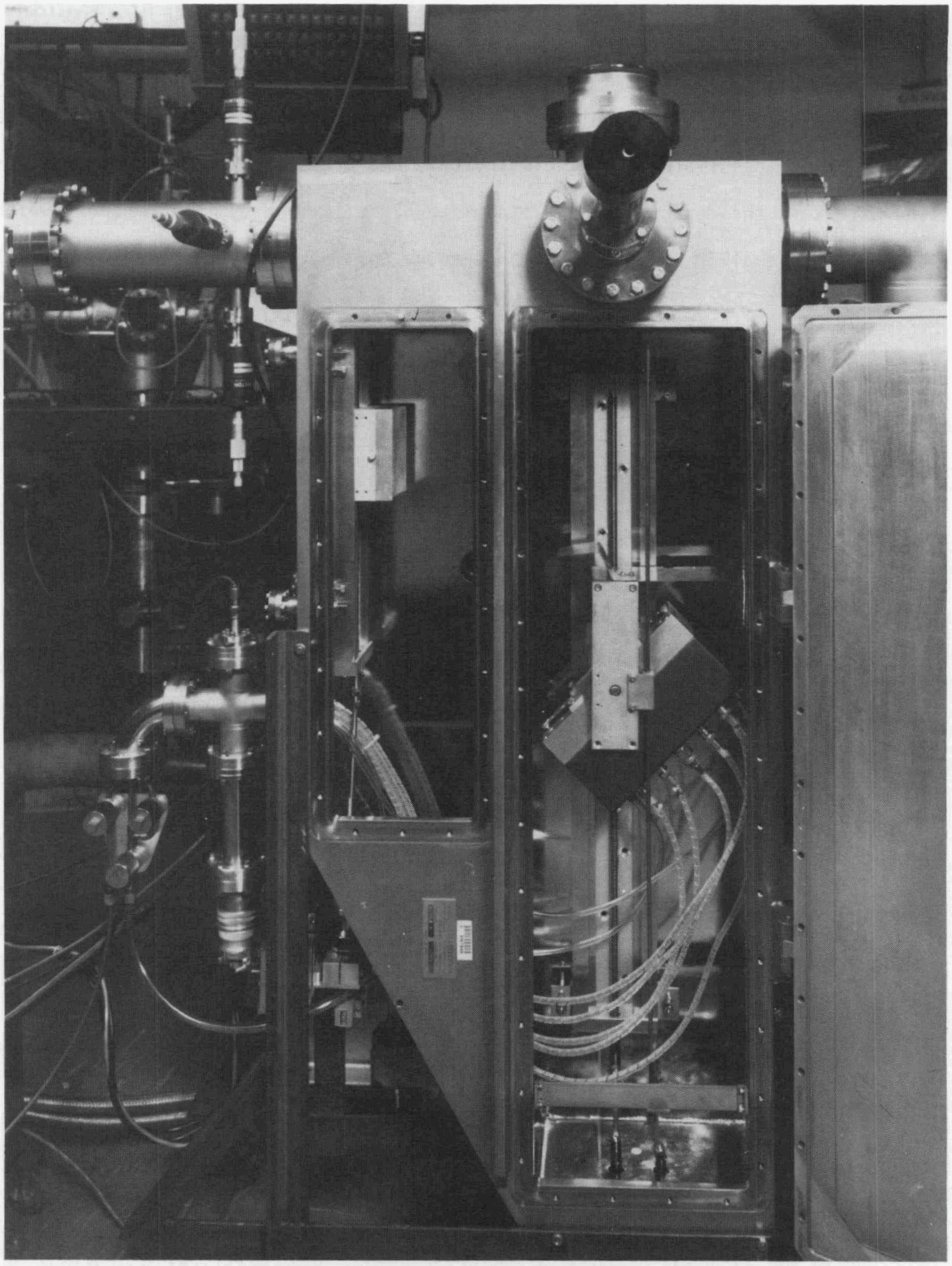

Fig. 20. Photograph of spectrometer as attached to the HHIRF tandem accelerator beam line. Ion beam enters from the left.

III. OPERATIONAL CHARACTERISTICS

III.A. Calculated and Measured Performance.

The selected 30°- 70° angle range and the Bragg relation [eq. (1)] determine the energies accessible to a single crystal. At a given positioning of crystal and detector, the detected energy bandwidth ΔE is limited by the component which subtends the smaller opening angle $\Delta\theta$ through eq. (2), rewritten here as

$$\Delta E/E = \cot\theta_{BC}\ \Delta\theta\ . \tag{19}$$

For our design parameters of ρ = 25.4 cm, detector length (ℓ_D) = 10 cm, and crystal length (ℓ_C) = 10 cm, the detector is the limiting component and $\Delta\theta$ is given by

$$\Delta\theta = \tan^{-1}[\ell_D/(2\rho\cdot\sin\Theta_{BC})]\ . \tag{20}$$

Figure 21 displays the energies diffracted by four example crystals which span the 1.25 to 10 keV energy region. The detector-limited bandwidth is also shown there. The x-ray energy scaling within a detected bandwidth is weakly non-linear. To a very close approximation,

$$E(n) = E_0 + A\cdot(n-n_0) + B\cdot(n-n_0)^2\ , \tag{21}$$

where E_0 is the x-ray energy at data channel n_0 near detector center, A is the dispersion in eV per data channel at channel n_0, and

$$B = \frac{(2E_0{}^2 - C_B^2)A^2}{2E_0(E_0^2-C_B^2)}\quad ;\quad C_B \equiv \frac{12.398}{2d(\text{Å})}\ . \tag{22}$$

In normal operation, an energy calibration is accomplished by measuring channel positions n_1 and n_2 of two lines of known energies E_1 and E_2, respectively. The energy per channel is given by $(E_2-E_1)/(n_2-n_1)$ and to a first approximation,

$$n_0 \simeq (n_2 + n_1)/2\ . \tag{23}$$

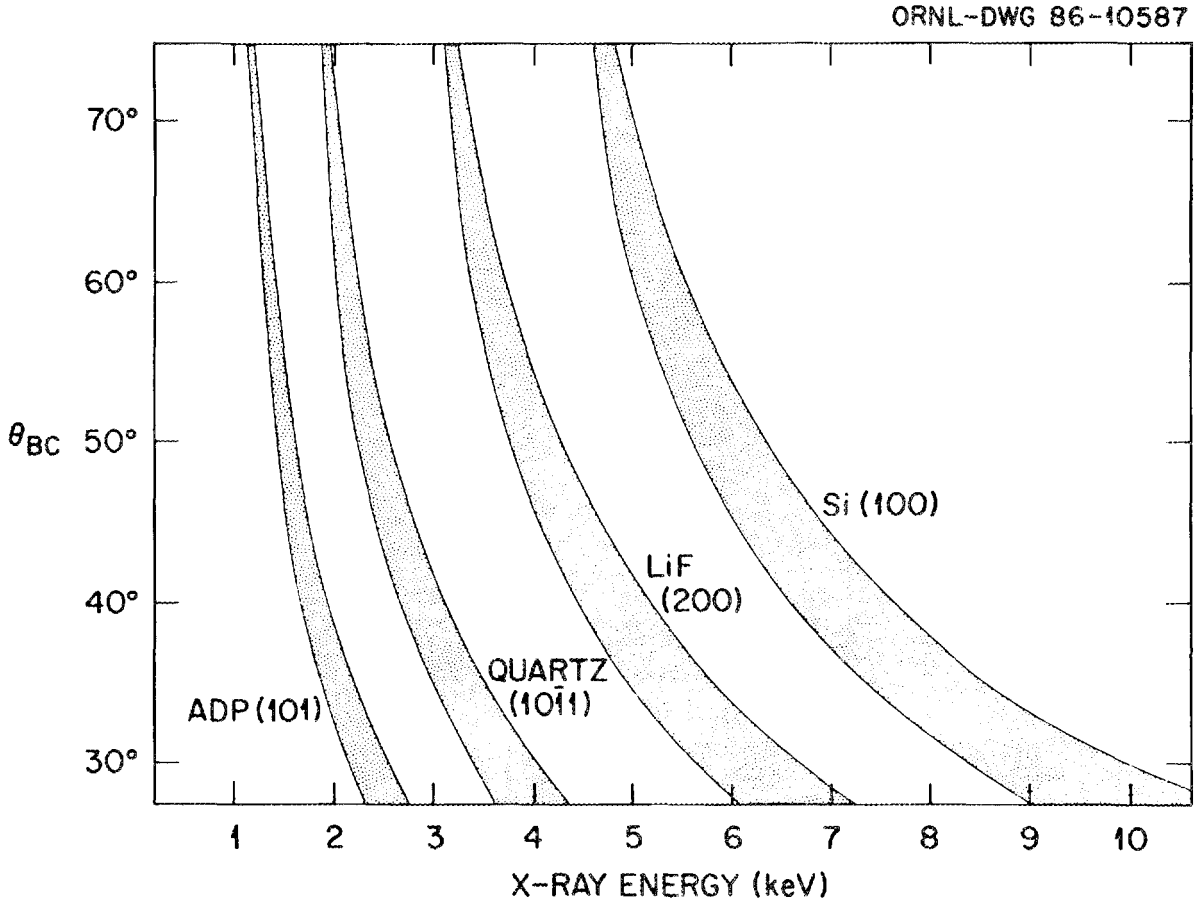

Fig. 21. Central Bragg angle θ_{BC} versus detected x-ray energy for four 10 cm long crystals. Shaded region indicates detector-limited bandwidth at a given central angle. Spectrometer allows $30° < \theta_{BC} < 70°$ range of operation.

The closer (in energy and channel number) E_1 and E_2 are, the more accurate the approximation for n_0, but the less precise the determination of A. A better approximation is given by

$$no \simeq \frac{(n_1+n_2)}{2} + \frac{(2E_0^2 - C_B^2)}{2E_0(E_0-C_B^2)} \cdot \frac{(E_2-E_1)}{4} \cdot (n_2-n_1). \qquad (24)$$

Figure 22 shows measured (points) and calculated (curve) energy vs. channel number data for electron-impact generated Zr L $\alpha_{1,2}$, β_1, $\beta_{6,4}$, β_3, $\beta_{2,15}$ lines using α_1 and β_1 for E_1, n_1 and E_2, n_2 determinations. The energy displacements of β_3 and $\beta_{2,15}$, from the calibration curve amount to less than one part in 1000.

ORNL-DWG 87-15895

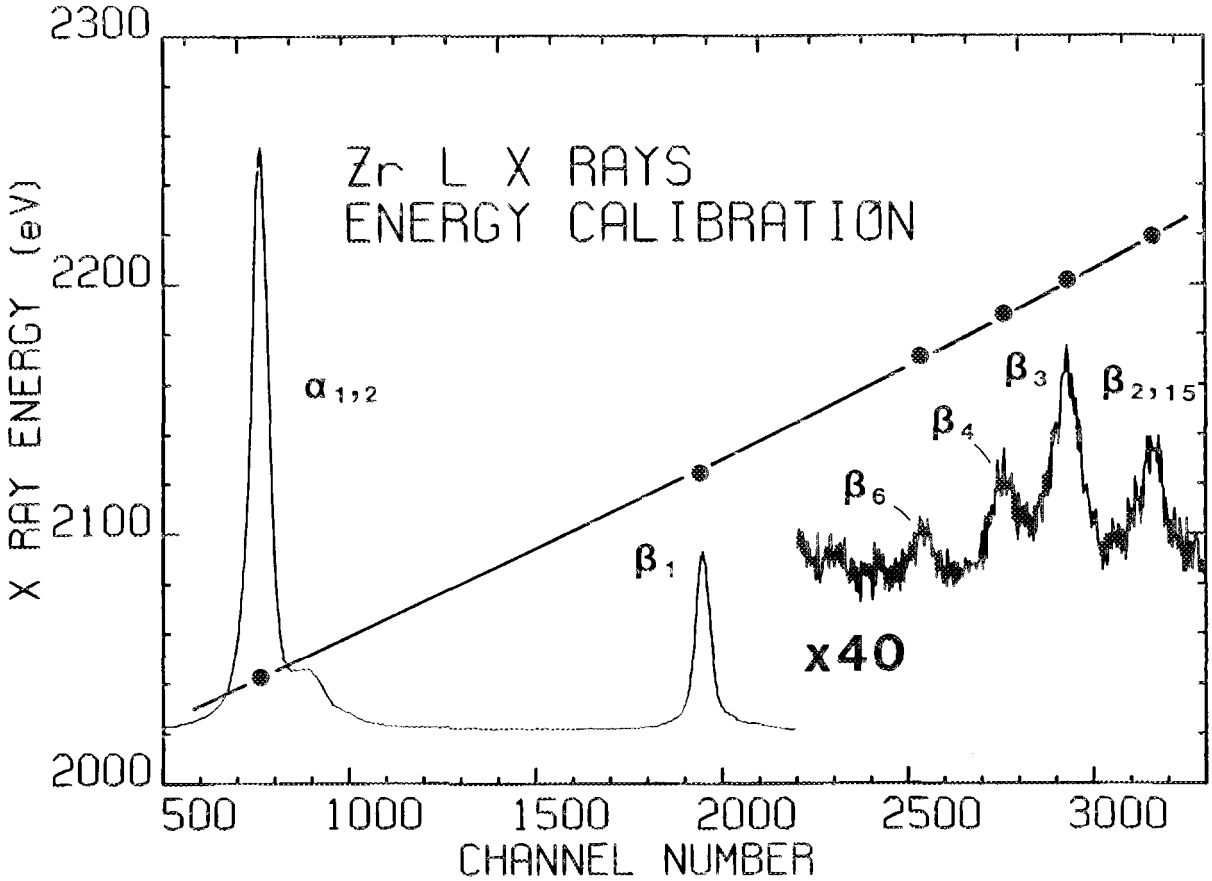

Fig. 22. Detected position versus x-ray energy in the 2.3 to 2.5 keV energy region using a quartz $(10\bar{1}1)$, 2d = 6.687Å crystal with radius of 25.4 cm. Points are 4 keV electron-excited zirconium $L_{\alpha,\beta}$ x-ray line positions measured from the displayed spectrum. The solid curve connecting the points is given by eq. 21 as explained in the text using $L_{\alpha_{1,2}}$ and L_{β_1} as calibration points.

The total energy resolution within a bandwidth varies with energy because of two effects. It was shown in Sect. II.B.2 that imaging distortions maximize for x-rays detected far from the central Bragg angle θ_{BC}. These distortions result in increased linewidth broadening by about 10% of the width for optimum resolution. Additionally, spatial broadening occurs for these off-normal rays due to conversion of x-rays at various depths within the working gas of the detector. To study this effect directly, a narrow line (Molybdenum $L_{\beta 1}$) excited by electron impact was located at the center of the detector and observed as a function of detector

orientation. The measured full-width-half-maximum is plotted in fig. 23 versus the angle of incidence. As shown there, deviations from 90° greater than about five degrees produce significant line broadening. Therefore, for optimized resolution the total opening angle must be limited to ~ ± 5°. At $\theta_{BC} \approx 51°$ the angular acceptance width of the 10 cm long detector is less than ± 5° as shown in fig. 23. However, at $\theta_{BC} = 70°$ the detector acceptance maximizes at ± 5.3° and there is noticeable (15%) resolution broadening at the ends of the detected bandwidth. These measurements were made with P10 detecting gas at 1 atmosphere

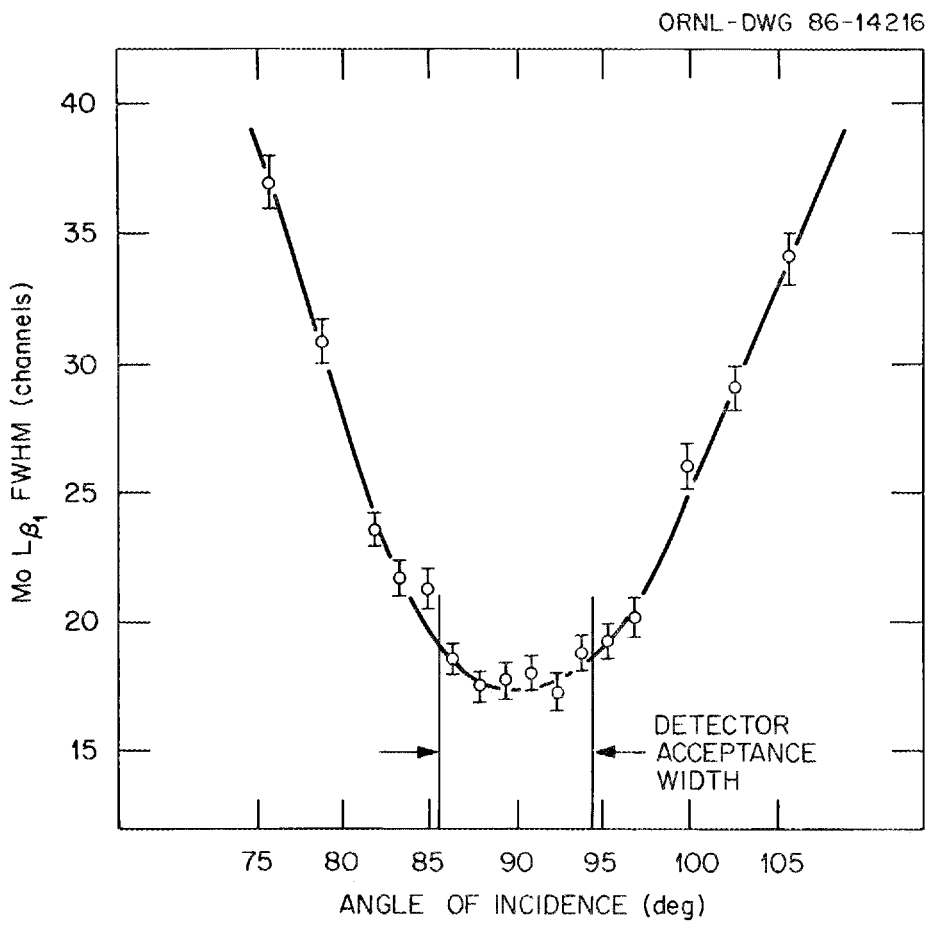

Fig. 23. Measured line width of electron-excited molybdenum L_{β_1} plotted versus detector orientation with respect to detected x-rays. When the detector is centered on the L_{β_1} line and oriented perpendicular to the incoming x-rays, it has the angular acceptance shown. Crystal used was quartz $(10\bar{1}1)$ and $\theta_{BC} = 51°$.

pressure. Higher pressures and/or heavier detection gases allow larger angles and therefore wider bandwidths. For example, Xe at 1 atmosphere should permit angles deviating from normal incidence that are ~ 5 times larger for 2.5 keV x-rays.

In practice total energy resolution depends on a variety of factors. An example is given below for Al $K\alpha_{1,2}$ x-rays at 1.49 keV excited by 5 keV electrons. The crystal used was ADP(101), 2d = 10.648Å with a 25.4 cm radius of curvature. Contributions to resolution loss include:

(a) finite source width ($w_S \simeq 250$ μm) and imaging distortion (F>1) effects

$$\delta E_S \simeq \frac{E\cos\Theta_B}{2\rho} w_S F_{fwhm} = 0.46 F_{fwhm} \text{ eV} .$$

(b) finite detector spatial resolution ($\Delta X_D \sim 150$μm)

$$\delta E_D \simeq \frac{E\cos\Theta_B}{2\rho} \Delta X_D = 0.27 \text{ eV} .$$

(c) Crystal resolving power ($R_C \sim 8000$)

$$\delta E_C \simeq (E/R_C) = 0.19 \text{ eV} .$$

(d) Natural (Lorentizian shaped) atomic line widths (0.43 eV) and $K\alpha_1,\alpha_2$ separation (0.43 eV) $\delta E_A \simeq 0.75$ eV .

One of the most distinctive features of this instrument is its high collection efficiency. While the "speed" of a crystal spectrometer can be expressed in several different ways, for estimates of count rates in a single line, the total efficiency for detection of x-rays within a resolution width is probably most useful. This can be defined as the ratio of the number of x-rays detected within a resolution width (I_d) to the total number emitted (I_{tot}). Assuming isotropic emission this ratio is given by

$$I_d/I_{tot} = R_{av}(\Delta\Omega/4\pi)D_{eff} . \qquad (25)$$

In eq. (25), R_{av} is the crystal reflectivity averaged over the crystal rocking angle, $\Delta\Omega$ is the product of the crystal height (in radians from the source) and the opening angle corresponding to the angular total system resolution which can be approximated as

$$\Delta\Omega = \frac{h_c \sin\theta}{\rho} \cdot \frac{w_s + w_d}{2\rho} \sin\Theta \tag{26}$$

Here, w_s is the width of the source and w_d is the detector spatial resolution width. In our instrument, the crystal rocking angle ω_c is usually insignificant. D_{eff} is the detector efficiency including window absorption. For a 10 cm high quartz($10\bar{1}1$) crystal, 250 μm wide source, 150 μm detector resolution, and at 2.3 keV, where the detection efficiency is estimated to be 35%, the calculated efficiency per resolution width is about 2×10^{-6}. The 10 cm long PSPC simultaneously intercepts over 300 resolution widths.

The spectrometer efficiency can vary significantly (even within a bandwidth) if the crystal reflectivity or detector efficiency changes with position due to imperfections. With our instrument, the portions of the crystal and detector being used to detect a particular energy x-ray can be varied in a controlled way, so that the relative instrumental efficiency as a function of x-ray energy can be measured directly as described in the next section.

III. B. Special Operational Considerations

III.B.1. Corrections for Crystal and Detector Efficiency Variations.

There are several subtle effects in the operation of a von Hamos geometry spectrometer which can significantly affect the acquired spectra. As with all wavelength dispersive instruments, spectral data must be interpreted cautiously in regions near strong reflectivity changes, e.g., near absorption edges especially those of the elements composing the crystal. In practice, care is taken to avoid known regions of rapid reflectivity variation, and data are corrected

by dividing the raw spectra by measured or calculated crystal integrated reflectivity as a function of Bragg angle. Detector efficiency may also vary substantially with energy near absorption edges. As an example, calculated detection efficiency as a function of x-ray energy is shown in fig. 24a for a 1 cm deep PSPC using P10 gas at 1, 2, and 3 atmospheres pressure. The window is 0.5 mil mylar. The drastic jump in efficiency is due to the Ar K edge at 3.203 keV. A similar plot for 90% Xe, 10% CH_4 is shown in fig. 24b.

In the position-sensitive von Hamos geometry, different x-ray energies are diffracted and focused at different points along the crystal and detected at different points along the PSPC axis. Localized anomalies in either the crystal or detector can therefore have severe effects on the observed data. Variations in crystal reflectivity along its length result in distortions in measured spectral intensity. Variations in detector counting efficiency along its active length result in intensity distortions as well. Focusing effects can also produce a modulation in the collected x-ray fraction as a function of Bragg angle and hence energy. Both spectral position and intensity can be distorted by these effects.

An important consequence of crystal and/or detector variations is the strong effect that source position instability can have on spectral data variations. One might expect a shift in source position to lead to a simple shift in spectral position without intensity distortion. However, since the position of the x-ray source determines which specific portions of the crystal and detector will be used in diffracting, focusing, and detecting the x-rays, small changes in the source position can have significant impact on the measured spectral intensity profiles when the crystal or detector have strong localized imperfections.

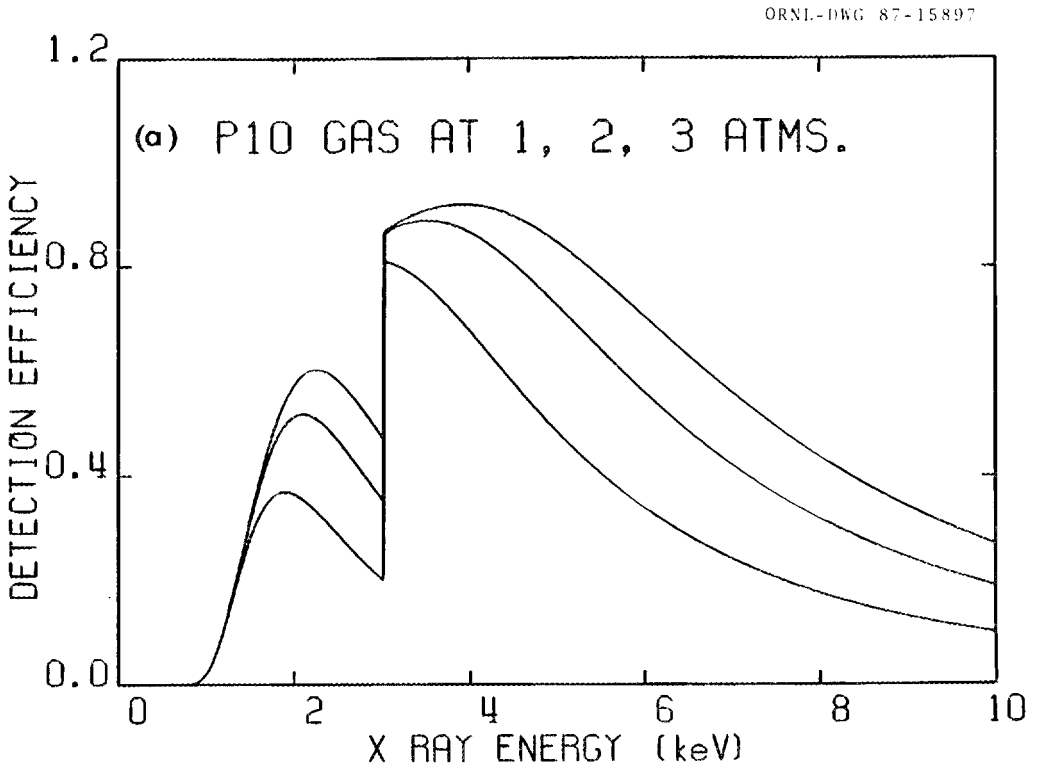

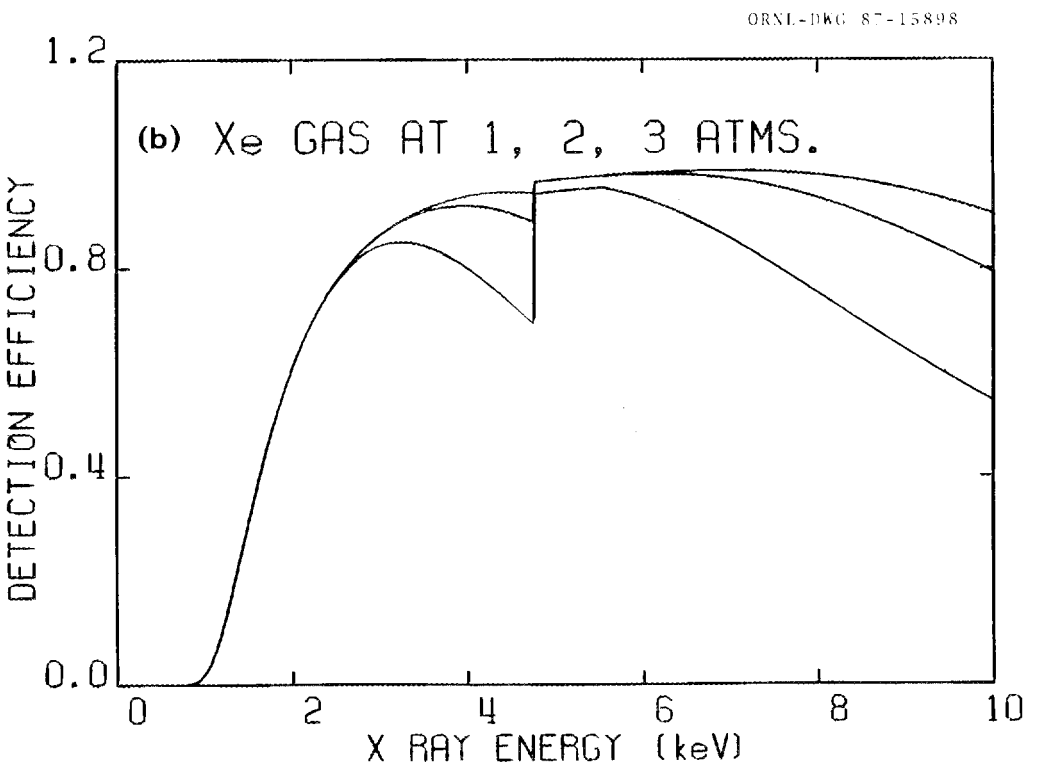

Fig. 24. Calculated detection efficiency including window absorption for (a) P10 (90% Ar, 10% CH_4) and (b) 90% Xe + 10% CH_4 gases at 1, 2, and 3 atmospheres pressure. The window is 1/2 mil Mylar. The efficiency increases with gas pressure.

To characterize the distorting properties of defects in the crystal and detector, we have studied their independent effects on a narrow x-ray line as a function of position in the wavelength dispersing plane. The characterization procedure for the detector is straightforward. Using an x-ray peak such as Al $K_{\alpha_{1,2}}$ produced by electron impact on a metallic target as the source, the detector is scanned uniformly along its mounting track, i.e., along the axis of the fixed, curved crystal. X-rays are counted in equal time intervals as the detector is translated. A spectrum of x-ray counts versus detector position is obtained which depicts the relative efficiency for collecting this energy x-ray as a function of detected position (which can be used for subsequent correction of data). Figure 25 displays Al $K_{\alpha_{1,2}}$ x-ray PSPC counts versus detected position.

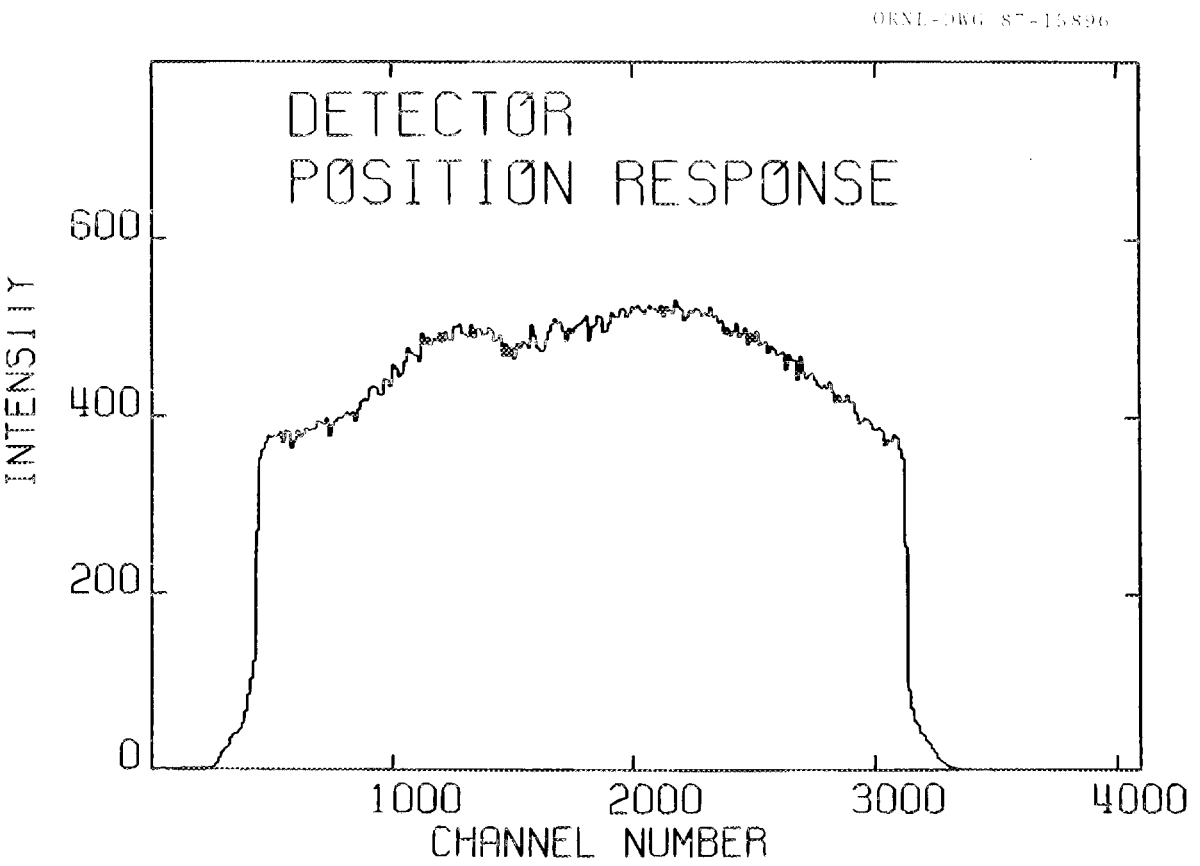

Fig. 25. Measured Al $K_{\alpha_{1,2}}$ count rate versus detector position for 5 keV electrons on aluminum metal. Crystal used was ADP(101), 2d = 10.648Å.

Characterization of the crystal proceeds in the same general fashion. A narrow line or peak is set to be counted near the center of the detector. Electronic upper- and lower-level discriminators are set at the FWHM points on the detected peak. The crystal is then uniformly scanned along its mounting track, i.e., parallel to its cylindrical axis, and x-rays are stored in multi-channel-scaling mode as the crystal is translated. The resulting curve contains effects of both changing collection/focusing efficiency along the crystal and distortion along the crystal straight edge direction which results in translation of the diffracted x-ray peak on the detector. A second crystal translation scan is taken in exactly the same manner except with much wider discriminator settings. These data exhibit only the focusing and gross reflectivity variations along the crystal axis. Differences in these two curves represent the non-planar distortions in the crystal which result in energy-dependent line shifting and therefore limit the confidence with which measured energies can be made. Figures 26 and 27 show characterization data collected for three typical commercial crystals, two ADP (one of good and one of poor quality) and one quartz crystal.

III.B.2. Doppler Effects for x-rays Emitted from Fast Projectiles.

Intensities and energies of x-rays arising from few-electron heavy ions are of fundamental interest. Preparation of these ions normally involves acceleration to high energies and subsequent stripping in thin targets to achieve the required high charge states. Observation in the laboratory of x-rays emitted from the moving ions results in unavoidable Doppler shifting and broadening. Measurements are often made on x-rays emitted in a direction normal to the beam velocity to minimize the shifts. The spectrometer described here sacrifices absolute energy determination somewhat but achieves low Doppler broadening and high efficiency by collecting projectile x-rays with large but nearly constant Doppler shifts. The geometric relationship between the Doppler and Bragg angles (θ_D and θ_B) in the lab frame is shown in fig. 28. When the cylindrical crystal

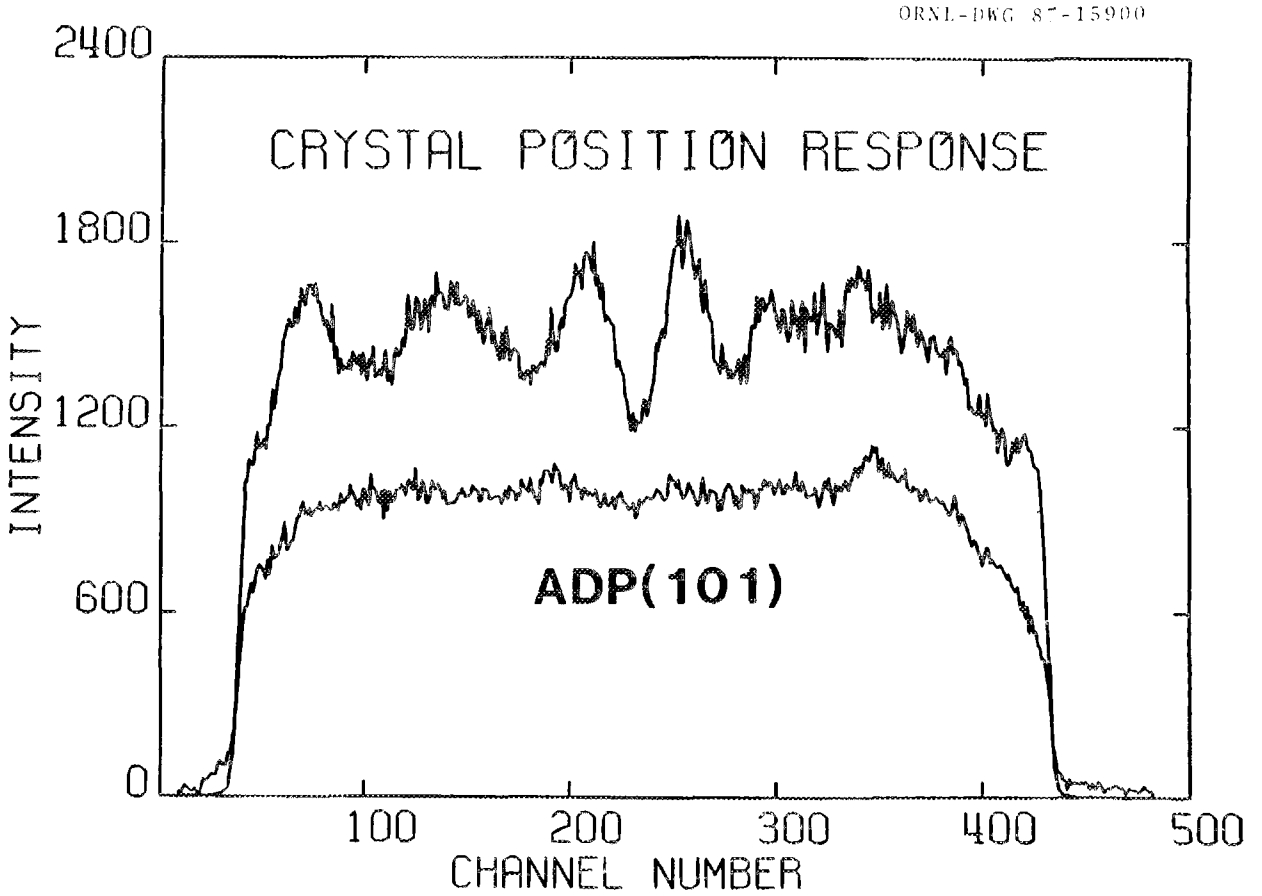

Fig. 26. Measured ADP(101) crystal relative efficiency versus position for electron-excited aluminum K_α x-rays. Data for two crystals from the same manufacturer are shown. The crystal characterized by the upper curve showed signs of separating from its mounting block.

axis is oriented exactly normal to the ion beam velocity vector $\vec{\beta}c$ (c is the velocity of light),

$$\cos \theta_D = \sin \theta_B \cos \psi \ . \tag{27}$$

The relativistic Doppler relation[12] between projectile and laboratory frame x-ray energies (E_P and E_L, respectively) can be expressed as

$$E_L = E_P/[\gamma\ (1 - \beta \cos \theta_D)] \ , \tag{28}$$

ORNL-DWG 87-15888

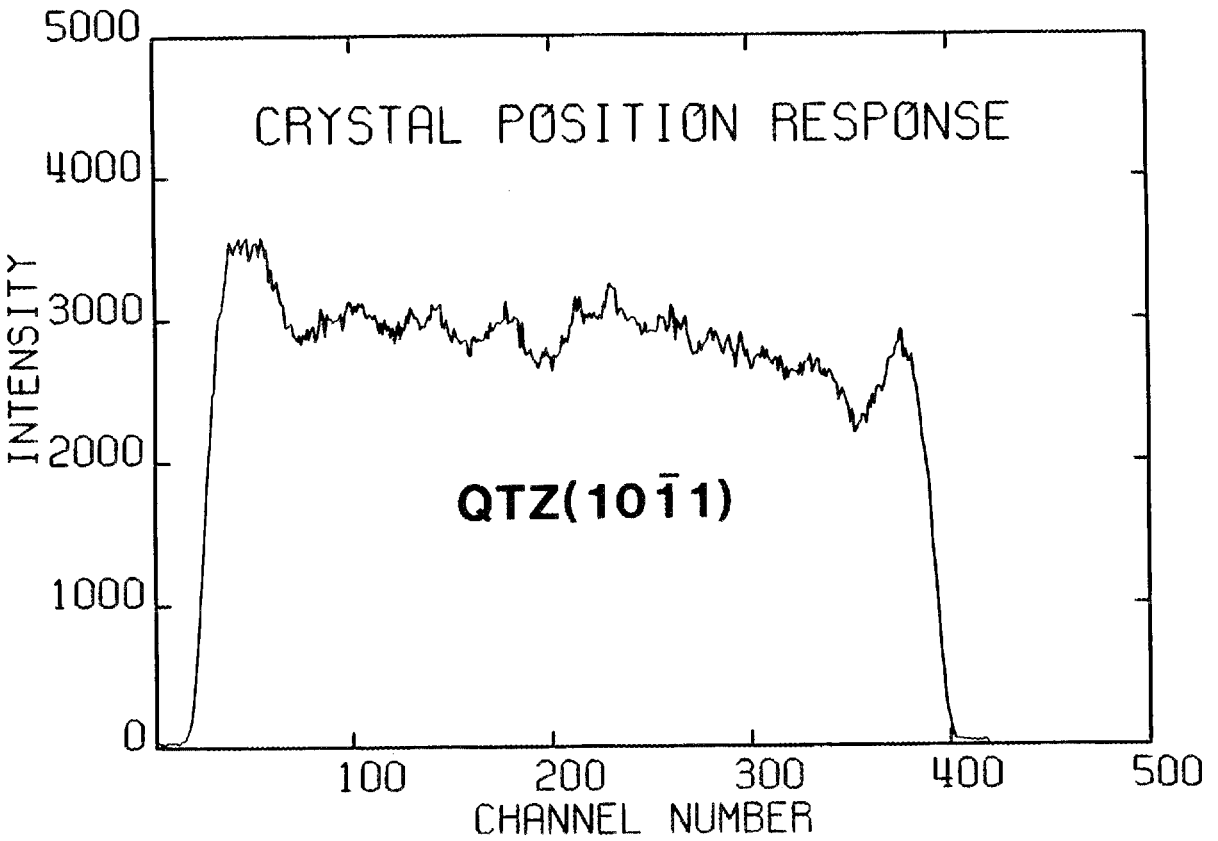

Fig. 27. Measured quartz (10$\bar{1}$1) crystal relative efficiency versus position for electron-excited molybdenum L_α x-rays.

where $\gamma = 1/\sqrt{1-\beta^2}$. When combined with eqs. (27) and (1) (the Bragg relation), the lab frame x-ray energy is given by

$$E_L = (E_P/\gamma) \pm C_B\, \beta \cos \psi \; ; \quad C_B \equiv 12.398/2d(\text{Å}) \; . \tag{29}$$

The sign of the second term depends on the direction of $\vec{\beta}$, being negative for the case shown in fig. 28 where $\vec{\beta}$ is directed away from the crystal. For a 10 cm high crystal ψ varies from 0° at the center to ψ_{max} = 11° at the crystal edge. This leads to a broadening and shifting of line energies such that the Doppler induced width δE_D and centroid energy $\langle E_L \rangle$ observed in the lab frame are given by

$$\delta E_D = C_B\, \beta\, (1 - \cos \psi_{max}) \; , \tag{30}$$

and $$\langle E_L \rangle = (E_P/\gamma) \pm [C_B\, \beta (1 - \cos \psi_{max})/2] \; . \tag{31}$$

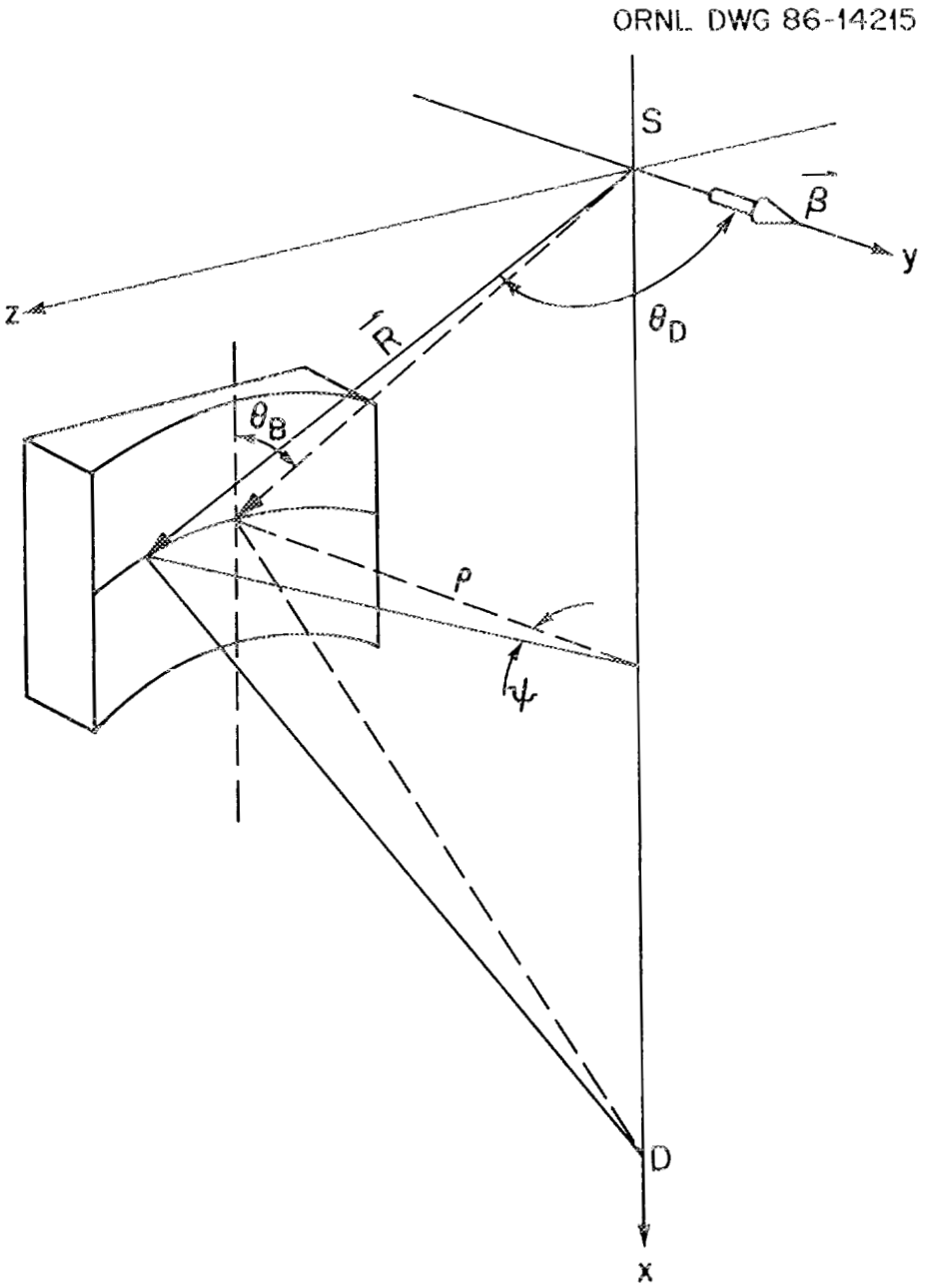

Fig. 28. Schematic showing geometric relationship between the laboratory frame Doppler angle θ_D and the Bragg angle θ_B. The velocity vector of the projectile is β. The angle ψ varies from 0° (at the crystal center) to $\pm\psi_{max}$ = 11.3° for a 10 cm high crystal of radius 25.4 cm.

The measured energy and resolution are only weakly dependent on ψ_{max} and the broadening is therefore relatively small even for large area (i.e., fast) crystals. As an example, a spectrum of silicon X-rays emitted from 2.6 MeV/u Si ions passing through a 5 $\mu g/cm^2$ carbon foil is shown in fig. 29. Silicon Lyman α_1 and α_2 separated by 1.8 eV are clearly resolved (see expanded fig. 30). Several lines from doubly-excited He-like Si are also identified there according to tabulated energies.[13] By limiting the crystal height to 7 cm (ψ_{max} = 7.8°), the overall energy resolution including Doppler broadening (~ 1 eV) has been held to < 1.5 eV at 2.14 keV while the high efficiency of the system has been retained. If the same height crystal were oriented in a configuration to collect X-rays emitted about a normal to the beam, the resulting Doppler spread would amount to > 40 eV.

III. C. Sample Data

Our principle goal in development of this spectrometer was to produce an instrument with sufficient resolution and bandwidth to permit us to efficiently measure chemically dependent spectral variations in heavy-ion induced satellite x-rays. In this section we present data exemplifying the utility of this spectrometer in studying these chemical effects, as well as in a variety of other areas. Descriptions of the data displayed (see Figs. 29-38) along with the relevant spectrometer operating conditions are given in the corresponding figure captions.

ORNL DWG 86-17793

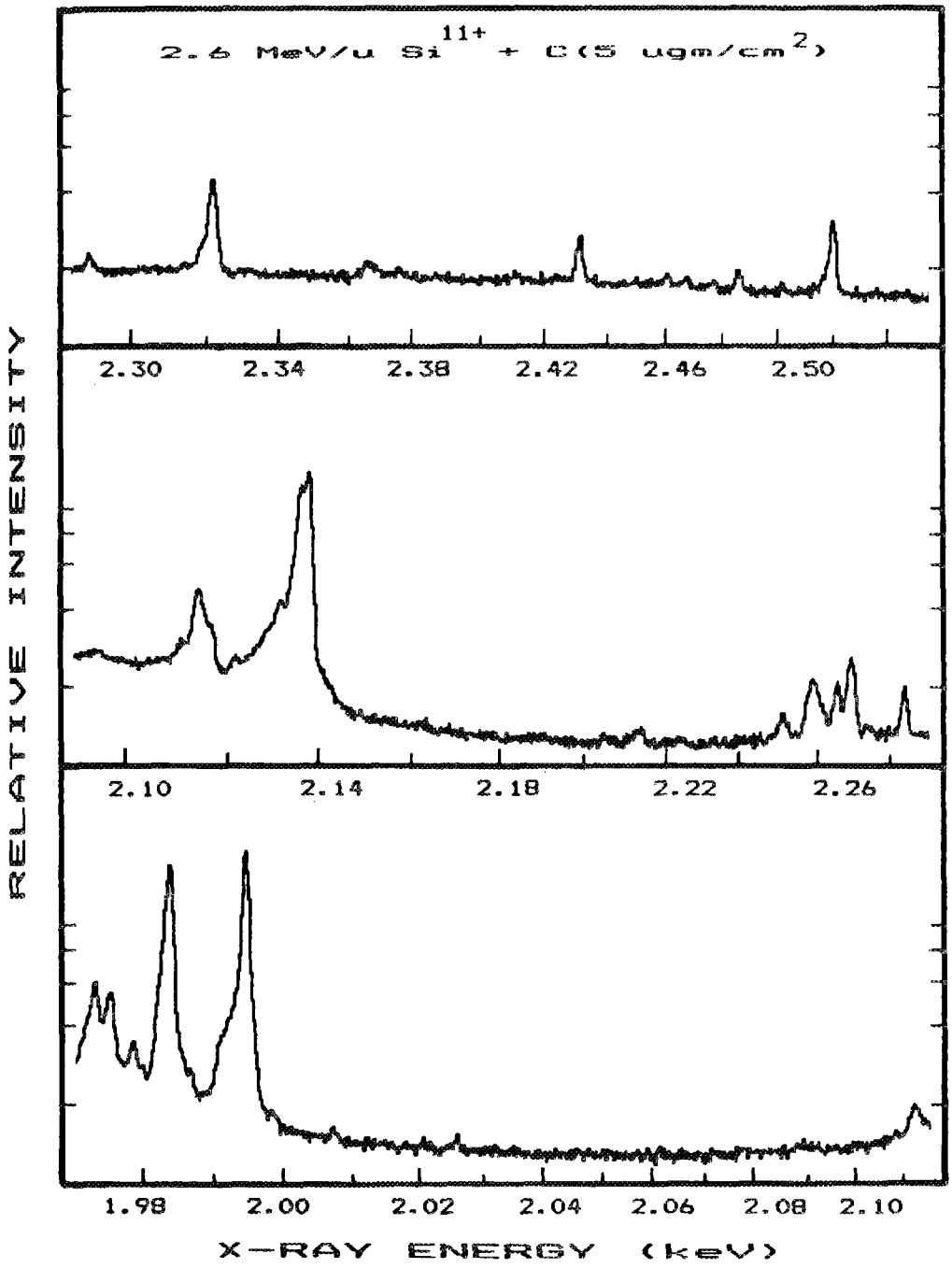

Fig. 29. X-ray spectra from 2.6 MeV/u Si^{q+} ions excited in passing through a 5μg/cm^2 thick carbon foil. A quartz $(10\bar{1}1)$ crystal was used with the spectrometer mounted such that the Si projectiles moved toward the crystal, i.e., + sign in eqs. (29) and (31). The outer 2.5 cm on each side of the crystal was masked so that ψ_{max} was limited to ±7.8°. Energy scale shown is for the laboratory frame.

ORNL DGW 86-17794

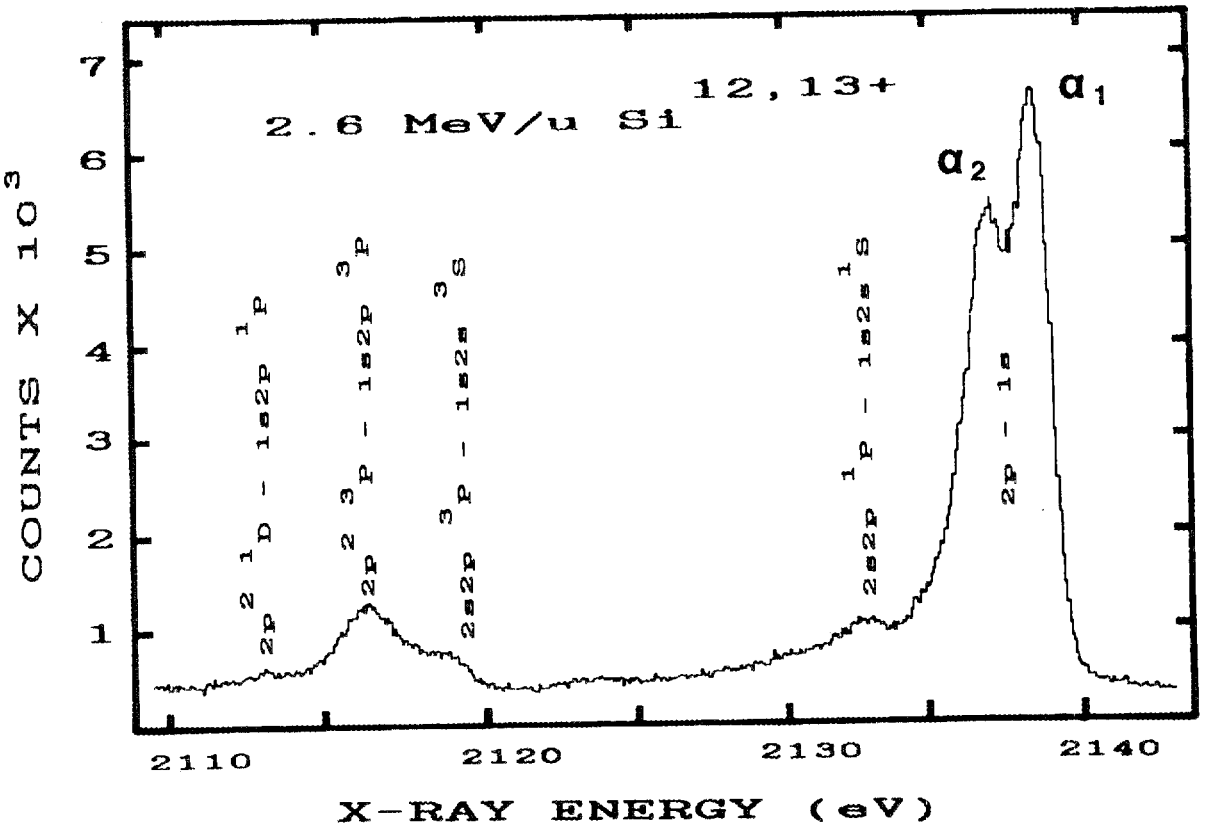

Fig. 30. Expanded 2.11 to 2.14 keV portion of fig. 29. Labeled transitions are from hydrogen-like and helium-like $Si^{12,13+}$ ions generated in the carbon foil.

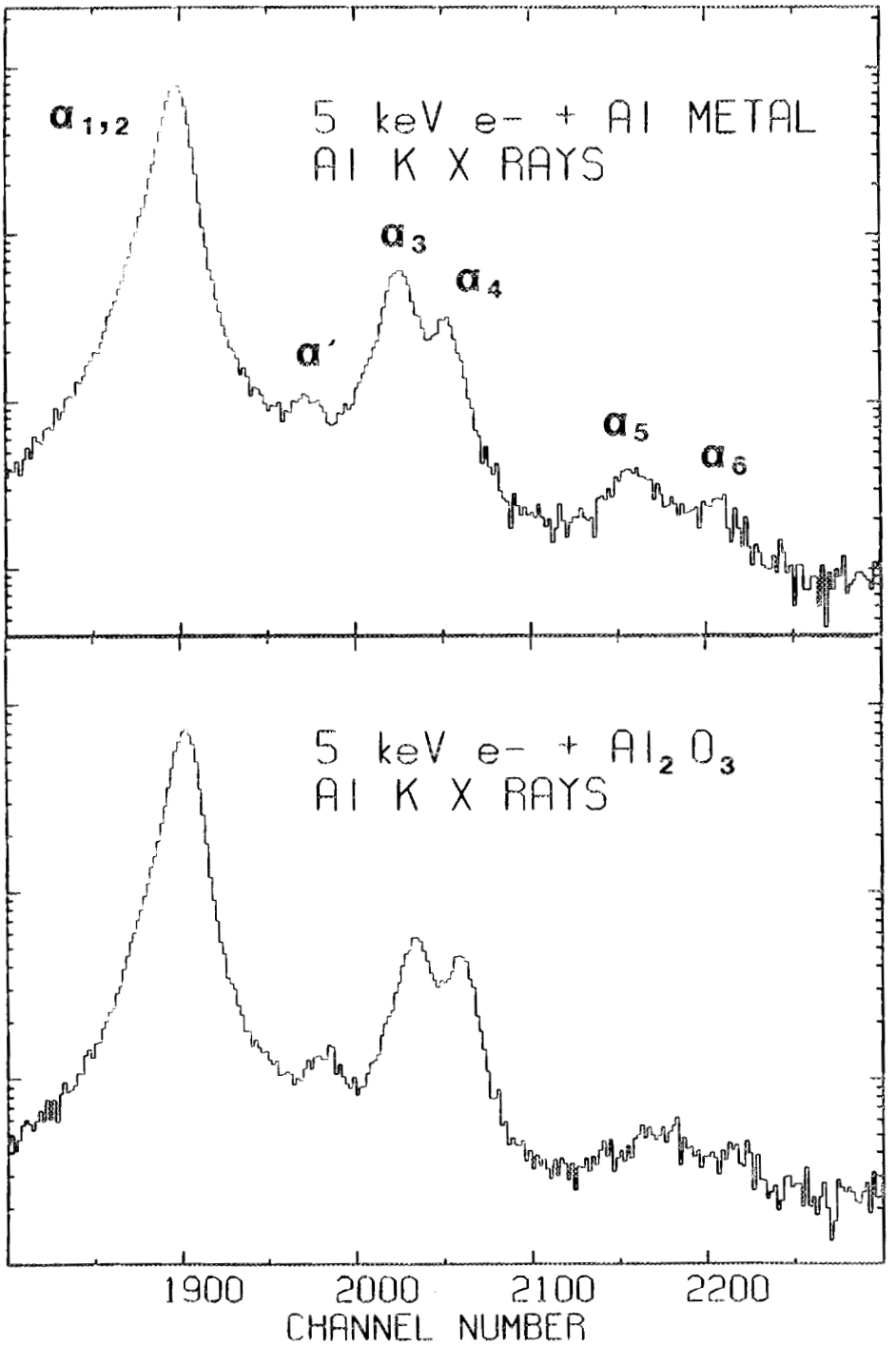

Fig. 31. Comparison of Aluminum K X rays generated by 5 keV e^- impact for aluminum metal and aluminum oxide targets. Note the difference in the relative intensity of the α_3 line with respect to α_4. The instrumental energy resolution here is 0.8 eV as determined from convolution of known α_1 and α_2 line widths and intensities with an assumed Gaussian instrument function of variable width. The times required to accumulate these spectra were 500 and 1000 seconds, respectively. The crystal used was ADP(101) in first order.

ORNL-DWG 87-15886

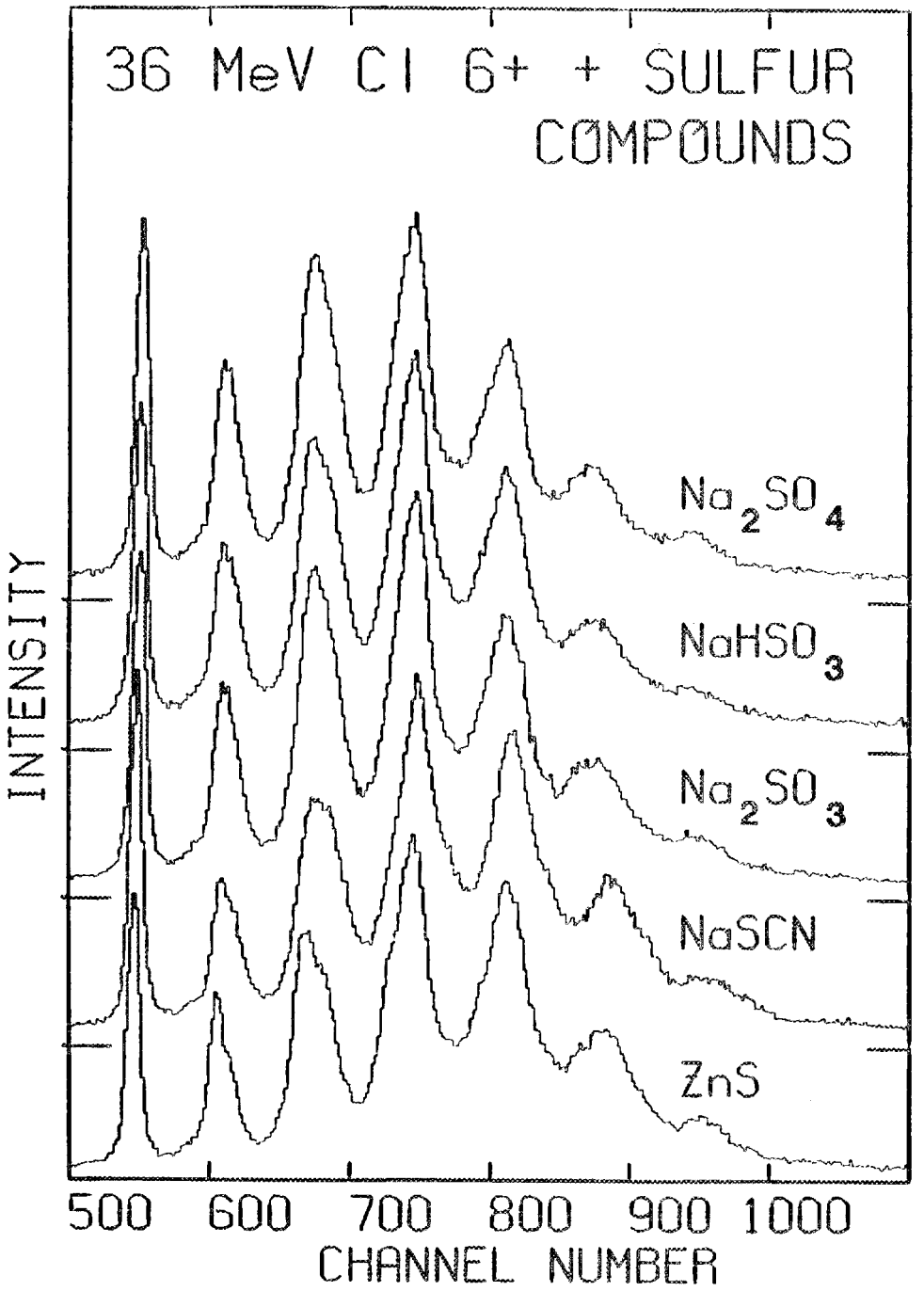

Fig. 32. Sulfur K x-ray spectra generated by 36 MeV Cl^{6+} ions incident on five different sulfur compounds. These data were acquired in about 1 hour per spectrum using 80 nA_e incident ion current. The crystal used was quartz($10\bar{1}1$) in first order. Vertical scales are zero-offset and linear.

ORNL-DWG 87-15890

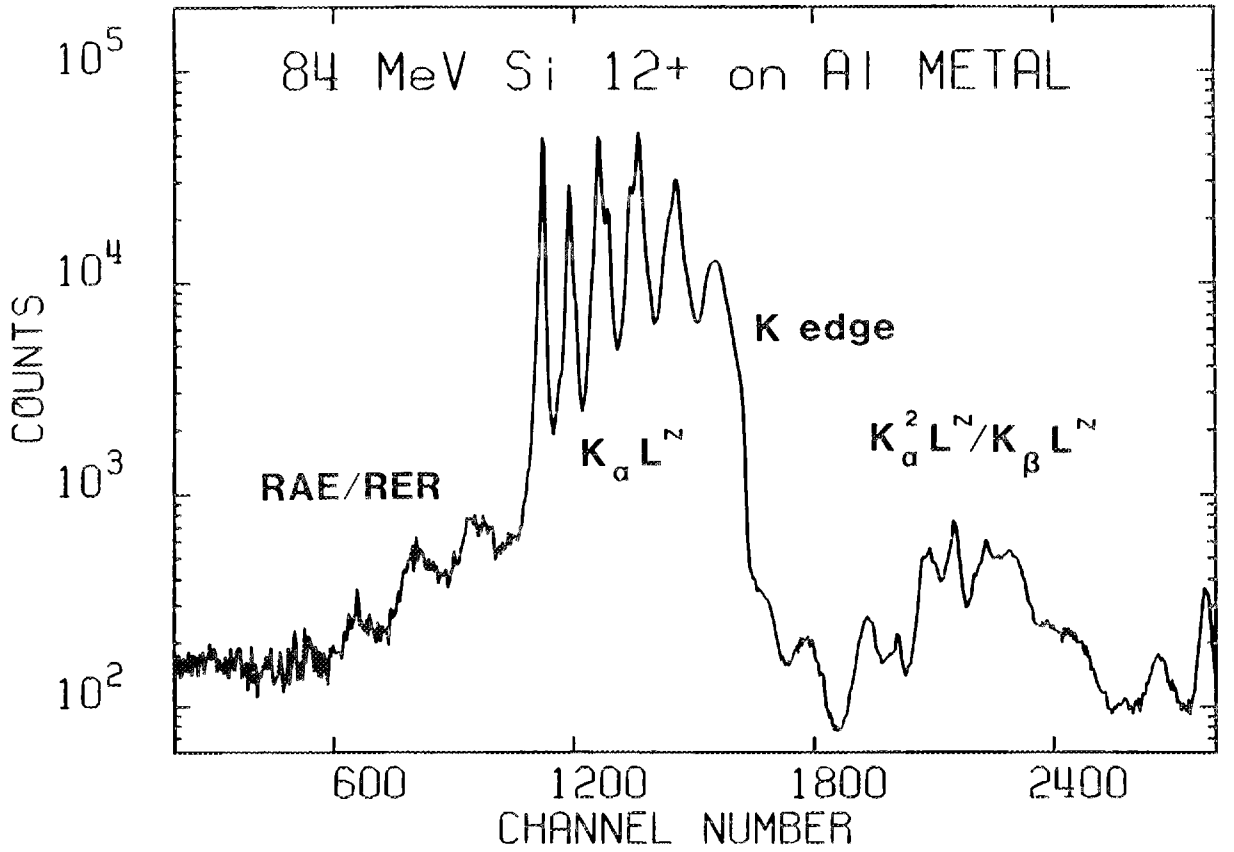

Fig. 33. Aluminum K X rays excited by 84 MeV Si^{12+} ions illustrating the importance of broad bandwidth for study of heavy ion generated X rays. The displayed spectrum extends from 1380 eV to 1750 eV and includes: low energy structures (labeled RAE/RER), $K_\alpha L^n$ satellites, the K absorption edge, $K_\alpha{}^2L^n$ hypersatellites, and $K_\beta L^n$ satellites. This spectrum was made by joining two separate spectra at the Al K edge. Ion current was 20 nA_e and total time required to accumulate the data was 2000 sec. Crystal used was ADP(101) in first order.

ORNL-DWG 87-15902

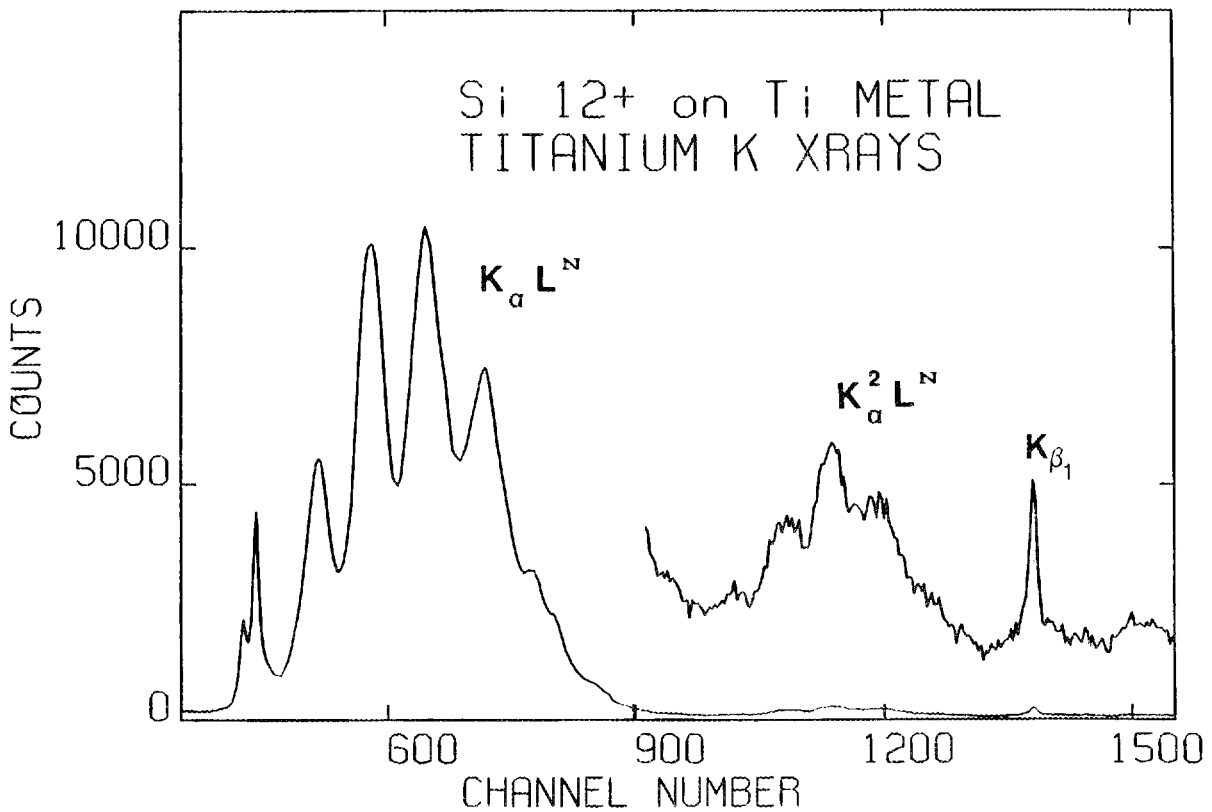

Fig. 34. Higher energies can be reached using diffraction orders greater than one. Crystal reflectivity is reduced, but for relatively intense emission the present instrument's good collection efficiency allows measurement in reasonable times. Displayed here are titanium K satellite and hypersatellite X rays generated by 84 MeV Si^{12+} ions on a thick titanium metal target. Ion current was 25 nA_e and the time required to accumulate spectrum was 2400 sec. Crystal used was quartz($10\bar{1}1$) in second order.

ORNL-DWG 87-15899

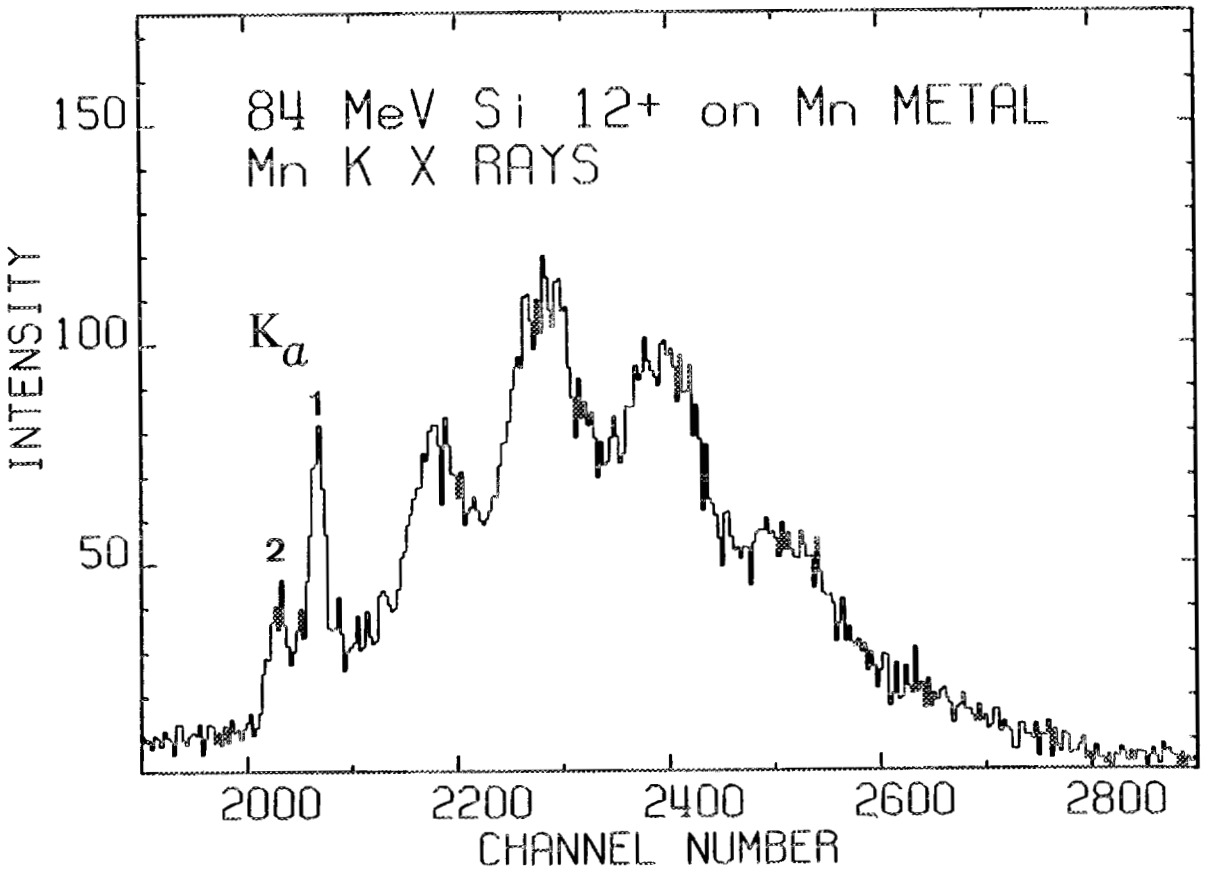

Fig. 35. Even higher energies may be reached using increased diffraction orders. Shown here are manganese $K_\alpha L^n$ X rays generated by 84 MeV Si^{12+} ions on a thick manganese metal target. The characteristic lines α_1 and α_2 occur at 5.9 keV. Ion current was 8 nA_e and time required to accumulate this spectrum was 800 sec. Crystal used was ADP(101) in fourth order.

ORNL-DWG 87-15892

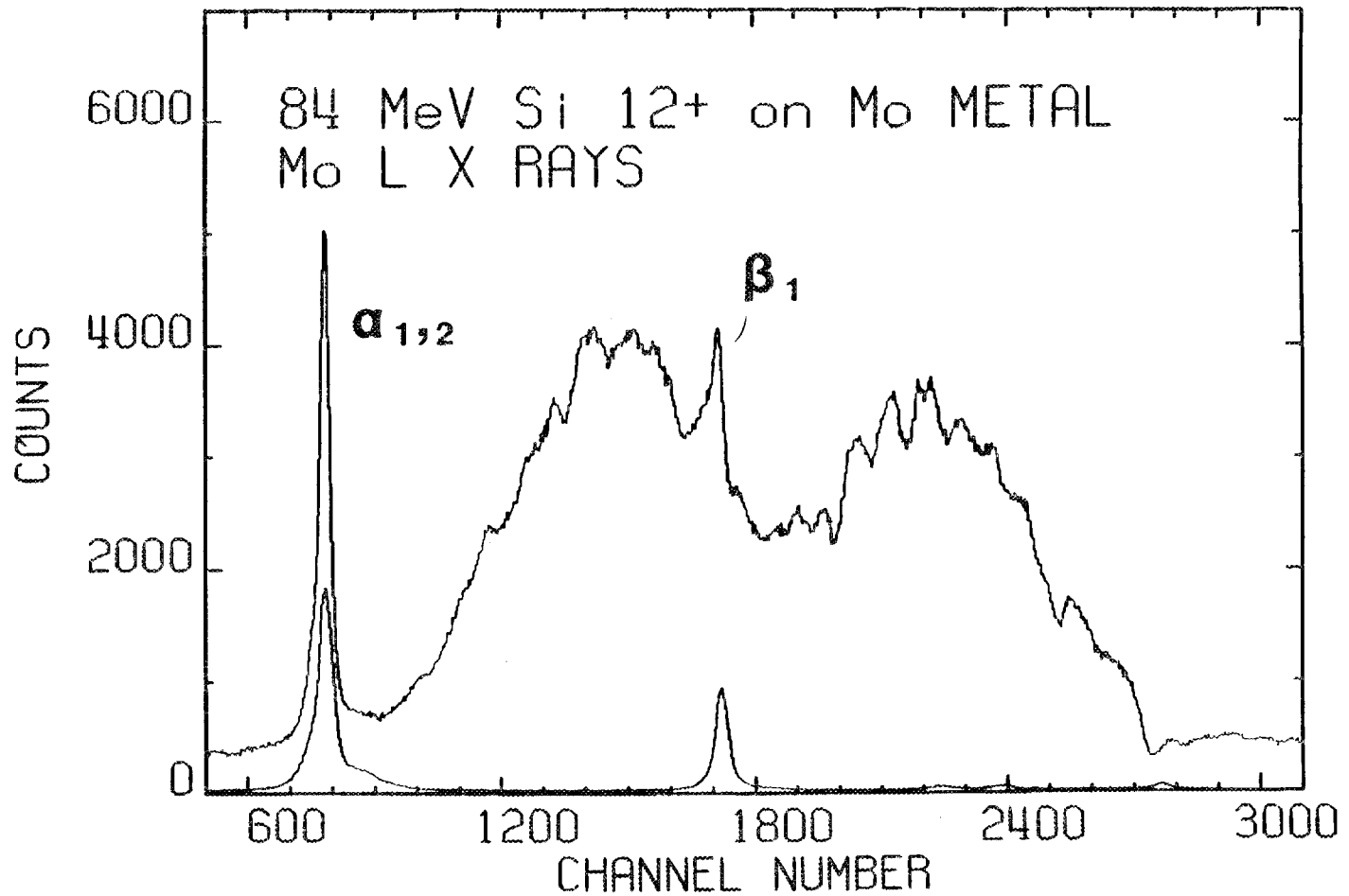

Fig. 36. Molybdenum L satellite spectrum from a molybdenum-titanium alloy excited by 84 MeV Si^{12+} ions. The time required for acquisition of this data using 20 nA_e of Si^{12+} ions on a thick target was about 2800 seconds. The crystal used was quartz($10\bar{1}1$) in first order. The bottom spectrum is Mo L X rays generated by 5 keV e^- impact. It was used for energy calibration.

ORNL-DWG 87-15894

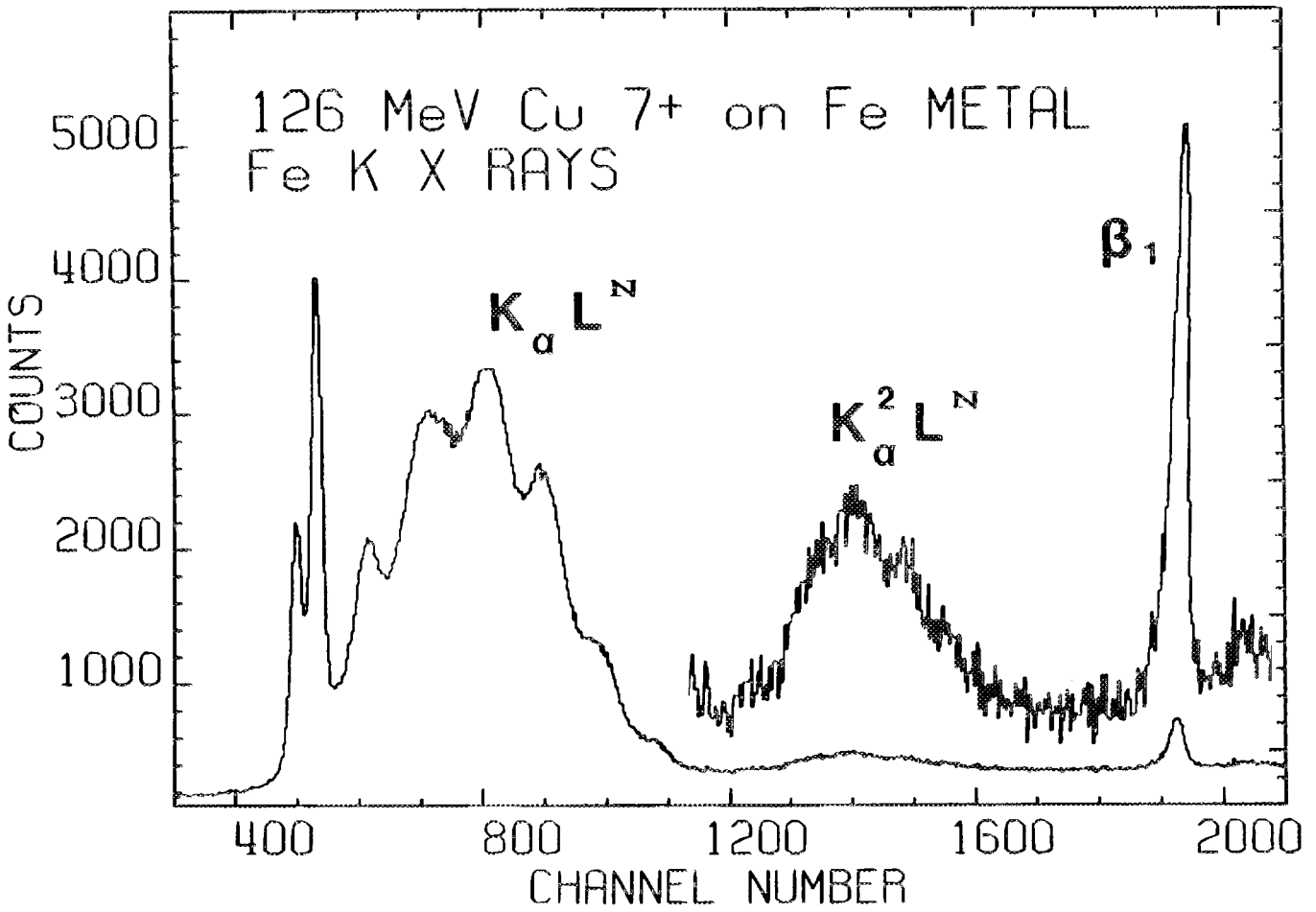

Fig. 37. Flat crystals can also be used, but at a great cost in efficiency. The time required to acquire data for weak spectral features becomes excessive. Displayed here are iron $K_\alpha L^n$, $K_\alpha{}^2 L^n$, and K_{β_1} X rays generated by 126 MeV Cu^{7+} ions on a thick iron target. Ion current was 120 nA_e and the time required to accumulate this spectrum was 24,000 sec. Crystal used was a flat Si(100) in fourth order.

ORNL-DWG 87-15893

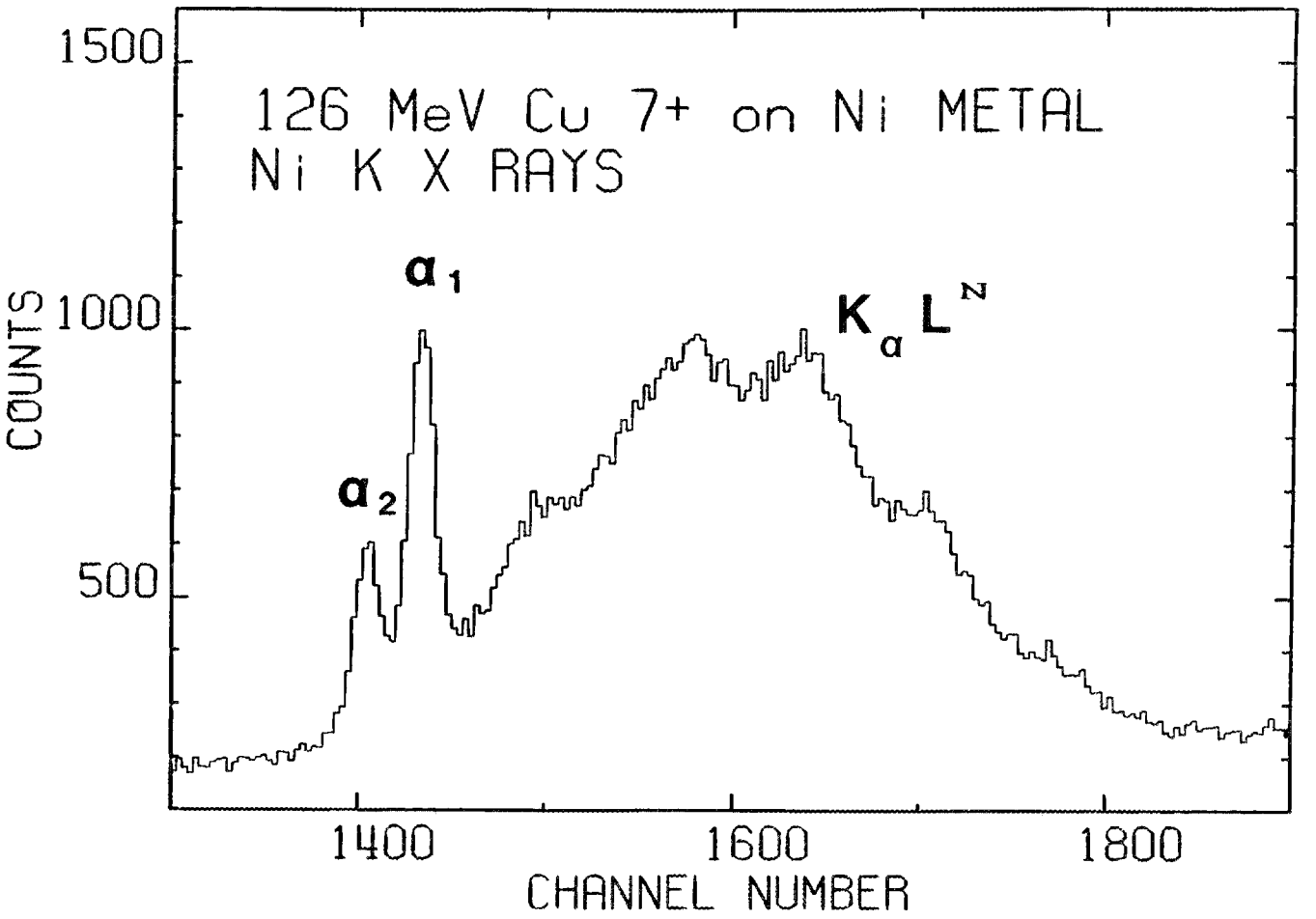

Fig. 38. The highest energy X rays studied to date with this instrument are at 7.5 keV. Displayed here are nickel $K_\alpha L^n$ X rays generated by 126 MeV Cu^{7+} ions on a thick nickel target. The K α_1 and α_2 occur at 7.460 and 7.477 keV, respectively. Ion current was 200 nA_e and the time required to accumulate this spectrum was 2400 sec. Crystal used was a flat Si(100) in fourth order.

IV. ACKNOWLEDGMENTS

Several people have been instrumental in the development of the spectrometer described here. In particular, we wish to acknowledge the invaluable assistance of E. Källne and J. Källne who were a great help in lending their narrow-band von Hamos instrument and in aiding us in testing it in an accelerator environment on the ORNL EN tandem Van de Graaff prior to the design of our new spectrometer. We also wish to thank B. Yaakobi of the University of Rochester for providing a copy of his ray-tracing program and for assistance in the initial design of the instrument. Finally, we wish to thank G. E. Ice and C. J. Sparks, Jr., of ORNL for reading this report and making critical comments.

V. REFERENCES

1. S. Raman et al., Nucl. Inst. Meth. B3, 71-103 (1984).
2. M. Gouy, Ann. Physique 5, 241 (1916).
3. L. v. Hámos, Ann. der Physik 17, 716 (1933); Z. Kristallogr. 101, 17 (1939); and Arkiv Mat. Astr. Fys. 31A, 1 (1945).
4. C. B. Van den Berg and H. Brinkman, Physica 21, 85 (1955).
5. B. Yaakobi and V. A. Bhagavatula, "Von Hamos Type Focusing X-ray Spectrograph," Report No. 89, Laboratory for Laser Energetics, Univ. of Rochester, 1979.
6. B. Yaakobi, H. W. Schnopper, R. E. Turner, and P. O. Taylor, Rev. Sci. Inst. 50, 12 (1979).
7. H. H. Johann, Z. Phys. 69, 185 (1931).
8. T. Johannson, Z. Phys. 82, 507 (1935).
9. P. O. Taylor and H. Schnopper, Progress Reports DOE COO-4021, 4022, 4023. (1977, 78, 79); E. Källne and J. Källne, Physica Scripta T3, 185 (1983).
10. R. Kappler, Kappler Crystal Optics, Inc. Holliston, MA, and W. Ruderman, Interactive Radiation, Inc. Northvale, NJ, private communication.
11. C. J. Borkowski and M. K. Kopp, J. Appl. Cryst. 11, 430 (1978).
12. J. D. Jackson, Classical Electrodynamics (John Wiley, New York, 1962), eq. 11.37.
13. J. F. Seeley, Atomic Data and Nucl. Data Tables 26, 137 (1981).
14. G. E. Ice, private communication.

Appendix A. Calculation of Images in Geometry 1

Figure 3 shows the point source $S = (0, y_S, z_S)$, the point of incidence $R = (x_R, y_R, z_R)$, and the coordinate axes. The reflected ray from R to P lies in the plane defined by S, R, and O' since the ray RO' is normal to the crystal at R (fig. 4a). Define A to be the projection of S into the plane $x = x_R$, and B to be the projection of A onto the line RO'; these points have coordinates

$$A = (x_R, y_S, z_S) ,$$

$$\text{and} \qquad B = (x_R, y_B, z_B) . \tag{A1}$$

Since SA is parallel to the x-axis, the plane SAB is normal to the plane $x = x_R$; hence SA is normal to AB, SB is normal to BR, and AB is normal to BR (fig. 4a). Construct RR' in the plane SRO' so that SB is parallel to RR' and R' lines in the x = 0 plane, and define $S' = (x_{S'}, y_{S'}, z_{S'})$ as the intersection of RP with the plane x = 0. The procedure is to find the coordinates of A, B, and R, allowing the coordinates of S' to be found. Then the image point $P = (x_P, y_P, z_P)$ can be found using the relation[4]

$$\frac{x_P}{x_R} = \frac{y_P - y_{S'}}{y_R - y_{S'}} = \frac{z_P - z_{S'}}{z_R - z_{S'}} . \tag{A2}$$

By fig. 4b, whenever $\psi \neq 0$, y_B and z_B satisfy

$$y_B = - z_B \cot\psi ,$$

$$\text{and} \qquad y_B = z_B \tan\psi + y_S - z_S \tan\psi , \tag{A3}$$

which follow from the equations of line RO' and the normal to RO' through A. By solving this system, we have

$$z_B = (z_S \tan\psi - y_S)/(\tan\psi + \cot\psi) \ , \tag{A4}$$

and $\quad y_B = -z_B \cot\psi$.

For $\psi = 0$, we clearly have

$$z_B = 0 \ , \text{ and } \ y_B = y_S \ . \tag{A5}$$

From figs. 4a and 4b,

$$|AB|^2 = (y_S - y_B)^2 + (z_S - z_B)^2 \ , \tag{A6}$$

$$|PB|^2 = x_R^2 + |AB|^2 \ ,$$

$$|BR|^2 = (y_B + \rho \cos\psi)^2 + (z_B - \rho \sin\psi)^2 \ ,$$

and $\quad \cot\theta_B = |PB| / |BR|$.

Equations (A6) combine to give

$$x_R = (|BR|^2 \cot^2\theta_B - |AB|^2)^{1/2} \tag{A7}$$

as the x-coordinate of the point of incidence. By figs. 4a-c we have

$$|SR'| = |R'S'| = |BR| \ ,$$

$$\cos\psi = (y_S - y_{S'})/2|BR| \ , \tag{A8}$$

and $\quad \sin\psi = (z_{S'} - z_S)/2|BR|$,

which gives us

$$y_{S'} = y_S - 2|BR| \cos\psi \ , \tag{A9}$$

and $\quad z_{S'} = z_S + 2|BR| \sin\psi$.

The coordinates of R and S' are, summarizing (A7) and (A9),

$$x_R = (|BR|^2 \cot^2\theta_B - |AB|^2)^{1/2} \quad , \tag{A10}$$

$$y_R = -\rho \cos\psi \ ,$$

$$z_R = \rho \sin\psi \ ,$$

$$x_S' = 0 \ ,$$

$$y_S' = y_S - 2|BR| \cos\psi \ ,$$

and $$z_S' = z_S + 2|BR| \sin\psi \ .$$

Employing (A2), the image point $P = (x_P, y_P, z_P)$ in the $y = 0$ plane has coordinates

$$x_P = x_R \, y_S'/(y_S' - y_R) \ , \tag{A11}$$

$$y_P = 0 \ ,$$

and $$z_P = (z_R - z_S') \, y_S'/(y_S' - y_R) \ .$$

Substituting in (A10) we have

$$x_P = \frac{(|BR|^2 \cot^2\theta_B - |AB|^2)^{1/2} \, (y_S - 2|BR| \cos\psi)}{(y_S + \rho \cos\psi - 2|BR| \cos\psi)} \quad , \tag{A12}$$

$$y_P = 0 \ ,$$

and $$z_P = \frac{(\rho \sin\psi - 2|BR| \sin\psi - z_S)(y_S - 2|BR| \cos\psi)}{(y_S + \rho \cos\psi - 2|BR| \cos\psi)} + z_S + 2|BR| \sin\psi \ ,$$

where from (A4) and (A6) for $\psi \neq 0$,

$$z_B = (z_S \tan\psi - y_S)/(\tan\psi + \cot\psi) \ , \tag{A13}$$

$$|AB| = ((y_S + z_B \cot\psi)^2 + (z_S - z_B)^2)^{1/2} \ ,$$

and $$|BR| = ((\rho \cos\psi - z_B \cot\psi)^2 + (z_B - \rho \sin\psi)^2)^{1/2} \ .$$

Vector analysis may also be employed[14] to obtain the coordinates of the image point P. Let $\vec{S}$ denote the vector to the source point, $\vec{R}$ the point of incidence on the crystal, $\vec{N}$ the unit normal to the crystal at $\vec{R}$, $\vec{Q}$ the reflected ray, and $\vec{P}$ the image point. The unit incident ray is $\vec{R}-\vec{S}/\left|\vec{R}-\vec{S}\right|$, and the Bragg angle is given by

$$\sin\theta_B = \vec{N}\cdot(\vec{R}-\vec{S})/\left|\vec{R}-\vec{S}\right| . \tag{A14}$$

The unit reflected ray is given by

$$\vec{Q} = (\vec{R}-\vec{S})/\left|\vec{R}-\vec{S}\right| + 2\sin\theta_B\,\vec{N} , \tag{A15}$$

and thus the image point can be expressed as

$$\vec{P}(\beta) = \vec{R} + \beta\vec{Q} , \tag{A16}$$

where β is a parameter chosen to allow $\vec{P}$ to lie in the desired detector plane. Employing

$$\vec{S} = (0,\ y_S,\ z_S) , \tag{A17}$$

$$\vec{R} = (x_R,\ -\rho\cos\psi,\ \rho\sin\psi) ,$$

and $$\vec{N} = (0,\ \cos\psi,\ -\sin\psi) ,$$

and using (A14) to solve for x_R and $\left|\vec{R}-\vec{S}\right|$:

$$x_R = (((z_S\sin\psi - y_S\cos\psi - \rho)/\sin\theta_B)^2 - (\rho^2 + y_S^2 + z_S^2 + 2\rho\,(y_S\cos\psi - z_S\sin\psi)))^{1/2} , \tag{A18}$$

and $\left|\vec{R}-\vec{S}\right| = (z_S\sin\psi - y_S\cos\psi - \rho)/\sin\theta_B$.

It follows from (A15) and (A18) that

$$x_Q = x_R / |\vec{R}-\vec{S}| \ ,$$

$$y_Q = -(\rho \cos\psi + y_S)/|\vec{R}-\vec{S}| + 2 \sin\theta_B \cos\psi \ , \tag{A19}$$

and $$z_Q = (\rho \sin\psi - z_S)/|\vec{R}-\vec{S}| - 2 \sin\theta_B \sin\psi \ .$$

Finally, (A16) gives us

$$x_P = x_R \ (1 + \beta/|\vec{R}-\vec{S}|) \ ,$$

$$y_P = -\rho \cos\psi + \beta \ y_Q \ , \tag{A20}$$

and $$z_P = \rho \sin\psi + \beta \ z_Q \ .$$

Choosing $\beta = \rho \cos\psi/(2 \sin\theta_B \cos\psi - (\rho \cos\psi + y_S)/|\vec{R}-\vec{S}|))$ gives us $y_P = 0$, and hence $\vec{P}$ lies in the detector plane. The result (A20) can be shown to agree numerically with the previous solution (A12).

Appendix B. Calculation of Images in Geometry 2

Using the method found in Appendix A, we may calculate the image point $P = (x_P, y_P, z_P)$ from the source $S = (0, y_S, z_S)$ by finding the intersection of the ray S'R with the detector plane defined by eq. (11). Once again the coordinates of R and S' are given by (A10), and the ray S'R defined by (A2). Solving this system

$$y = -x \cot\theta_{BC} + 2\,\rho \cot^2\theta_{BC} \,, \tag{B1}$$

and $$\frac{x_P}{x_R} = \frac{y_P - y_S'}{y_R - y_S'} = \frac{z_P - z_S'}{z_R - z_S'} \,,$$

gives the result

$$x_P = (2\,\rho \cot^2\theta_{BC} - y_S')/((y_R - y_S')/x_R + \cot\theta_{BC}) \,, \tag{B2}$$

$$y_P = -x_P \cot\theta_{BC} + 2\,\rho \cot^2\theta_{BC} \,,$$

and $$z_P = x_P\,(z_R - z_S')/x_R + z_S' \,.$$

Substituting in (A10), this becomes

$$x_P = \frac{2\,\rho \cot^2\theta_{BC} + 2\,|BR|\cos\psi - y_S}{(2\,|BR|\cos\psi - \rho\cos\psi - y_S)/x_R + \cot\theta_{BC}} \,, \tag{B3}$$

$$y_P = -x_P \cot\theta_{BC} + 2\,\rho \cot^2\theta_{BC} \,,$$

and $$z_P = x_P\,(\rho \sin\psi - 2\,|BR|\sin\psi - z_S)/x_R + z_S + 2\,|BR|\sin\psi \,.$$

Appendix C. Detector Location in Geometry 3

Figure 11b gives the point and angles necessary to calculate the detector location in Geometry 3 by the method described in Section II.4: the Lensmaker's Law shows that a partial focus of the source point $Q = (0, y_{SO}, 0)$, the center of the slit, occurs at the intersection of rays R3 and R4. The angles θ_{BC} and α are given by eq. (15), and $N = (x_N, y_N, 0)$ has coordinates

$$x_N = x_C + \rho \sin\alpha \ , \tag{C1}$$

and $$y_N = \rho\ (\cos\alpha - 1) \ .$$

The angle β is given by

$$\beta = \mathrm{atan}((y_{SO} - y_N)/x_N) \ , \tag{C2}$$

and the point $S' = (0, y_S', z_S')$ in the source plane has coordinates

$$y_S' = x_C \tan\ (\alpha - \theta_{BC}) - \rho \ , \tag{C3}$$

and $$z_S' = 0 \ ,$$

for the case when $\psi = 0$. Rays R3 and R4 thus have equations

$$\mathrm{R3} : y = (x - x_C) \tan\gamma - \rho \ , \tag{C4}$$

and $$\mathrm{R4} : y = -x \tan\beta + y_{SO} \ .$$

The intersection gives us the coordinates of $D = (x_D, y_D, 0)$:

$$x_D = (y_{SO} + \rho + x_C \tan\gamma)/(\tan\gamma + (y_{SO} - y_N)/x_N) \ , \tag{C5}$$

and $$y_D = \tan\gamma\ (x_D - x_C) - \rho \ .$$

When the slit is correctly aligned, y_{SO} is equal to zero and (C5) reduces to

$$x_D = (\rho + x_C \tan\gamma)/(\tan\gamma - y_N/x_N) \ , \tag{C6}$$

and $$y_D = \tan\gamma \ (x_D - x_C) - \rho \ .$$

This is the location of the detector center, dependent upon y_{SO}, θ_{BC}, ρ, and x_C. The orientation is normal to ray R3.

Appendix D. Calculation of Images in Geometry 3

The coordinate transformation described in Sect. II.4 is shown in fig. 12a-b. We will examine the transformation of four points: the source point $S = (0, y_S, z_S)$; the slit center $Q = (0, y_{SO}, 0)$; and the detector center $D = (x_D, y_D, 0)$; and the crystal center $C = (x_C, -\rho, 0)$. We first translate to a coordinate system with origin at C, and then perform a clockwise rotation through the angle α given by eq. (12). The points have new coordinates

$$S = (-x_C \cos\alpha - (y_S + \rho) \sin\alpha,\ -x_C \sin\alpha + (y_S + \rho) \cos\alpha,\ z_S) \ , \tag{D1}$$

$$Q = (-x_C \cos\alpha - (y_S + \rho) \sin\alpha,\ -x_C \sin\alpha + (y_{SO} + \rho) \cos\alpha,\ 0) \ ,$$

$$D = ((x_D - x_C) \cos\alpha - (y_D + \rho) \sin\alpha \ ,$$

$$(x_D - x_C) \sin\alpha + (y_D + \rho) \cos\alpha,\ 0) \ ,$$

and $C = (0, 0, 0)$.

Translating to a coordinate system in which S has an x-component equal to zero (and is thus in the "source plane"), we have

$$S = (0, y_{SR}, z_S) \ , \tag{D2}$$

$$Q = (x_{SOR}, y_{SOR}, 0) \ ,$$

$$D = (x_{DR}, y_{DR}, 0) \ ,$$

and $C = (x_{CR}, -\rho, 0)$.

where

$$y_{SR} = -x_C \sin\alpha + (y_S + \rho) \cos\alpha - \rho \ ,$$

$$x_{SOR} = (y_S - y_{SO}) \sin\alpha \ , \tag{D3}$$

$$y_{SOR} = -x_C \sin\alpha + (y_{SO} + \rho) \cos\alpha - \rho \ ,$$

$$x_{DR} = x_D \cos\alpha + (y_S - y_D) \sin\alpha \ ,$$

$$y_{DR} = (x_D - x_C) \sin\alpha + (y_D + \rho) \cos\alpha - \rho \ ,$$

and $x_{CR} = x_C \cos\alpha + (y_S + \rho) \sin\alpha$.

Now the x-axis is the axis of revolution of the crystal, the point source S lies in the x = 0 plane, and the slit center Q is off of the source plane. We have transformed the coordinates so that the source and crystal are in the configuration of Geometry 2, and the new detector plane is given by

$$y - y_{DR} = -(x - x_{DR}) \cot\theta_{BC} \ . \tag{D4}$$

The coordinates of R and S' are found by replacing y_S by y_{SR} in (A4), (A6), and (A10) to get

$$\begin{aligned} x_R &= (|BR|^2 \cot^2\theta_B - |AB|^2)^{1/2} \ , \\ y_R &= -\rho \cos\psi \ , \\ z_R &= \rho \sin\psi \ , \\ x_S' &= 0 \ , \\ y_S' &= y_{SR} - 2|BR| \cos\psi \ , \\ \text{and} \quad z_S' &= z_S + 2|BR| \sin\psi \ . \end{aligned} \tag{D5}$$

For $\psi \neq 0$

$$\begin{aligned} z_B &= (z_S \tan\psi - y_{SR})/(\tan\psi + \cot\psi) \ , \\ |AB| &= ((y_{SR} + z_B \cot\psi)^2 + (z_S - z_B)^2)^{1/2} \ , \\ \text{and} \quad |BR| &= ((\rho \cos\psi - z_B \cot\psi)^2 + (z_B - \rho \sin\psi)^2)^{1/2} \ , \end{aligned} \tag{D6}$$

and for $\psi = 0$

$$\begin{aligned} z_B &= 0 \ , \\ |AB| &= z_S \ , \\ \text{and} \quad |BR| &= y_{SR} + \rho \ . \end{aligned} \tag{D7}$$

The ray S'R is again given by (A2). The intersection of this ray with the plane of the detector gives the system

$$y_P - y_{DR} = -(x_P - x_{DR}) \cot\theta_{BC} , \tag{D8}$$

and $$\frac{x_P}{x_R} = \frac{y_P - y_S'}{y_R - y_S'} = \frac{z_P - z_S'}{z_R - z_S'} ,$$

which has the solution

$$x_P = (x_{DR} - y_S' + x_{DR} \cot\theta_{BC})/(\cot\theta_{BC} + (y_R - y_S')/x_R) , \tag{D9}$$

$$y_P = -(x_P - x_{DR}) \cot\theta_{BC} + Y_{DR} ,$$

and $$z_P = x_P (z_R - z_S')/x_R + z_S' .$$

Inserting (D5) we get

$$x_P = \frac{x_{DR} - y_{SR} + 2|BR| \cos\psi + x_{DR} \cot\theta_{BC}}{(y_S - y_{SR} + 2|BR| \cos\psi)/x_R + \cot\theta_{BC}} , \tag{D10}$$

$$y_P = -(x_P - x_{DR}) \cot\theta_{BC} + y_{DR} ,$$

and $$z_P = x_P (\rho \sin\psi - z_S - 2|BR| \sin\psi)/x_R + z_S + 2|BR| \sin\psi .$$

Appendix E. Computer Programs for Image Calculations and Analysis

Listings of the following programs are given, along with sample output. The programs are written in FORTRAN VIID on a Perkin-Elmer system.

1. MOSY.FTN: calculates images of the line sources on the detector in Geometry 2.

2. Input (entered interactively):

   xmin = 0.00 cm

   xmax = 0.005 cm

   zmin = -0.75 cm

   zmax = 0.75 cm

   ρ = 25.4 cm

   θ_B = 32.42°

   ψ_0 = 12.0°

   H = 0.5 cm

   y_S = 0.0 mm

   x_C = 40.0 cm

The output contains listing of all (441) image points $P(\psi)$ if "LIST" is entered at line 2, in addition to the figure shown.

2. ROTO.FTN: calculates images of line sources on the detector in Geometry 3.

   Input:

   xmin = -0.01 cm

   xmax = 0.03 cm

   zmin = -1.25 cm

   zmax = 1.25 cm

ρ = 25.4 cm

x_C = 40.0 cm

CL(crystal length) = 10.16 cm

ψ_0 = 12.0°

ymin,ymax (top and bottom of rectangular slit) = -0.015 cm, 0.015 cm

y_S = 0.0 cm

θmin,θmax (desired Bragg angle range) = 30.0°, 40.0°

θ_B = 35.0°

The output is again an optional image point listing and the figure shown (identical to fig. 16c).

3. EFFIGY.FTN: graphs $\Delta\xi$ vs θ_B and F_{fw} vs θ_B for a rectangular slit source in Geometry 2, for a Bragg angle range $\Delta\theta_B$ striking the crystal.

Input:

ρ = 25.4 cm

ψ_0 = 12.0°

H = 0.5 cm

2d = 6.687Å

CL = 10.16 cm

DL (detector length) = 10.0 cm

ymin,ymax = -0.015 cm, 0.015 cm

E_{01}, E_{02} (desired energy range) = 2.0, 2.5 keV

The output lists the actual Bragg angle and energy range reaching the crystal, a

listing of 11 values of θ_B, $\Delta\xi$, and F_{fw}, and plots of $\Delta\xi$ vs θ_B and F_{fw} vs θ_B.

4. REFUGEE.FTN: graphs $\Delta\xi$ vs θ_B and F_{fw} vs θ_B for a rectangular slit source in Geometry 3, for a Bragg angle range $\Delta\theta_B$ striking the crystal.

Input:

ρ = 25.4 cm

x_C = 30.0 cm

ψ_o = 12.0°

H = 0.5 cm

2d = 6.687Å

CL = 10.16 cm

DL = 10.0 cm

ymin,ymax = -0.015, 0.015 cm

E_{01},E_{02} = 2.0, 2.5 keV

The output is similar to that of EFFIGY.FTN.

5. FISHY.FTN: graphs intensity vs ξ in Geometry 2 for a rectangular slit source in Geometry 2 for one Bragg angle θ_B striking the crystal.

Input:

ρ = 25.4 cm

ψ_o = 12.0°

H = 0.5 cm

2d = 6.687Å

CL = 10.16 cm

ymin,ymax = -0.015, 0.015 cm

θ_1, θ_2 (desired Bragg angle range) = 29.0°, 35.0°

θ_B (Bragg angle to be considered) = 29.4°

The output gives the actual Bragg angle and energy range reaching the crystal, a list of number of image points N(I) vs position on crystal XB(I), and a plot of N(I) vs XB(I).

6. FISHROT.FTN: graphs intensity vs ξ for a rectangular slit source in Geometry 3, for one Bragg angle θ_B striking the crystal.

Input:

ρ = 25.4 cm

x_C = 40.0 cm

ψ_0 = 12.0°

H = 0.5 cm

2d = 6.687Å

CL = 10.16 cm

ymin,ymax = -0.015, 0.015 cm

θ_1, θ_2 = 30.0°, 40.0°

θ_B = 35.0°

The output is similar to FISHY.FTN.

Listings and sample output for the above six programs follow.

FILE : MCSY.FTN 11:30 20 MAR 85

```
C
C                                MCSY.FTN
C
C     ************************************************************
C     THIS  PROGRAM CALCULATES IMAGES IN THE PLANE OF THE
C     DETECTOR IN THE CONFIGURATION OF GEOMETRY 2.
C     ************************************************************
      DIMENSION X(21),Z(21),SCALEX(2),SCALEZ(2)
C
      COMMON/XXX/ XX(21,21),ZZ(21,21)
C
      PI=2.0*ASIN(1.0)
C
    2 WRITE(5,*)'TYPE "LIST" FOR FULL LISTING,END TO END,OR RETURN'
      READ(3,5)IPLOF
    5 FORMAT(A4)
      IF(IPLOF.EQ.'END ') CALL EXIT(0)
C
      WRITE(5,*)'ENTER X-MIN,X-MAX,Z-MIN,Z-MAX (CM) FOR PLOTTING'
      READ(3,*)SCALEX,SCALEZ
C
      WRITE(5,*)'ENTER RHO (RADIUS OF CURVATURE OF CRYSTAL IN CM.)'
      READ(3,*)RHO
C
      WRITE(5,*)'ENTER THETAB (BRAGG ANGLE IN DEGREES)'
      READ(3,*)THETAB1
      THETAB=THETAB1*PI/180.0
C
      WRITE(5,*)'ENTER PSIMAX (HALF-SECTOR MAX ANGLE OF XTAL (DEG))'
      READ(3,*)PSIMAX1
      PSIMAX=PSIMAX1*PI/180.0
C
      WRITE(5,*)'ENTER HALF-SLIT LENGTH H IN CM.'
      READ(3,*)H
C
      WRITE(5,*)'ENTER Y-AXIS TRANSLATION IN MM'
      READ(3,*)SHIFT1
      SHIFT=0.1*SHIFT1
C
      WRITE(5,*)'ENTER XC (COORDINATE OF CRYSTAL CENTER) IN CM.'
      READ(3,*)XC
      THETABC=ATAN(RHO/XC)
C
C     ************************************************************
C     CALCULATION OF IMAGE DISTRIBUTION
C     ZS     = POINT ON SOURCE SLIT,Z-COORDINATE
C     YS     = POINT ON SOURCE SLIT,Y-COORDINATE
C     ************************************************************
C
      DO 100 J=1,21
      ZS=2.0*H*FLOAT(J-1)/20.0-H
      YS=SHIFT
      CALL IMDSTRB(RHO,THETAB,PSIMAX,X,Z,YS,ZS,THETABC)
C
      DO 25 I=1,21
      XX(I,J)=X(I)
      ZZ(I,J)=Z(I)
   25 CONTINUE
      IF(IPLOF.NE.'LIST') GO TO 100
C
      WRITE(6,50)RHO,THETAB1
      WRITE(6,30)H
   30 FORMAT(1H ,4X,'H=',F12.4,2X,'CM'/)
      WRITE(6,40)SHIFT*10.0
   40 FORMAT(1H ,'     Y-AXIS TRANSLATION IN MM =',F7.3/)
   50 FORMAT(1H ,///,5X,'X-TAL RADIUS OF CURVATURE =',F5.2,2X,'CM.',
     &          5X,'BRAGG ANGLE =',F6.2,2X,'DEGREES'/)
      WRITE(6,60)
   60 FORMAT(1H ,14X,'X=',14X,'Z=')
      WRITE(6,70)(X(K)*1.E4,Z(K)*1.E4,K=1,21)
   70 FORMAT(1H ,2F16.4)
C
  100 CONTINUE
C
```

```
      CALL PPLOT(SCALEX,SCALEZ)
C
C
      WRITE(6,300)RHO
  300 FORMAT(1H ,'RHO =',F6.2,'  CM')
C
      WRITE(6,301)THETAB1
  301 FORMAT(1H ,'THETAB = ',F6.2,'  DEGREES')
C
      WRITE(6,302)PSIMAX1
  302 FORMAT(1H ,'PSIMAX = ',F6.2,'  DEGREES')
C
      WRITE(6,303)H
  303 FORMAT(1H ,'H = ',F6.2,'  CM')
C
      WRITE(6,305)SHIFT1
  305 FORMAT(1H ,'Y-TRANSLATION = ',F7.3,'  MM')
C
      WRITE(6,310)
  310 FORMAT(1H1)
      GO TO 2
      END

C
      SUBROUTINE IMDSTRB(RHO,THETAB,PSIMAX,X,Z,YS,ZS,THETABC)
C
      DIMENSION X(21),Z(21)
C
      DO 30 I=1,21
C
      PSIVAR=PSIMAX*(1.0-2.0*(FLOAT(I-1))/20.0)
C
      T1=SIN(PSIVAR)
      T2=COS(PSIVAR)
      T5=SIN(THETAB)
      T6=COS(THETAB)
      T7=T6/T5
      T8=T1/T2
C
      S1=SIN(THETABC)
      S2=COS(THETABC)
      S3=S2/S1
C
C
      IF(PSIVAR.EQ.0.0) GO TO 20
C
      T9=T2/T1
      ZB=(ZS*T8-YS)/(T8+T9)
      AB=SQRT(((YS+T9*ZB)**2+(ZS-ZB)**2)
      BS=SQRT(((RHO*T2-ZB*T9)**2+(ZB-RHO*T1)**2)
      GO TO 25
C
   20 AB=ZS
      BS=RHO+YS
C
   25 XS=SQRT(T7**2*BS**2-AB**2)
      DD=YS-(2*BS*T2)
      EE=((RHO*T2+DD)/(-XS))+S3
C
      XD=(S3**2*RHO*2-DD)/EE
C
      X(I)=(XD-2*RHO*S3)/(-S1)
      Z(I)=((XD*(RHO*T1-2*BS*T1-ZS))/XS)+2*BS*T1+ZS
C
      GO TO 30
C
C
   30 CONTINUE
      RETURN
      END
```

```
      SUBRCUTINE PPLOT(SCALEX,SCALEZ)
C
      COMMCN/XXX/ XX(21,21),ZZ(21,21)
C
      INTEGER*4 IWD(25,100)
C
      DIMENSION SCALEX(2),SCALEZ(2)
C
      DC 2C J=1,100
      DO 1C I=1,25
      IWD(I,J)=4H
   10 CONTINUE
   20 CONTINUE
C
      EX=99.0/(SCALEX(2)-SCALEX(1))
      EZ=99.0/(SCALEZ(2)-SCALEZ(1))
C
      AX=1.C-BX*SCALEX(1)
      AZ=1.0-BZ*SCALEZ(1)
C
      DO 1CO J=1,21
      DC 8C  I=1,21
C
      IC=AZ+BZ*ZZ(I,J)+0.5
      JL=AX+BX*XX(I,J)+C.5
C
      IF(IC.LT.1)   IC=1
      IF(IC.GT.100) IC=100
      IF(JL.LT.1)   JL=1
      IF(JL.GT.1CO) JL=100
C
      CALL ISBYTE(Y'2A',IWD(1,JL),IC-1)
C
   80 CONTINUE
  100 CONTINUE
C
      WRITE(6,110)
  110 FCRMAT(1H1)
      WRITE(6,120)
  120 FCRMAT(1H ,1X,25('----'))
C
      DC 140 J=1,1CC
      WRITE(6,130)(IWD(I,J),I=1,25)
  130 FCRMAT(1H ,'!',25A4,'!')
  140 CONTINUE
C
      WRITE(6,120)
      WRITE(6,15C)SCALEX,SCALEZ
  150 FCRMAT(1H ,'X-MIN,X-MAX,Z-MIN,Z-MAX (CM) =',4F10.4)
      RETURN
      END
```

X-TAL RADIUS OF CURVATURE =25.40 CM. BRAGG ANGLE = 32.42 DEGREES

H= 0.5000 CM

Y-AXIS TRANSLATION IN MM = 0.000

X=	Z=
40.1355	4952.9570
41.5588	4957.4100
43.2667	4961.9960
44.1206	4966.6020
45.8285	4971.3520
46.9671	4976.1560
47.5364	4980.9920
48.6750	4985.9220
48.9597	4990.8440
49.2443	4995.8320
49.2443	5000.8200
48.9597	5005.8090
48.9597	5010.7970
48.1057	5015.7660
47.5364	5020.7230
46.9671	5025.5860
45.8285	5030.4410
44.9746	5035.1990
43.2667	5039.9300
42.1281	5044.5660
39.8509	5049.1130

X-TAL RADIUS OF CURVATURE =25.40 CM. BRAGG ANGLE = 32.42 DEGREES

H= 0.5000 CM

Y-AXIS TRANSLATION IN MM = 0.000

X=	Z=
35.5812	4461.3440
36.4351	4464.9770
37.5737	4468.7540
39.2816	4472.6050
40.1355	4476.4610
40.9895	4480.3980
41.2741	4484.3670
42.6974	4488.4100
42.6974	4492.4610
42.4127	4496.5510
42.9820	4500.6410
42.6974	4504.7270
42.6974	4508.8360
42.4127	4512.8980
41.5588	4516.9410
40.9895	4520.9570
39.8509	4524.9530
38.9969	4528.8550
38.1430	4532.6990
36.7196	4536.4730
35.0119	4540.2620

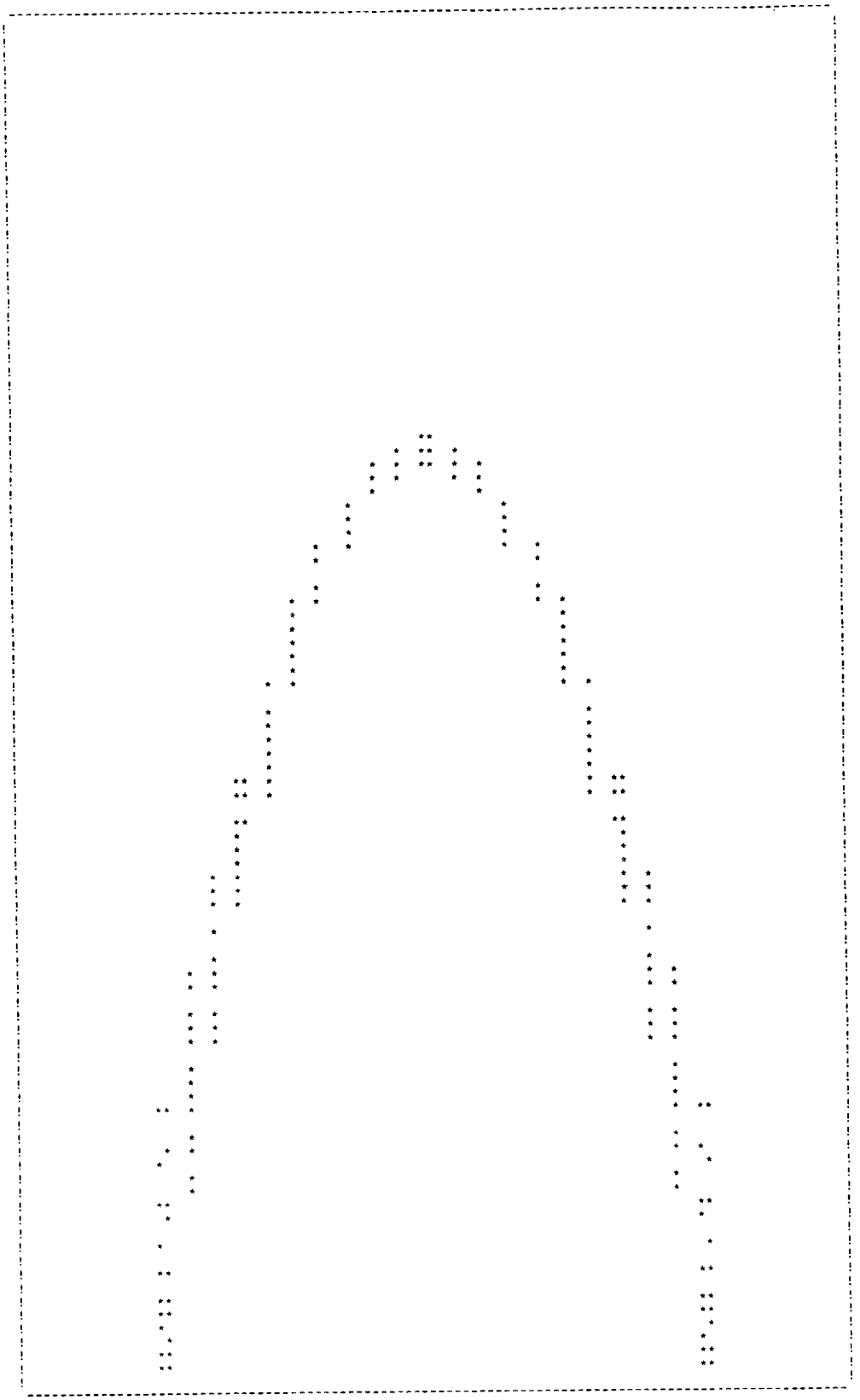

X-MIN,X-MAX,Z-MIN,Z-MAX (CM) = 0.0000 0.0050 -0.7500 0.7500
RHO = 25.40 CM
THETAB = 32.42 DEGREES
PSIMAX = 12.00 DEGREES
H = 0.50 CM
Y-TRANSLATION = 0.000 CM

FILE : ROTO.FTN 11:30 20 MAR 85

```
C
C                                ROTO.FTN
C
C      ************************************************************
C      THIS PROGRAM CALCULATES IMAGES IN THE PLANE OF THE DETECTOR
C      IN GEOMETRY 3:  ROTATION OF THE CRYSTAL IS EMPLOYED TO ALTER
C      THE BRAGG ANGLE RANGE.
C      ************************************************************
C
C
       DIMENSION X(21),Z(21),SCALEX(2),SCALEZ(2)
C
       COMMON/XXX/ XX(21,21),ZZ(21,21)
C
       PI=2.0*ASIN(1.0)
C
     2 WRITE(5,*)'TYPE "LIST" FOR FULL LISTING - OTHERWISE, RETURN'
       READ(3,5)IPLOF
     5 FORMAT(A4)
       IF(IPLOF.EQ.'END ') CALL EXIT(0)
C
       WRITE(5,*)'ENTER X-MIN,X-MAX,Z-MIN,Z-MAX (CM) FOR PLOTTING'
       READ(3,*)SCALEX,SCALEZ
C
       WRITE(5,*)'ENTER RHO (RADIUS OF CURVATURE OF CRYSTAL IN CM.)'
       READ(3,*)RHO
C
       WRITE(5,*)'ENTER XC (COORDINATE OF CRYSTAL CENTER) IN CM.'
       READ(3,*)XC
C
       WRITE(5,*)'ENTER CL (CRYSTAL LENGTH) IN CM.'
       READ(3,*)CL
C
       WRITE(5,*)'ENTER PSIMAX (HALF-SECTOR ANGLE) IN DEG.'
       READ(3,*)PSIMAX1
       PSIMAX=PSIMAX1*PI/180.0
C
       WRITE(5,*)'ENTER YMIN,Y-MAX(COORD. OF SLIT)IN CM.'
       READ(3,*)YMIN,YMAX
C
    6  WRITE(5,*)'ENTER Y-AXIS TRANSLATION OF SLIT IN CM.'
       READ(3,*)YS
C
       IF((YS.GE.YMIN).AND.(YS.LE.YMAX)) GO TO 8
       WRITE(5,*)'Y-AXIS TRANSLATION INCOMPATIBLE WITH YMIN,YMAX'
       GO TO 6
C
    8  WRITE(5,*)'ENTER DESIRED BRAGG ANGLE RANGE IN DEG.'
       READ(3,*)THETAMIN1,THETAMAX1
       THETAMIN=THETAMIN1*PI/180.0
       THETAMAX=THETAMAX1*PI/180.0
C
       THETABC=(THETAMAX+THETAMIN)/2.0
       THETABC1=THETABC*180.0/PI
C
       YSO=(YMIN+YMAX)/2.0
C   ** YSO = CENTER OF SLIT ALONG Y-AXIS **
C
       ALPHA=ATAN((RHO+YSO)/XC)-THETABC
C**    ALPHA=ANGLE OF ROTATION OF CRYSTAL    **
C
C**    XCR=X-COORDINATE OF CRYSTAL IN NON-ROTATED FRAME   **
       XCR=XC*COS(ALPHA)+(RHO+YS)*SIN(ALPHA)
C
       YSR=(YS+RHO)*COS(ALPHA)-XC*SIN(ALPHA)-RHO
       YSOR=(YSO+RHO)*COS(ALPHA)-XC*SIN(ALPHA)-RHO
C
       XSOR=(YS-YSO)*SIN(ALPHA)
C
       THETA1=ATAN((RHO+YSR)/(XCR-0.5*CL))
       THETA2=ATAN((RHO+YSR)/(XCR+0.5*CL))
C
C
```

```
      WRITE(5,*)'ENTER HALF-SLIT LENGTH H IN CM.'
      READ(3,*)H
C
C
    9 WRITE(5,*)'ENTER THETAB (BRAGG ANGLE) IN DEG.'
      READ(3,*)THETAB1
      THETAB=THETAB1*PI/180.0
C
      IF((THETAB.GE.THETA2).AND.(THETAB.LE.THETA1)) GO TO 10
      WRITE(5,*)'BRAGG ANGLE UNACCEPTABLE WITH CL,XC,AND RHO'
      GO TO 9
C
C
C
C     ************************************************************
C     CALCULATION OF IMAGE DISTRIBUTION
C     ZS     = POINT ON SOURCE SLIT,Z-COORDINATE
C     YS     = POINT ON SOURCE SLIT,Y-COORDINATE
C     ************************************************************
C
C ** XSOR=X-COORDINATE OF CENTER OF SLIT **
C ** YSOR=Y-COORDINATE OF CENTER OF SLIT **
C
   10 CH=ATAN((YSOR+RHO)/(XOR-XSOR))
C
C
C** DETECTOR LOCATION IN ROTATED AND NON-ROTATED FRAMES **
C
      GAMMA=THETABC-ALPHA
      DEN=((YSO+RHO-RHO*COS(ALPHA))/(XC+RHO*SIN(ALPHA)))+TAN(GAMMA)
C
      XD=(YSO+RHO+XC*TAN(GAMMA))/DEN
      YD=TAN(GAMMA)*(XD-XC)-RHO
C
      XDR=XD*COS(ALPHA)+(YS-YD)*SIN(ALPHA)
      YDR=(XD-XC)*SIN(ALPHA)+(RHO+YD)*COS(ALPHA)-RHO
C
C
C     WRITE(6,12)THETABC,CH,THETABC1,CH*180.0/PI,ALPHA*180.0/PI
C  12 FORMAT(1H ,5(F8.4,2X)/)
C
C     WRITE(6,14)XD,YD,XDR,YDR
C  14 FORMAT(1H ,4(F8.4,2X)/)
C
C     WRITE(6,16)YSOR,YSR
C  16 FORMAT(1H ,2(F8.4,2X)/)
C
C     WRITE(6,18)THETA1*180.0/PI,THETA2*180.0/PI,GAMMA*180.0/PI
C  18 FORMAT(1H ,3(F8.4,2X)/)
      DO 100 J=1,21
      ZS=2.0*H*FLOAT(J-1)/20.0-H
      CALL IMDSTRB(RHO,THETAB,PSIMAX,X,Z,YSR,ZS,XDR,YDR,THETABC)
C
      DO 25 I=1,21
      XX(I,J)=X(I)
      ZZ(I,J)=Z(I)
   25 CONTINUE
      IF(IPLOF.NE.'LIST') GO TO 100
C
      WRITE(6,50)RHO,THETAB1
      WRITE(6,30)H
   30 FORMAT(1H ,4X,'H=',F12.4,2X,'CM'/)
      WRITE(6,40)YS
   40 FORMAT(1H ,'     Y-AXIS TRANSLATION OF SLIT IN CM= ',F7.3/)
   50 FORMAT(1H ,//,5X,'X-TAL RADIUS OF CURVATURE =',F5.2,2X,'CM.',
     &          5X,'BRAGG ANGLE =',F6.2,2X,'DEGREES'/)
      WRITE(6,60)
   60 FORMAT(1H ,14X,'X=',14X,'Z=')
      WRITE(6,70)(X(K)*1.E4,Z(K)*1.E4,K=1,21)
   70 FORMAT(1H ,2F16.4)
C
  100 CONTINUE
C
```

```
      CALL PPLOT(SCALEX,SCALEZ)
C
      WRITE(6,300)RHO,XC,CL
  300 FORMAT(1H ,'RHO =',F6.2,' CM,',2X,'XC = ',F6.2,' CM,',2X,
     &       'CL = ',F6.2,' CM'/)
C
      WRITE(6,301)THETAB1,THETABC1,ALPHA*180.0/PI
  301 FORMAT(1H ,'THETAB = ',F8.4,' DEG,',2X,'THETABC = ',F8.4,
     &       ' DEG,',2X,'ALPHA = ',F8.4,' DEG'/)
C
      WRITE(6,302)PSIMAX1,THETA2*180.0/PI,THETA1*180.0/PI
  302 FORMAT(1H ,'PSIMAX = ',F6.2,' DEG,',3X,'BRAGG ANGLE RANGE = ',
     &       F8.4,' TO ',F8.4,' DEG'/)
      WRITE(6,303)H,XD,YD
  303 FORMAT(1H ,'H = ',F6.2,' CM,',3X,'DETECTOR LOCATION = (',
     &       F6.3,',',F6.3,', 0.000)'/)
C
      WRITE(6,305)YS,YMIN,YMAX
  305 FORMAT(1H ,'Y-TRANSLATION = ',F7.3,' CM,',3X,'SLIT COORDS = '
     &       F6.4,' TO ',F6.4,' CM'/)
C
      WRITE(6,310)
  310 FORMAT(1H1)
      GO TO 2
      END

C
      SUBROUTINE IMDSTRB(RHO,THETAB,PSIMAX,X,Z,YSR,ZS,XDR,YDR,THETABC)
C
      DIMENSION X(21),Z(21)
C
      DO 30 I=1,21
C
      PSIVAR=PSIMAX*(1.0-2.0*(FLOAT(I-1))/20.0)
C
      T1=SIN(PSIVAR)
      T2=COS(PSIVAR)
      T5=SIN(THETAB)
      T6=COS(THETAB)
      T7=T6/T5
      T8=T1/T2
C
C
      S1=SIN(THETABC)
      S2=COS(THETABC)
      S3=S2/S1
C
C
      IF(PSIVAR.EQ.0.0) GO TO 20
C
      T9=T2/T1
      ZB=(ZS*T8-YSR)/(T8+T9)
      AB=SQRT((YSR+T9*ZB)**2+(ZS-ZB)**2)
      BS=SQRT((RHO*T2-ZB*T9)**2+(ZB-RHO*T1)**2)
      GO TO 25
C
   20 AB=ZS
      BS=RHO+YSR
C
   25 XS=SQRT(T7**2*BS**2-AB**2)
      DD=YSR-(2*BS*T2)
      EE=((RHO*T2+DD)/(-XS))+S3
C
      XINT=(XDR*S3+YDR-DD)/EE
      ZINT=((XINT*(RHO*T1-2*BS*T1-ZS))/XS)+2*BS*T1+ZS
C
      X(I)=(XDR-XINT)/S1
      Z(I)=ZINT
C
      GO TO 30
C
   30 CONTINUE
      RETURN
      END
```

```
      SUBROUTINE PPLOT(SCALEX,SCALEZ)
C
      COMMON/XXX/ XX(21,21),ZZ(21,21)
C
      INTEGER*4 IWD(25,100)
C
      DIMENSION SCALEX(2),SCALEZ(2)
C
      DO 20 J=1,100
      DO 10 I=1,25
      IWD(I,J)=4H
   10 CONTINUE
   20 CONTINUE
C
      BX=99.0/(SCALEX(2)-SCALEX(1))
      BZ=99.0/(SCALEZ(2)-SCALEZ(1))
C
      AX=1.0-BX*SCALEX(1)
      AZ=1.0-BZ*SCALEZ(1)
C
      DO 100 J=1,21
      DO 80  I=1,21
C
      IC=AZ+BZ*ZZ(I,J)+0.5
      JL=AX+BX*XX(I,J)+0.5
C
      IF(IC.LT.1)    IC=1
      IF(IC.GT.100) IC=100
      IF(JL.LT.1)    JL=1
      IF(JL.GT.100) JL=100
C
      CALL ISBYTE(Y'2A',IWD(1,JL),IC-1)
C
   80 CONTINUE
  100 CONTINUE
C
      WRITE(6,110)
  110 FORMAT(1H1)
      WRITE(6,120)
  120 FORMAT(1H ,1X,25('----'))
C
      DO 140 J=1,100
      WRITE(6,130)(IWD(I,J),I=1,25)
  130 FORMAT(1H ,'!',25A4,'!')
  140 CONTINUE
C
      WRITE(6,120)
      WRITE(6,150)SCALEX,SCALEZ
  150 FORMAT(1H ,'X-MIN,X-MAX,Z-MIN,Z-MAX (CM) =',4F10.4)
      RETURN
      END
```

X-TAL RADIUS OF CURVATURE =25.40 CM. BRAGG ANGLE = 35.0C DEGREES

H= 0.5000 CM

Y-AXIS TRANSLATION OF SLIT IN CM= 0.00C

X=	Z=
-63.0489	4391.7380
-59.0584	4388.5700
-53.7378	4385.6450
-47.3531	4383.1250
-38.8402	4381.1130
-29.7952	4379.7190
-19.6861	4379.0820
-7.7148	4379.3400
5.5866	4380.5590
19.9522	4382.9410
35.1158	4386.5350
50.8115	4391.4800
68.1034	4397.8980
86.4594	4405.8790
105.0814	4415.5390
124.7676	4426.9450
144.4537	4440.2890
165.2040	4455.5080
186.2203	4472.8090
207.5025	4492.3400
229.0509	4513.9960

X-TAL RADIUS OF CURVATURE =25.40 CM. BRAGG ANGLE = 35.0C DEGREES

H= 0.5000 CM

Y-AXIS TRANSLATION OF SLIT IN CM= 0.00C

X=	Z=
-54.0039	3954.0840
-51.0776	3951.4710
-47.6192	3948.9630
-42.8307	3946.6550
-36.1799	3944.7290
-28.4651	3943.2890
-19.4201	3942.4690
-9.0450	3942.3930
1.8622	3943.1650
14.3656	3944.9370
28.1991	3947.7940
42.5647	3951.8820
58.2603	3957.2700
75.0202	3964.1080
92.8441	3972.4810
110.6680	3982.5330
129.5561	3994.3110
148.4441	4007.9590
168.6623	4023.4640
188.6145	4041.0790
208.8327	4060.7720

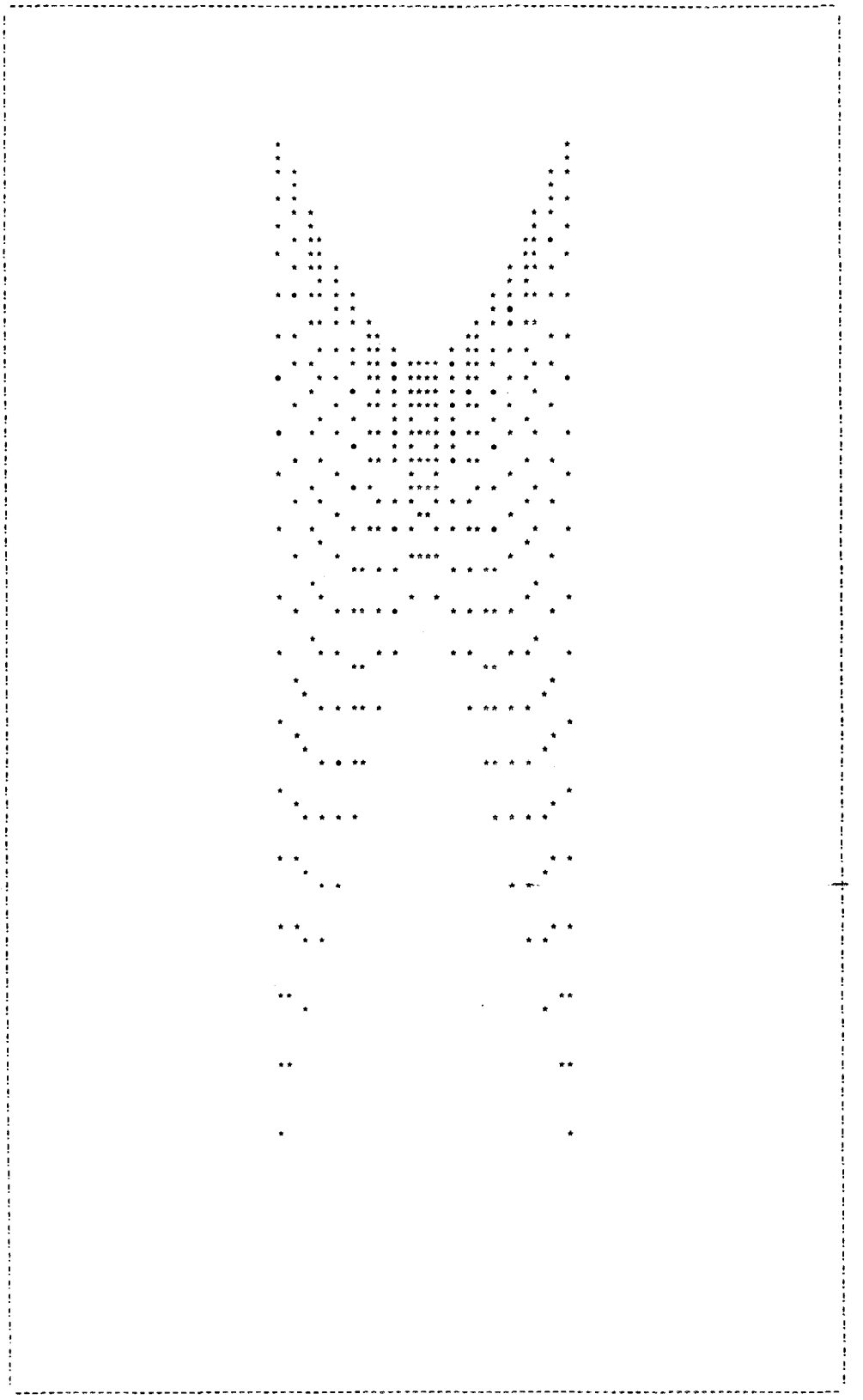

X-MIN,X-MAX,Z-MIN,Z-MAX (CM) = -0.0100 0.0300 -1.2500 1.2500
RHO = 25.40 CM, XC = 40.00 CM, CL = 10.16 CM

THETAB = 35.0000 DEG, THETABC = 35.0000 DEG, ALPHA = -2.5945 DEG

PSIMAX = 12.00 DEG, BRAGG ANGLE RANGE = 31.7646 TO 35.8568 DEG

H = 0.50 CM, DETECTOR LOCATION = (72.938,-0.048, 0.000)

Y-TRANSLATION = 0.000 CM, SLIT COORDS = -.0150 TO 0.0150 CM

FILE : EFFIGY.FTN 11:40 20 MAR 85

```
C
C                                EFFIGY.FTN
C
C  ***************************************************************
C     PROGRAM TO CALCULATE SPECTROMETER PERFORMANCE
C     BY FINDING THE HEIGTH OF THE IMAGE OF A
C     FINITE EXTENDED SLIT ON THE DETECTOR.  GRAPHS OF
C     EFFECTIVE SOURCE HEIGTH VS. BRAGG ANGLE AND
C     (EFFECTIVE SOURCE HEIGTH/ACTUAL SOURCE HEIGTH) VS. BRAGG ANGLE
C     ARE PLOTTED FOR A GIVEN SET OF INPUT PARAMETERS.  THIS PROGRAM
C     UTILIZES GEOMETRY 2:  THE CRYSTAL IS TRANSLATED TO VARY THE
C     BRAGG ANGLE RANGE.
C  ***************************************************************
C
C
      DIMENSION YS(2),X(2,21,21),NCH(100),NCD(100),THETAB(11)
      DIMENSION DELX(11),THETAB1(11),RATIO(11)
C
      INTEGER*4 U
      PI=2.0*ASIN(1.0)
C
C ****INTERACTIVELY ENTER INPUT PARAMETERS****
C
    1 WRITE(5,*)'TYPE "END" TO END, OTHERWISE RETURN'
      READ(3,2)IPLOF
    2 FORMAT(A4)
C
      IF(IPLOF.EQ.'END')CALL EXIT(0)
C
C
      WRITE(5,*)'ENTER RHO (CRYSTAL RADIUS OF CURVATURE) IN CM.'
      READ(3,*)RHO
C
      WRITE(5,*)'ENTER PSIMAX (HALF-SECTOR ANGLE OF CRYSTAL) IN DEG.'
      READ(3,*)PSIMAX1
      PSIMAX=PSIMAX1*PI/180.0
C
      WRITE(5,*)'ENTER HALF-SLIT LENGTH H IN CM.'
      READ(3,*)H
C
      WRITE(5,*)'ENTER TWOD (LATTICE SPACING) IN ANGSTROMS'
      READ(3,*)TWOD
C
      WRITE(5,*)'ENTER CL (CRYSTAL LENGTH) IN CM.'
      READ(3,*)CL
C
      WRITE(5,*)'ENTER DETECTOR LENGTH DL IN CM.'
      READ(3,*)DL
C
      WRITE(5,*)'ENTER YMIN(COORDINATE OF BOTTOM OF SLIT)IN CM.'
      READ(3,*)YMIN
C
      WRITE(5,*)'ENTER YMAX(COORDINATE OF TOP OF SLIT)IN CM.'
      READ(3,*)YMAX
C
C ****"STANDARD VALUES" OF INPUT PARAMETERS****
C
C
C     RHO=25.4
C     PSIMAX1=12.0
C     PSIMAX=PSIMAX1*PI/180.0
C     H=0.5
C     TWOD=6.687
C     CL=10.16
C     DL=10.0
C     YMIN=-0.015
C     YMAX=0.015
C
C ***********************************************************
C *   DESIRED ENERGY RANGE DETERMINES BRAGG ANGLE TO THE    *
C *   CENTER OF THE CRYSTAL, THETABC, WHICH IN TURN DETER-  *
C *   MINES THE X-COORDINATE OF THE CRYSTAL CENTER, XC.     *
C ***********************************************************
C
      WRITE(5,*)'ENTER DESIRED ENERGY RANGE IN KEV'
      READ(3,*)E01,E02
      EOC=(E01+E02)/2.0
```

```
C
C ************************************************************
C *    END OF INPUT PHASE.  THETABC, XC, BRAGG ANGLE RANGE, AND*
C *    ACTUAL ENERGY RANGE ARE NOW CALCULATED.                 *
C ************************************************************
C
      THETABC=ASIN(12.396/(TWOD*EOC))
      THETABC1=THETABC*180.0/PI
C
      XC=RHO/TAN(THETABC)
C
C
      THETA1=ATAN(RHO/(XC-(CL/2.0)))
      THETA2=ATAN(RHO/(XC+(CL/2.0)))
      DELTHE=THETA1-THETA2
C
      E1=12.396/(TWOD*SIN(THETA1))
      E2=12.396/(TWOD*SIN(THETA2))
      DELEN=E2-E1
      WRITE(5,3)E1,E2
    3 FORMAT(1H ,'ACTUAL ENERGY RANGE = ',F8.4,' TO ',F8.4,' KEV'/)
C
C ****INITIALIZE THE ARRAY THETAB****
C
      DO 4 U=1,11
      THETAB(U)=0.0
    4 CONTINUE
C
C ****FIRST OUTPUT PHASE****
C
      WRITE(6,5)RHO
    5 FORMAT(1H1,'CRYSTAL RADIUS OF CURVATURE = ',F6.2,2X,'CM'/)
C
      WRITE(6,10)XC
   10 FORMAT(1H ,'COORDINATE OF CRYSTAL CENTER = ',F6.2,2X,'CM'/)
C
      WRITE(6,15)PSIMAX1
   15 FORMAT(1H ,'HALF-SECTOR ANGLE OF CRYSTAL = ',F6.2,2X,'DEG'/)
C
      WRITE(6,20)H
   20 FORMAT(1H ,'HALF-SLIT LENGTH = ', F6.2,2X,'CM'/)
C
      WRITE(6,25)TWOD
   25 FORMAT(1H ,'2*LATTICE SPACING = ',F8.4,2X,'ANGSTROMS'/)
C
      WRITE(6,30)CL
   30 FORMAT(1H ,'CRYSTAL LENGTH = ',F8.2,2X,'CM'/)
C
      WRITE(6,35)THETA1*180.0/PI
   35 FORMAT(1H ,'MAXIMUM BRAGG ANGLE = ',F6.2,2X,'DEG'/)
      WRITE(6,40)THETA2*180.0/PI
   40 FORMAT(1H ,'MINIMUM BRAGG ANGLE = ',F6.2,2X,'DEG'/)
C
      WRITE(6,45)DELTHE*180.0/PI
   45 FORMAT(1H ,'BRAGG ANGLE RANGE = ',F6.2,2X,'DEG'/)
C
      WRITE(6,50)E1
   50 FORMAT(1H ,'MINIMUM X-RAY ENERGY = ',F8.4,2X,'KEV'/)
      WRITE(6,55)E2
   55 FORMAT(1H ,'MAXIMUM X-RAY ENERGY = ',F8.4,2X,'KEV'/)
C
      WRITE(6,60)DELEN
   60 FORMAT(1H ,'ENERGY RANGE = ',F8.4,2X,'KEV'/)
C
      WRITE(6,65)YMIN,YMAX
   65 FORMAT(1H ,'SLIT COORDINATES ALONG Y-AXIS = ',F8.4,'CM, ',
     2        F8.4,'CM'//)
C
C ************************************************************
C *    MAIN DO LOOP OF PROGRAM.  DIVIDES BRAGG ANGLE RANGE INTO *
C *    11 EQUAL INCREMENTS, AND REPEATS THE BELOW CALCULATIONS  *
C *    FOR EACH BRAGG ANGLE.                                    *
C ************************************************************
C
      DO 500 U=1,11
C
      THETAB(U)=THETA2+(FLOAT(U-1))*DELTHE/10.0
```

```
155         THETAB1(U)=THETAB(U)*180.0/PI
156   C
157         WRITE(6,70)THETAB1(U)
158      70 FORMAT(1H ,'BRAGG ANGLE = ',F6.2,2X,'DEG.'/)
159   C
160   C ****INITIALIZE ARRAY X****
161   C
162         DO 85 I=1,2
163   C
164         DO 80 K=1,21
165   C
166         DO 75 L=1,21
167   C
168         X(I,K,L)=0.0
169   C
170      75 CONTINUE
171   C
172      80 CONTINUE
173   C
174      85 CONTINUE
175   C
176   C ***********************************************************
177   C *   CALCULATE X-COORDINATES OF THE TOP AND BOTTOM OF THE RECT-*
178   C *   ANGULAR SLIT SOURCE, AND CALL THE SUBROUTINE IMDSTRB TO   *
179   C *   CALCULATE IMAGE POINTS FOR EACH OF THESE 2 LINE SLIT      *
180   C *   SOURCES; STORE THE IMAGE POINTS IN THE ARRAY X.           *
181   C ***********************************************************
182   C
183         DO 90 I=1,2
184   C
185         YS(I)=YMIN+(YMAX-YMIN)*FLOAT(I-1)
186   C
187   C
188         CALL IMDSTRB(THETAB,PSIMAX,RHO,THETABO,I,H,X,YS,U)
189   C
190      90 CONTINUE
191   C
192   C ***************************************************************
193   C *   INITIALIZE XMIN AND XMAX; THEN PROCEED TO SET XMIN TO MIN-   *
194   C *   IMUM X-VALUE OF IMAGE POINTS FROM TOP SLIT, AND XMAX TO MAX- *
195   C *   IMUM X-VALUE OF IMAGE POINTS FROM BOTTOM SLIT; DELX IS THE   *
196   C *   ABSOLUTE IMAGE EXTENSION ON THE DETECTOR, AND RATIO IS THE   *
197   C *   RATIO OF ACTUAL IMAGE EXTENSION TO ACTUAL SOURCE EXTENSION.  *
198   C ***************************************************************
199         XMIN=100.0
200         XMAX=-100.0
201   C
202         DO 100 K=1,21
203         DO 95 L=1,21
204   C
205         XMAX=AMAX1(XMAX,X(1,K,L))
206         XMIN=AMIN1(XMIN,X(2,K,L))
207   C
208      95 CONTINUE
209     100 CONTINUE
210   C
211         DELX(U)=XMAX-XMIN
212         RATIO(U)=DELX(U)/(YMAX-YMIN)
213   C
214   C ****SECOND OUTPUT PHASE BEGINS ON LINE 134, ENDS ON 188****
215   C
216         WRITE(6,105)XMIN,XMAX
217     105 FORMAT(1H ,'IMAGE RANGE ON DETECTOR IS ',F8.4,2X,' CM TO',
218        &        F8.4,2X,'CM'/)
219   C
220   C ***********************************************************
221   C *   IMAGE IS OFF OF DETECTOR WHEN XMIN IS BELOW DETECTOR BOTTOM *
222   C *   OR XMAX IS ABOVE DETECTOR TOP.                              *
223   C ***********************************************************
224   C
225         IF((XMIN.GE.(-DL*0.5)).AND.(XMAX.LE.(DL*0.5))) GO TO 115
226         WRITE(6,110)
227     110 FORMAT(1H ,'IMAGE IS OFF DETECTOR'/)
228   C
229     115 WRITE(6,120)DELX(U)
230     120 FORMAT(1H ,'EFFECTIVE SOURCE HEIGTH = ',F8.4,' CM'/)
231   C
```

```
      WRITE(6,125)RATIO(U)
  125 FORMAT(1H ,'EFFECTIVE SOURCE HEIGTH RATIO = ',F8.4//)
C
C
C
C
  500 CONTINUE
C
C ****END OF MAIN DO LOOP****
C
      DO 600 I=1,100
      NCD(I)=1H-
      NCH(I)=1H
  600 CONTINUE
C
C ****CALL PLOTTING SUBROUTINE****
C
      CALL BBAR(DELX,RATIO,NCD,THETAB1)
C
      GO TO 1
C
      END
      SUBROUTINE IMDSTRB(THETAB,PSIMAX,RHO,THETABC,I,H,X,YS,U)
C
C ***************************************************************
C *   THIS SUBROUTINE TAKES THE ABOVE INPUT PARAMETERS AND CAL-  *
C *   CULATES THE X-COORDINATES OF THE IMAGE POINTS, STORING THE *
C *   VALUES IN THE ARRAY X                                      *
C ***************************************************************
C
      DIMENSION YS(2),X(2,21,21),THETAB(11)
      INTEGER*4 U
C
      DO 50 K=1,21
C
      PSIVAR=PSIMAX*(1.0-2.0*(FLOAT(K-1))/20.0)
C
      DO 40 L=1,21
C
      ZS=2.0*H*FLOAT(L-1)/20.0-H
C
      T1=SIN(PSIVAR)
      T2=COS(PSIVAR)
      T5=SIN(THETAB(U))
      T6=COS(THETAB(U))
      T7=T6/T5
      T8=T1/T2
C
      S1=SIN(THETABC)
      S2=COS(THETABC)
      S3=S2/S1
C
      IF(PSIVAR.EQ.0.0) GO TO 20
C
      T9=T2/T1
      ZB=(ZS*T8-YS(I))/(T8+T9)
      AB=SQRT((YS(I)+T9*ZB)**2+(ZS-ZB)**2)
      BS=SQRT((RHO*T2-ZB*T9)**2+(ZS-RHO*T1)**2)
      GO TO 25
C
   20 AB=ZS
      BS=RHO+YS(I)
C
   25 XS=SQRT(T7**2*BS**2-AB**2)
      DD=YS(I)-(2*BS*T2)
      EE=((RHO*T2+DD)/(-XS))+S3
C
      XD=(S3**2*RHO+2-DD)/EE
C
      X(I,K,L)=(XD-2*RHO*S3)/(-S1)
C
   40 CONTINUE
C
   50 CONTINUE
C
      END
```

```
      SUBROUTINE BRAR(DELX,RATIO,NCD,THETAB1)
C
C ****THIS IS THE PLOTTING SUBROUTINE****
C
      DIMENSION DELX(11),RATIO(11),NCD(100),NCH(100),THETAB1(11)
      DIMENSION NCE(100)
      INTEGER*4 U
C
C
      DO 2 I=1,100
      NCE(I)=1H
    2 CONTINUE
C
      DO 4 I=1,10
      J=I*10
      NCE(J)=1H!
    4 CONTINUE
C
      WRITE(6,8)
    8 FORMAT(1H1,35X,'EFFECTIVE SOURCE HEIGTH ON DETECTOR'/)
C
      WRITE(6,10)(0.015*FLOAT(J),J=1,10)
   10 FORMAT(1H ,13X,10(5X,F5.3)/)
C
C
      WRITE(6,14)NCE
   14 FORMAT(1H ,13X,100A1/)
C
C
      WRITE(6,18)NCD
   18 FORMAT(1H ,13X,100A1/)
C
      DO 100 U=1,11
C
      DO 50 I=1,100
      NCH(I)=4H
   50 CONTINUE
C
      J=IFIX(DELX(U)/0.0015)
      NCH(J)=4H*
C
      WRITE(6,60)THETAB1(U),NCH
   60 FORMAT(1H ,F10.4,2X,'!',100A1,'!'/)
C
      WRITE(6,62)
   62 FORMAT(1H ,12X,'!',100X,'!'/)
C
  100 CONTINUE
C
      WRITE(6,110)NCD
  110 FORMAT(1H ,13X,100A1/)
C
C
      RMAX=RATIO(1)
      DO 120 J=1,11
      RMAX=AMAX1(RMAX,RATIO(J))
  120 CONTINUE
C
      WRITE(6,130)
  130 FORMAT(1H1,35X,'RATIO OF EFFECTIVE SOURCE WIDTH TO SOURCE WIDTH'/)
C
      DEL=(RMAX-1.00)/10.0
      WRITE(6,140)(1.00+DEL*FLOAT(J),J=1,10)
  140 FORMAT(1H ,8X,'1.000',10(5X,F5.3)/)
C
      WRITE(6,150)NCE
  150 FORMAT(1H ,12X,'!',100A1/)
C
      WRITE(6,160)NCD
  160 FORMAT(1H ,13X,100A1/)
C
      DO 200 U=1,11
C
      DO 150 I=1,100
      NCH(I)=4H
  160 CONTINUE
C
```

```
      CAL=IFIX((RATIO(L)-1.00)*10.0/DEL)
C
      IF(CAL.GT.0.0) GO TO 185
      NCH(1)=4H*
      GO TO 187
C
  185 J=CAL
      NCH(J)=4H*
C
  187 WRITE(6,190)THETAB1(L),NCH
  190 FORMAT(1H ,F10.4,2X,'!',100A1,'!',/)
C
      WRITE(6,195)
  195 FORMAT(1H ,12X,'!',100X,'!'/)
C
  200 CONTINUE
C
      WRITE(6,210)NCD
  210 FORMAT(1H ,13X,100A1/)
C
C
      END
```

```
CRYSTAL RADIUS OF CURVATURE =  25.40  CM
COORDINATE OF CRYSTAL CENTER =  17.95  CM
HALF-SECTOR ANGLE OF CRYSTAL =  12.00  DEG
HALF-SLIT LENGTH =   0.50  CM
2*LATTICE SPACING =   6.6870  ANGSTROMS
CRYSTAL LENGTH =    10.16  CM
MAXIMUM BRAGG ANGLE =  63.13  DEG
MINIMUM BRAGG ANGLE =  47.80  DEG
BRAGG ANGLE RANGE =  15.33  DEG
MINIMUM X-RAY ENERGY =   2.0782  KEV
MAXIMUM X-RAY ENERGY =   2.5024  KEV
ENERGY RANGE =   0.4242  KEV
SLIT COORDINATES ALONG Y-AXIS =  -0.0150CM,   0.0150CM

BRAGG ANGLE =  47.80  DEG.
IMAGE RANGE ON DETECTOR IS  -7.5924   CM TO -7.4878  CM
IMAGE IS OFF DETECTOR
EFFECTIVE SOURCE HEIGTH =   0.1046 CM
EFFECTIVE SOURCE HEIGTH RATIO =   3.4360

BRAGG ANGLE =  49.33  DEG.
IMAGE RANGE ON DETECTOR IS  -5.9084   CM TO -5.8230  CM
IMAGE IS OFF DETECTOR
EFFECTIVE SOURCE HEIGTH =   0.0854 CM
EFFECTIVE SOURCE HEIGTH RATIO =   2.8457

BRAGG ANGLE =  50.86  DEG.
IMAGE RANGE ON DETECTOR IS  -4.2330   CM TO -4.1655  CM
EFFECTIVE SOURCE HEIGTH =   0.0675 CM
EFFECTIVE SOURCE HEIGTH RATIO =   2.2503

BRAGG ANGLE =  52.40  DEG.
IMAGE RANGE ON DETECTOR IS  -2.5636   CM TO -2.5128  CM
EFFECTIVE SOURCE HEIGTH =   0.0508 CM
EFFECTIVE SOURCE HEIGTH RATIO =   1.6947
```

```
BRAGG ANGLE =  53.93  DEG.
IMAGE RANGE ON DETECTOR IS  -0.8979   CM TO -0.8625  CM
EFFECTIVE SOURCE HEIGTH =   0.0354 CM
EFFECTIVE SOURCE HEIGTH RATIO =   1.1803

BRAGG ANGLE =  55.46  DEG.
IMAGE RANGE ON DETECTOR IS   0.7608   CM TO  0.7955  CM
EFFECTIVE SOURCE HEIGTH =   0.0347 CM
EFFECTIVE SOURCE HEIGTH RATIO =   1.1579

BRAGG ANGLE =  57.00  DEG.
IMAGE RANGE ON DETECTOR IS   2.4148   CM TO  2.4617  CM
EFFECTIVE SOURCE HEIGTH =   0.0470 CM
EFFECTIVE SOURCE HEIGTH RATIO =   1.5652

BRAGG ANGLE =  58.53  DEG.
IMAGE RANGE ON DETECTOR IS   4.0730   CM TO  4.1315  CM
EFFECTIVE SOURCE HEIGTH =   0.0585 CM
EFFECTIVE SOURCE HEIGTH RATIO =   1.9489

BRAGG ANGLE =  60.06  DEG.
IMAGE RANGE ON DETECTOR IS   5.7380   CM TO  5.8073  CM
IMAGE IS OFF DETECTOR
EFFECTIVE SOURCE HEIGTH =   0.0693 CM
EFFECTIVE SOURCE HEIGTH RATIO =   2.3095

BRAGG ANGLE =  61.59  DEG.
IMAGE RANGE ON DETECTOR IS   7.4124   CM TO  7.4917  CM
IMAGE IS OFF DETECTOR
EFFECTIVE SOURCE HEIGTH =   0.0793 CM
EFFECTIVE SOURCE HEIGTH RATIO =   2.6440

BRAGG ANGLE =  63.13  DEG.
IMAGE RANGE ON DETECTOR IS   9.0935   CM TO  9.1871  CM
IMAGE IS OFF DETECTOR
EFFECTIVE SOURCE HEIGTH =   0.0887 CM
EFFECTIVE SOURCE HEIGTH RATIO =   2.9554
```

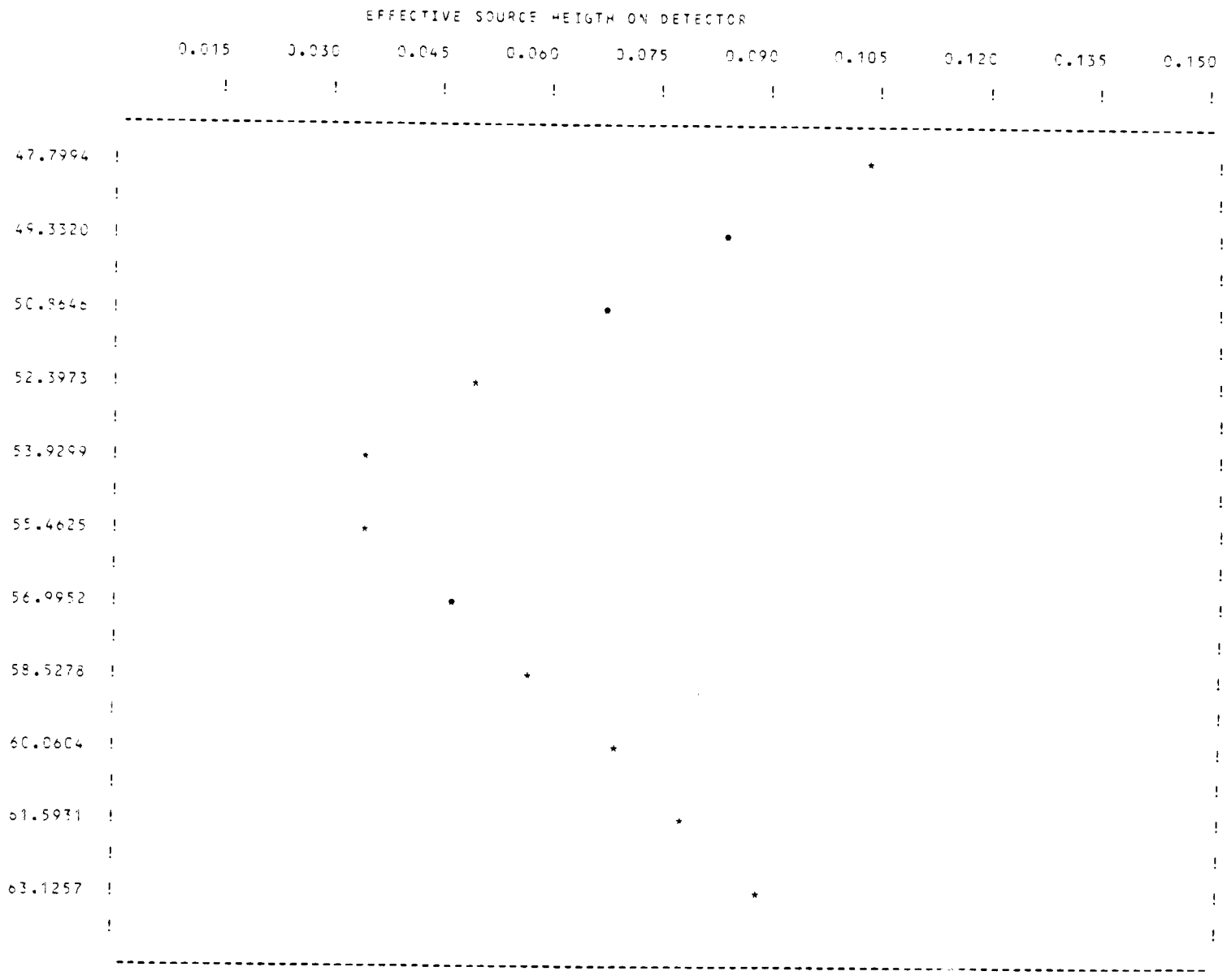
EFFECTIVE SOURCE HEIGTH ON DETECTOR
0.015
0.030
0.045
0.060
0.075
0.090
0.105
0.120
0.135
0.150
47.7994
49.3320
50.8646
52.3973
53.9299
55.4625
56.9952
58.5278
60.0604
61.5931
63.1257

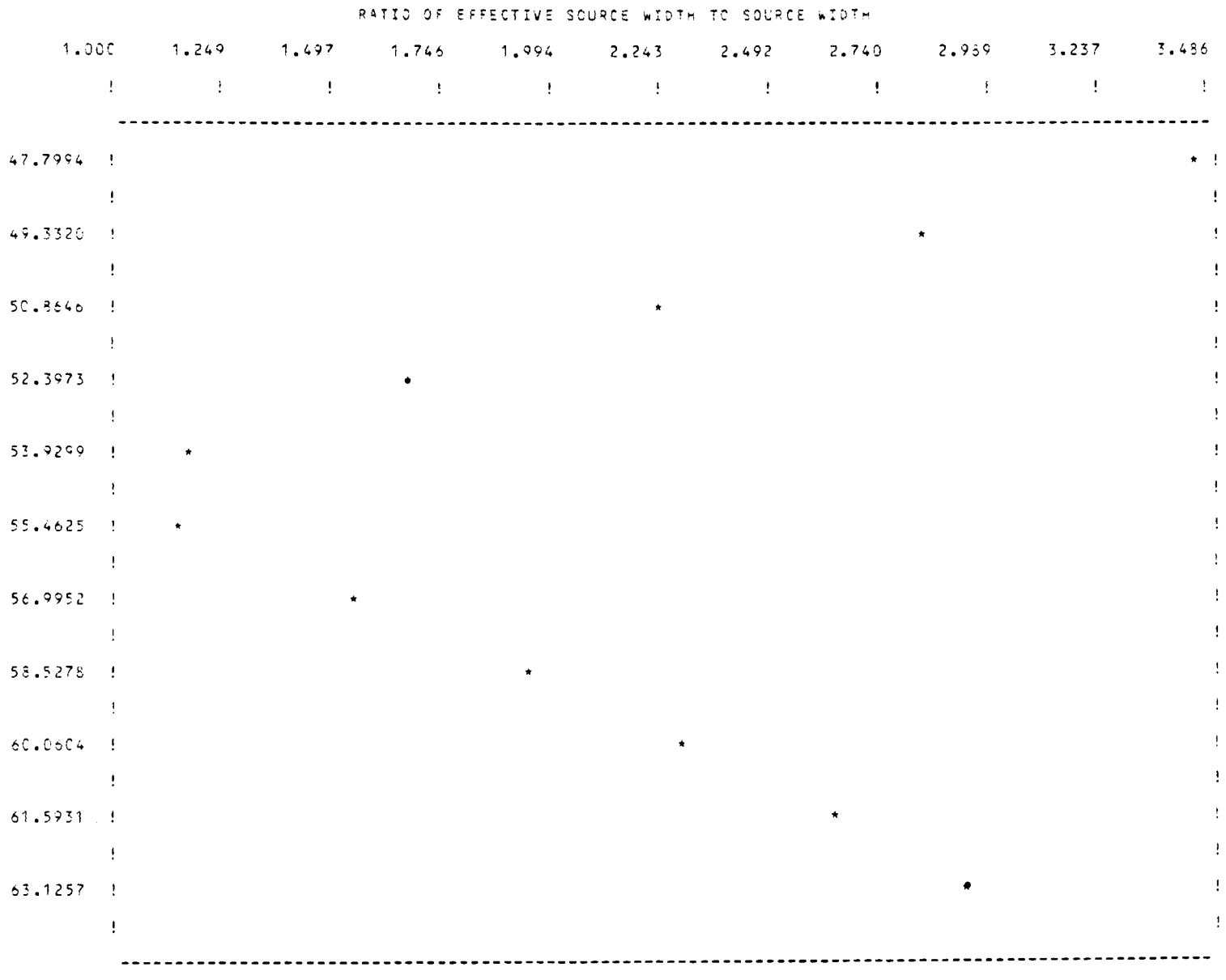
RATIO OF EFFECTIVE SOURCE WIDTH TO SOURCE WIDTH
1.000
1.249
1.497
1.746
1.994
2.243
2.492
2.740
2.989
3.237
3.486
47.7994
49.3320
50.8646
52.3973
53.9299
55.4625
56.9952
58.5278
60.0604
61.5931
63.1257

FILE : REFUGEE.FTN 11:41 20 MAR 85

```
C
C                                REFUGEE.FTN
C
C  ************************************************************
C      PROGRAM TO CALCULATE SPECTROMETER PERFORMANCE
C      BY FINDING THE HEIGTH OF THE IMAGE OF A
C      FINITE EXTENDED SLIT ON THE DETECTOR.  GRAPHS
C      OF EFFECTIVE SOURCE HEIGTH VS. BRAGG ANGLE AND
C      (EFFECTIVE SOURCE HEIGTH/ACTUAL SOURCE HEIGTH) VS. BRAGG ANGLE
C      ARE PLOTTED FOR A GIVEN SET OF INPUT PARAMETERS.  THIS PROGRAM
C      UTILIZES GEOMETRY 3:  THE CRYSTAL IS ROTATED TO VARY THE BRAGG
C      ANGLE RANGE.
C  ************************************************************
C
      DIMENSION YS(2),X(2,21,21),NCH(100),NCD(100),THETAB(11)
      DIMENSION DELX(11),THETAB1(11),RATIO(11),YSR(2)
C
      INTEGER*4 U
      PI=2.0*ASIN(1.0)
C
C *****INTERACTIVELY ENTER INPUT PARAMETERS******
C
    1 WRITE(5,*)'TYPE "END" TO END, OTHERWISE RETURN'
      READ(3,2)IPLOF
    2 FORMAT(A4)
      IF(IPLOF.EQ.'END')CALL EXIT(0)
C
C
      WRITE(5,*)'ENTER RHO (CRYSTAL RADIUS OF CURVATURE) IN CM.'
      READ(3,*)RHO
C
      WRITE(5,*)'ENTER XC (COORDINATE OF CRYSTAL CENTER) IN CM.'
      READ(3,*)XC
C
      WRITE(5,*)'ENTER PSIMAX (HALF-SECTOR ANGLE OF CRYSTAL) IN DEG.'
      READ(3,*)PSIMAX1
      PSIMAX=PSIMAX1*PI/180.0
C
      WRITE(5,*)'ENTER HALF-SLIT LENGTH H IN CM.'
      READ(3,*)H
C
      WRITE(5,*)'ENTER TWOD (LATTICE SPACING) IN ANGSTROMS'
      READ(3,*)TWOD
C
      WRITE(5,*)'ENTER CL (CRYSTAL LENGTH) IN CM.'
      READ(3,*)CL
C
      WRITE(5,*)'ENTER DETECTOR LENGTH DL IN CM.'
      READ(3,*)DL
C
      WRITE(5,*)'ENTER YMIN(COORDINATE OF BOTTOM OF SLIT)IN CM.'
      READ(3,*)YMIN
C
      WRITE(5,*)'ENTER YMAX(COORDINATE OF TOP OF SLIT)IN CM.'
      READ(3,*)YMAX
C
C
C ****"STANDARD VALUES" OF THE INPUT PARAMETERS****
C
C     RHO=25.4
C     PSIMAX1=12.0
C     PSIMAX=PSIMAX1*PI/180.0
C     H=0.5
C     TWOD=6.687
C     CL=10.16
C     DL=10.0
C     YMIN=-0.015
C     YMAX=0.015
C     XC=20.0
C
```

```
C ***********************************************************
C *     DESIRED ENERGY RANGE DETERMINES BRAGG ANGLE TO       *
C *     CENTER OF CRYSTAL, THETABC; THIS, ALONG WITH XC,     *
C *     DETERMINES THE ANGLE OF ROTATION OF THE CRYSTAL      *
C *     ALPHA                                                *
C ***********************************************************
C
      WRITE(5,*)'ENTER DESIRED ENERGY RANGE IN KEV.'
      READ(3,*)E01,E02
      EOC=(E01+E02)/2.0
C
C ***********************************************************
C *   END OF INPUT PHASE.DETECTOR POSITION, SLIT POSITION,   *
C *   CRYSTAL ROTATION, BRAGG ANGLE RANGE, AND ACTUAL ENERGY*
C *   RANGE ARE CALCULATED NEXT.                             *
C ***********************************************************
C
      THETABC=ASIN(12.396/(TWOD*EOC))
      THETABC1=THETABC*180.0/PI
C
      YSO=(YMIN+YMAX)/2.0
      ALPHA=ATAN((RHO+YSO)/XC)-THETABC
      GAMMA=THETABC-ALPHA
      DEN=((YSO+RHO-RHO*COS(ALPHA))/(XC+RHO*SIN(ALPHA)))+TAN(GAMMA)
C
      XD=(YSO+RHO+XC*TAN(GAMMA))/DEN
      YD=TAN(GAMMA)*(XD-XC)-RHO
C
      YSOR=(YSO+RHO)*COS(ALPHA)-XC*SIN(ALPHA)-RHO
      YDR=(XD-XC)*SIN(ALPHA)+(RHO+YD)*COS(ALPHA)-RHO
C
      FF=XC*COS(ALPHA)+(YSO+RHO)*SIN(ALPHA)
      THETA1=ATAN((RHO+YSOR)/(FF-0.5*CL))
      THETA2=ATAN((RHO+YSOR)/(FF+0.5*CL))
      DELTHE=THETA1-THETA2
C
      E1=12.396/(TWOD*SIN(THETA1))
      E2=12.396/(TWOD*SIN(THETA2))
      DELEN=E2-E1
C
      WRITE(5,3)E1,E2
    3 FORMAT(1H ,'ACTUAL ENERGY RANGE = ',F8.4,' TO ',F8.4,' KEV'/)
C
C ****INITIALIZE THE ARRAY THETAB****
C
      DO 5 U=1,11
      THETAB(U)=0.0
    5 CONTINUE
C
C ****FIRST OUTPUT PHASE****
C
      WRITE(6,10)RHO
   10 FORMAT(1H1,'CRYSTAL RADIUS OF CURVATURE = ',F6.2,2X,'CM'/)
C
      WRITE(6,15)XC
   15 FORMAT(1H ,'COORDINATE OF CRYSTAL CENTER = ',F6.2,2X,'CM'/)
C
      WRITE(6,20)PSIMAX1
   20 FORMAT(1H ,'HALF-SECTOR ANGLE OF CRYSTAL = ',F6.2,2X,'DEG'/)
C
      WRITE(6,25)H
   25 FORMAT(1H ,'HALF-SLIT LENGTH = ', F6.2,2X,'CM'/)
C
      WRITE(6,30)TWOD
   30 FORMAT(1H ,'2*LATTICE SPACING = ',F8.4,2X,'ANGSTROMS'/)
C
      WRITE(6,35)CL
   35 FORMAT(1H ,'CRYSTAL LENGTH = ',F8.2,2X,'CM'/)
C
      WRITE(6,40)YMIN,YMAX
   40 FORMAT(1H ,'SLIT COORDINATES ALONG Y-AXIS = ',F8.4,'CM, ',
     &       F8.4,'CM'/)
```

```
C
      WRITE(6,45)ALPHA*180.0/PI
   45 FORMAT(1H ,'ANGLE OF ROTATION OF CRYSTAL = ',F8.4,' DEG'/)
C
      WRITE(6,50)THETA2*180.0/PI,THETA1*180.0/PI
   50 FORMAT(1H ,'MINIMUM BRAGG ANGLE = ',F8.4,' DEG',/,
     &            ' MAXIMUM BRAGG ANGLE = ',F8.4,' DEG'/)
C
      WRITE(6,55)DELTHE*180.0/PI
   55 FORMAT(1H ,'BRAGG ANGLE RANGE = ',F8.4,' DEG'/)
C
      WRITE(6,60)E1,E2
   60 FORMAT(1H ,'MINIMUM X-RAY ENERGY = ',F8.4,' KEV',/,
     &            ' MAXIMUM X-RAY ENERGY = ',F8.4,' KEV'/)
C
      WRITE(6,65)DELEN
   65 FORMAT(1H ,'ENERGY RANGE = ',F8.4,' KEV'/)
C
      WRITE(6,70)XD,YD
   70 FORMAT(1H ,'DETECTOR LOCATION = (',F8.4,', ',F8.4,',0.0000)'//)
C
C ************************************************************
C *   MAIN DO LOOP OF PROGRAM.  DIVIDES BRAGG ANGLE RANGE INTO  *
C *   11 EQUAL INCREMENTS, AND REPEATS THE BELOW CALCULATIONS   *
C *   FOR EACH BRAGG ANGLE.                                     *
C ************************************************************
C
C
      DO 500 U=1,11
C
      THETAB(U)=THETA2+(FLOAT(U-1))*DELTHE/10.0
      THETAB1(U)=THETAB(U)*180.0/PI
C
      WRITE(6,75)THETAB1(U)
   75 FORMAT(1H ,'BRAGG ANGLE = ',F6.2,2X,'DEG.'/)
C
C ****INITIALIZE ARRAY X****
      DO 90 I=1,2
C
      DO 85 K=1,21
C
      DO 80 L=1,21
C
      X(I,K,L)=0.0
C
   80 CONTINUE
C
   85 CONTINUE
C
   90 CONTINUE
C
C ************************************************************
C *   CALCULATE NEW COORDINATES FOR CRYSTAL CENTER, SLIT CEN-*
C *   TER, DETECTOR, AND Y-COORDINATE OF SLIT FOR THE TOP    *
C *   AND BOTTOM SLITS AFTER THE COORDINATE TRANSFORMATION   *
C ************************************************************
C
      DO 95 I=1,2
C
      YS(I)=YMIN+(YMAX-YMIN)*FLOAT(I-1)
C
      XCR=XC*COS(ALPHA)+(RHO+YS(I))*SIN(ALPHA)
      YSR(I)=(YS(I)+RHO)*COS(ALPHA)-XC*SIN(ALPHA)-RHO
      XSOR=(YS(I)-YSO)*SIN(ALPHA)
C
C
      XDR=XD*COS(ALPHA)+(YS(I)-YD)*SIN(ALPHA)
C
```

```
C ************************************************************
C *    CALL SUBROUTINE IMDSTRB TO FIND THE X-COORDINATES OF    *
C *     THE IMAGE POINTS ON THE DETECTOR; STORE IN THE ARRAY X *
C ************************************************************
C
C
      CALL IMDSTRB(THETAB,PSIMAX,RHO,THETABC,I,H,X,YS,U,YSR,XDR,YDR)
C
   95 CONTINUE
C
C ***********************************************************
C *    INITIALIZE XMIN, XMAX; THEN PROCEED TO SET XMIN       *
C *    TO MINIMUM X-VALUE OF IMAGE POINTS FROM TOP SLIT,AND  *
C *    XMAX TO MAXIMUM X-VALUE OF IMAGE POINTS FROM BOTTOM   *
C *    SLIT; DELX IS THE ACTUAL IMAGE EXTENSION, RATIO IS THE*
C *    RATIO OF ACTUAL IMAGE EXTENSION TO ACTUAL SOURCE EX-  *
C *    TENSION.                                              *
C ***********************************************************
C
      XMIN=100.0
      XMAX=-100.0
C
      DO 105 K=1,21
      DO 100 L=1,21
C
      XMAX=AMAX1(XMAX,X(1,K,L))
      XMIN=AMIN1(XMIN,X(2,K,L))
C
  100 CONTINUE
  105 CONTINUE
C
      DELX(U)=XMAX-XMIN
      RATIO(U)=DELX(U)/(YMAX-YMIN)
C
C ****SECOND OUTPUT PHASE COMPLETED****
C
      WRITE(6,110)XMIN,XMAX
  110 FORMAT(1H ,'IMAGE RANGE ON DETECTOR IS ',F8.4,2X,' CM TO',
     &       F8.4,2X,'CM'/)
C ***************************************************************
C *    IMAGE IS OFF OF THE DETECTOR WHEN XMIN IS BELOW DETECTOR  *
C *    BOTTOM OR XMAX IS ABOVE DETECTOR TOP.                     *
C ***************************************************************
C
      IF((XMIN.GE.(-DL*0.5)).AND.(XMAX.LE.(DL*0.5))) GO TO 120
      WRITE(6,115)
  115 FORMAT(1H ,'IMAGE IS OFF DETECTOR'/)
C
  120 WRITE(6,125)DELX(U)
  125 FORMAT(1H ,'EFFECTIVE SOURCE HEIGTH = ',F8.4,' CM'/)
C
      WRITE(6,130)RATIO(U)
  130 FORMAT(1H ,'EFFECTIVE SOURCE HEIGTH RATIO = ',F8.4//)
C
C
C
C
  500 CONTINUE
C ****END OF THE MAIN DO LOOP****
C
      DO 600 I=1,100
      NCD(I)=1H-
      NCH(I)=1H
  600 CONTINUE
C
C ****CALL PLOTTING SUBROUTINE****
C
      CALL BBAR(DELX,RATIO,NCD,THETAB1)
C
      GO TO 1
C
      END
```

```
      SUBROUTINE IMDSTRB(THETAB,PSIMAX,RHO,THETABC,I,H,X,YS,U,YSR,
     3                   XDR,YDR)
C
C ***************************************************************
C *   THIS SUBROUTINE TAKES THE ABOVE INPUT PARAMETERS AND CAL-  *
C *   CULATES THE X-COORDINATES OF THE IMAGE POINTS, STORING     *
C *   THE VALUES IN THE ARRAY X                                  *
C ***************************************************************
C
      DIMENSION YS(2),X(2,21,21),THETAB(11),YSR(2)
      INTEGER*4 U
C
      DO 50 K=1,21
C
      PSIVAR=PSIMAX*(1.0-2.0*(FLOAT(K-1))/20.0)
C
      DO 40 L=1,21
C
      ZS=2.0*H*FLOAT(L-1)/20.0-H
C
      T1=SIN(PSIVAR)
      T2=COS(PSIVAR)
      T5=SIN(THETAB(U))
      T6=COS(THETAB(U))
      T7=T6/T5
      T8=T1/T2
C
      S1=SIN(THETABC)
      S2=COS(THETABC)
      S3=S2/S1
C
      IF(PSIVAR.EQ.0.0) GO TO 20
C
      T9=T2/T1
      ZB=(ZS*T8-YSR(I))/(T8+T9)
      AB=SQRT((YSR(I)+T9*ZB)**2+(ZS-ZB)**2)
      BS=SQRT((RHO*T2-ZB*T9)**2+(ZB-RHO*T1)**2)
      GO TO 25
C
   20 AB=ZS
      BS=RHO+YSR(I)
C
   25 XS=SQRT(T7**2*BS**2-AB**2)
      DD=YSR(I)-(2*BS*T2)
      EE=((RHO*T2+DD)/(-XS))+S3
C
      XINT=(XDR*S3+YDR-DD)/EE
C
      X(I,K,L)=(XDR-XINT)/S1
C
   40 CONTINUE
C
   50 CONTINUE
C
      END

      SUBROUTINE BBAR(DELX,RATIO,NCD,THETAB1)
C
C ****THIS IS THE PLOTTING SUBROUTINE****
C
C
      DIMENSION DELX(11),RATIO(11),NCD(100),NCH(100),THETAB1(11)
      DIMENSION NCE(100)
      INTEGER*4 U
C
C
      DO 2 I=1,100
      NCE(I)=1H
    2 CONTINUE
C
      DO 4 I=1,10
      J=I*10
      NCE(J)=1H!
    4 CONTINUE
C
      WRITE(6,8)
    8 FORMAT(1H1,35X,'EFFECTIVE SOURCE HEIGTH ON DETECTOR'/)
C
```

```
      WRITE(6,10)(0.020*FLOAT(J),J=1,10)
   10 FORMAT(1H ,13X,10(5X,F5.3)/)
C
C
      WRITE(6,14)NCE
   14 FORMAT(1H ,13X,100A1/)
C
C
      WRITE(6,18)NCD
   18 FORMAT(1H ,13X,100A1/)
C
      DO 100 U=1,11
C
      DO 50 I=1,100
      NCH(I)=4H
   50 CONTINUE
C
      J=IFIX(DELX(U)/0.0020)
      NCH(J)=4H*
C
      WRITE(6,60)THETAB1(U),NCH
   60 FORMAT(1H ,F10.4,2X,'!',100A1,'!'/)
C
      WRITE(6,62)
   62 FORMAT(1H ,12X,'!',100X,'!'/)
C
  100 CONTINUE
C
      WRITE(6,110)NCD
  110 FORMAT(1H ,13X,100A1/)
C
C
      RMAX=RATIO(1)
      DO 120 J=1,11
      RMAX=AMAX1(RMAX,RATIO(J))
  120 CONTINUE
C
      WRITE(6,130)
  130 FORMAT(1H1,35X,'RATIO OF EFFECTIVE SOURCE WIDTH TO SOURCE WIDTH'/)
C
      DEL=(RMAX-1.00)/10.0
      WRITE(6,140)(1.00+DEL*FLOAT(J),J=1,10)
  140 FORMAT(1H ,8X,'1.000',10(4X,F6.3)/)
C
      WRITE(6,150)NCE
  150 FORMAT(1H ,12X,'!',100A1/)
C
      WRITE(6,160)NCD
  160 FORMAT(1H ,13X,100A1/)
C
      DO 200 U=1,11
C
      DO 180 I=1,100
      NCH(I)=4H
  180 CONTINUE
C
      CAL=IFIX((RATIO(U)-1.00)*10.0/DEL)
C
      IF(CAL.GT.0.0) GO TO 185
      NCH(1)=4H*
      GO TO 187
C
  185 J=CAL
      NCH(J)=4H*
C
  187 WRITE(6,190)THETAB1(U),NCH
  190 FORMAT(1H ,F10.4,2X,'!',100A1,'!',/)
C
      WRITE(6,195)
  195 FORMAT(1H ,12X,'!',100X,'!'/)
C
  200 CONTINUE
C
      WRITE(6,210)NCD
  210 FORMAT(1H ,13X,100A1/)
C
C
      END
```

```
CRYSTAL RADIUS OF CURVATURE =  25.40  CM

COORDINATE OF CRYSTAL CENTER =  30.00  CM

HALF-SECTOR ANGLE OF CRYSTAL =  12.00  DEG

HALF-SLIT LENGTH =   0.50  CM

2*LATTICE SPACING =   6.6870  ANGSTROMS

CRYSTAL LENGTH =    10.16  CM

SLIT COORDINATES ALONG Y-AXIS =  -0.0150CM,   0.0150CM

ANGLE OF ROTATION OF CRYSTAL = -14.8555 DEG

MINIMUM BRAGG ANGLE =  49.4713 DEG
MAXIMUM BRAGG ANGLE =  61.6390 DEG

BRAGG ANGLE RANGE =  12.1671 DEG

MINIMUM X-RAY ENERGY =   2.1066 KEV
MAXIMUM X-RAY ENERGY =   2.4389 KEV

ENERGY RANGE =   0.3323 KEV

DETECTOR LOCATION = ( 38.7519,  -1.4007,0.0000)

BRAGG ANGLE =  49.47  DEG.

IMAGE RANGE ON DETECTOR IS  -6.4149   CM TO -6.1733  CM

IMAGE IS OFF DETECTOR

EFFECTIVE SOURCE HEIGTH =   0.2416 CM

EFFECTIVE SOURCE HEIGTH RATIO =   2.0544

BRAGG ANGLE =  50.69  DEG.

IMAGE RANGE ON DETECTOR IS  -5.0269   CM TO -4.6008  CM

IMAGE IS OFF DETECTOR

EFFECTIVE SOURCE HEIGTH =   0.2262 CM

EFFECTIVE SOURCE HEIGTH RATIO =   7.5395

BRAGG ANGLE =  51.91  DEG.

IMAGE RANGE ON DETECTOR IS  -3.6436   CM TO -3.4313  CM

EFFECTIVE SOURCE HEIGTH =   0.2122 CM

EFFECTIVE SOURCE HEIGTH RATIO =   7.0740

BRAGG ANGLE =  53.12  DEG.

IMAGE RANGE ON DETECTOR IS  -2.2641   CM TO -2.0637  CM

EFFECTIVE SOURCE HEIGTH =   0.2004 CM

EFFECTIVE SOURCE HEIGTH RATIO =   6.6809
```

BRAGG ANGLE = 54.34 DEG.

IMAGE RANGE ON DETECTOR IS -0.5966 CM TO -0.6965 CM

EFFECTIVE SOURCE HEIGTH = 0.1901 CM

EFFECTIVE SOURCE HEIGTH RATIO = 6.3374

BRAGG ANGLE = 55.56 DEG.

IMAGE RANGE ON DETECTOR IS 0.4899 CM TO 0.6715 CM

EFFECTIVE SOURCE HEIGTH = 0.1816 CM

EFFECTIVE SOURCE HEIGTH RATIO = 6.0533

BRAGG ANGLE = 56.77 DEG.

IMAGE RANGE ON DETECTOR IS 1.8664 CM TO 2.0416 CM

EFFECTIVE SOURCE HEIGTH = 0.1752 CM

EFFECTIVE SOURCE HEIGTH RATIO = 5.8407

BRAGG ANGLE = 57.99 DEG.

IMAGE RANGE ON DETECTOR IS 3.2443 CM TO 3.4151 CM

EFFECTIVE SOURCE HEIGTH = 0.1708 CM

EFFECTIVE SOURCE HEIGTH RATIO = 5.6937

BRAGG ANGLE = 59.21 DEG.

IMAGE RANGE ON DETECTOR IS 4.6248 CM TO 4.7934 CM

EFFECTIVE SOURCE HEIGTH = 0.1686 CM

EFFECTIVE SOURCE HEIGTH RATIO = 5.6199

BRAGG ANGLE = 60.42 DEG.

IMAGE RANGE ON DETECTOR IS 6.0089 CM TO 6.1777 CM

IMAGE IS OFF DETECTOR

EFFECTIVE SOURCE HEIGTH = 0.1688 CM

EFFECTIVE SOURCE HEIGTH RATIO = 5.6280

BRAGG ANGLE = 61.64 DEG.

IMAGE RANGE ON DETECTOR IS 7.3981 CM TO 7.5696 CM

IMAGE IS OFF DETECTOR

EFFECTIVE SOURCE HEIGTH = 0.1715 CM

EFFECTIVE SOURCE HEIGTH RATIO = 5.7154

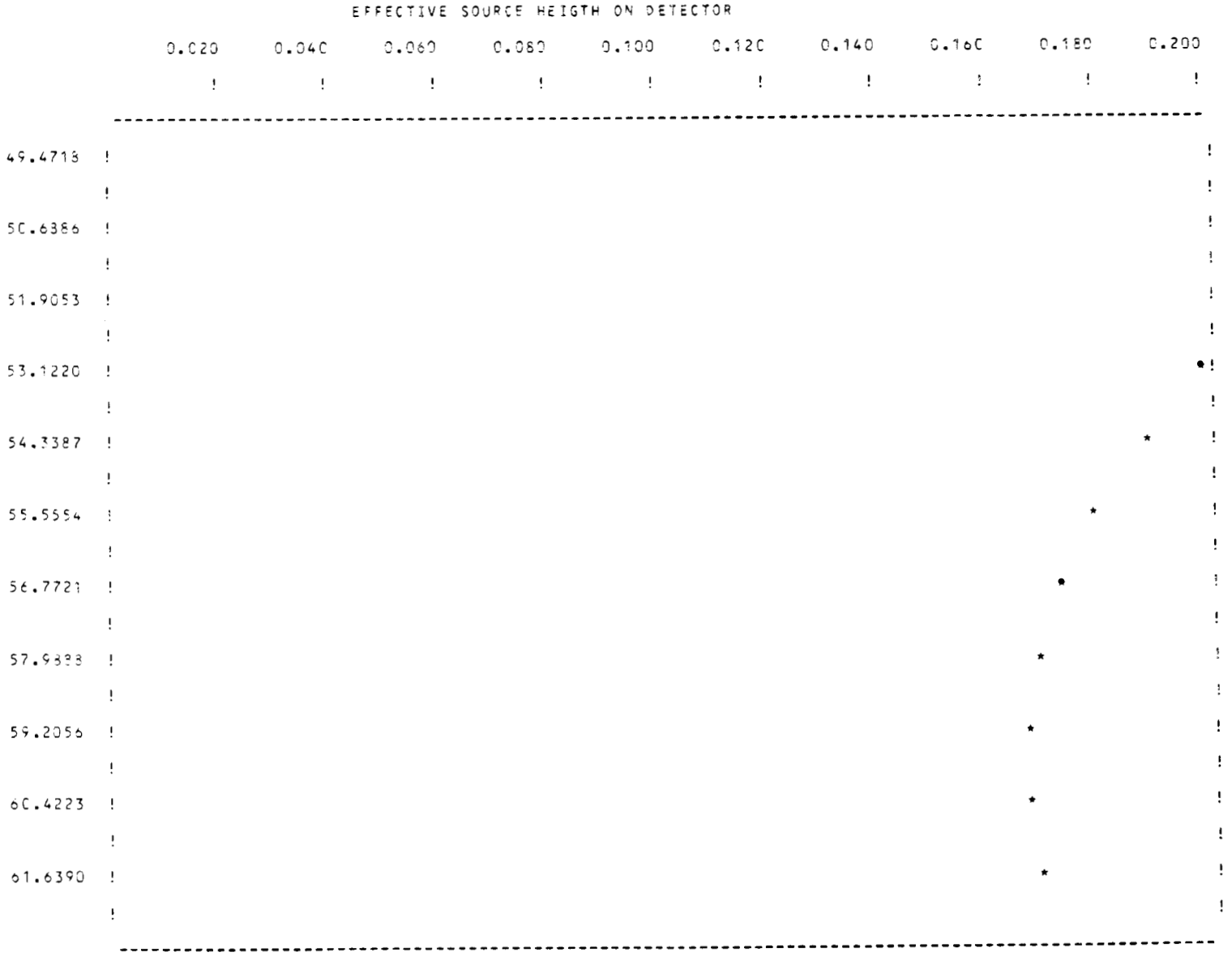
EFFECTIVE SOURCE HEIGTH ON DETECTOR
0.020
0.040
0.060
0.080
0.100
0.120
0.140
0.160
0.180
0.200
49.4718
50.6386
51.9053
53.1220
54.3387
55.5554
56.7721
57.9888
59.2056
60.4223
61.6390

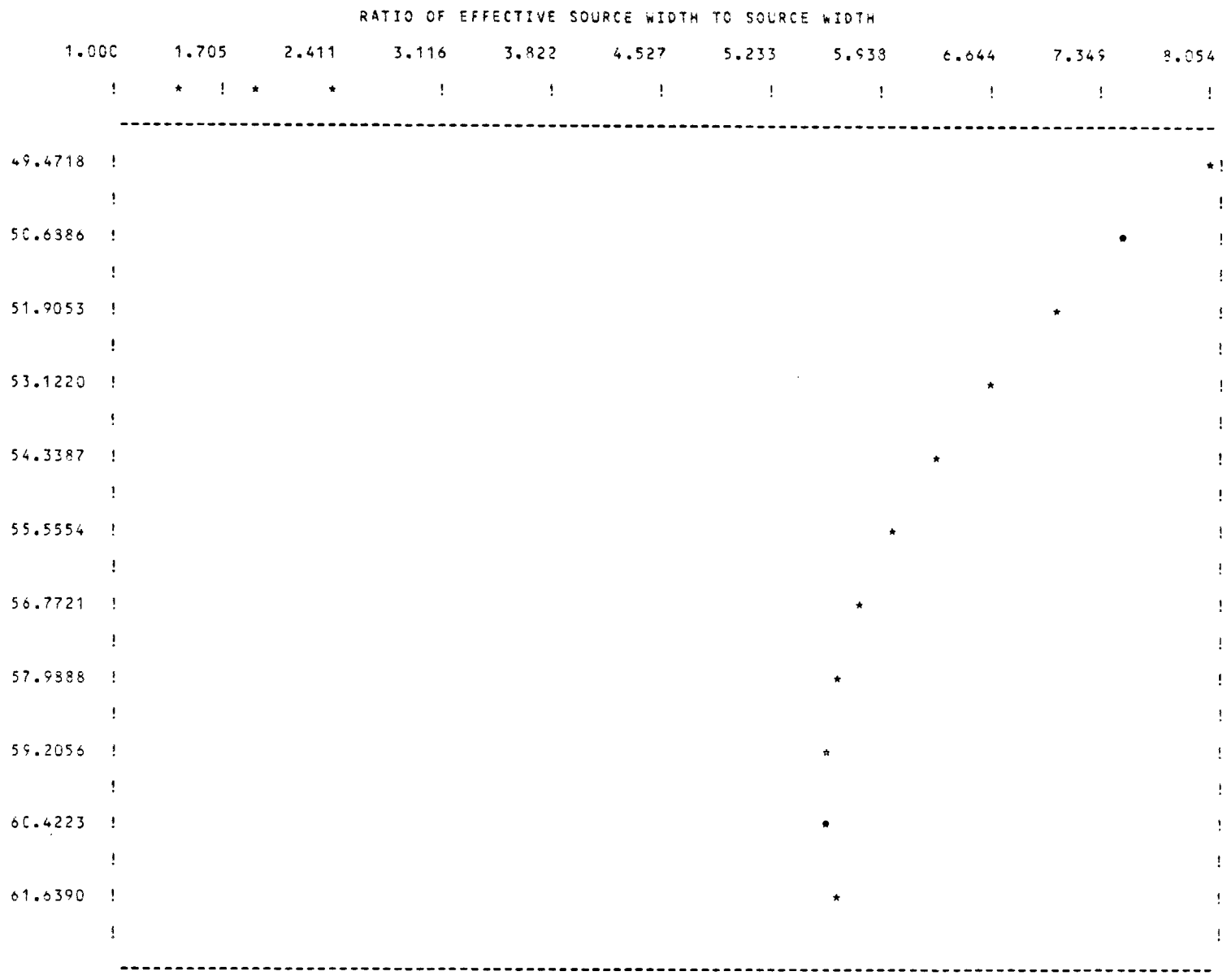
RATIO OF EFFECTIVE SOURCE WIDTH TO SOURCE WIDTH
1.000
1.705
2.411
3.116
3.822
4.527
5.233
5.938
6.644
7.349
8.054
49.4718
50.6386
51.9053
53.1220
54.3387
55.5554
56.7721
57.9888
59.2056
60.4223
61.6390

FILE : FISHY.FTN 11:30 20 MAR 85

```
C
C                                FISHY.FTN
C
C  ***************************************************************
C      PROGRAM TO CALCULATE SPECTROMETER PERFORMANCE
C      BY FINDING THE INTENSITY OF THE IMAGE OF A
C      FINITE EXTENDED SLIT AS A FUNCTION OF POSITION
C      ALONG THE DETECTOR. THE PROGRAM UTILIZES GEOMETRY 2:
C      TRANSLATION OF THE CRYSTAL IS EMPLOYED TO VARY THE BRAGG
C      ANGLE RANGE.
C  ***************************************************************
C
C
      DIMENSION YS(9),X(9,21,21),XB(21),N(20),NCH(100),NCD(100)
C
      PI=2.0*ASIN(1.0)
C
C ****INTERACTIVELY ENTER INPUT PARAMETERS****
C
    1 WRITE(5,*)'TYPE "END" TO END, OTHERWISE RETURN'
      READ(3,2)IPLOF
    2 FORMAT(A4)
      IF(IPLOF.EQ.'END')CALL EXIT(0)
C
      WRITE(5,*)'ENTER RHO (CRYSTAL RADIUS OF CURVATURE) IN CM.'
      READ(3,*)RHO
C
      WRITE(5,*)'ENTER PSIMAX (HALF-SECTOR ANGLE OF CRYSTAL) IN DEG.'
      READ(3,*)PSIMAX1
      PSIMAX=PSIMAX1*PI/180.0
C
      WRITE(5,*)'ENTER HALF-SLIT LENGTH H IN CM.'
      READ(3,*)H
C
      WRITE(5,*)'ENTER TWOD (LATTICE SPACING) IN ANGSTROMS'
      READ(3,*)TWOD
C
      WRITE(5,*)'ENTER CL (CRYSTAL LENGTH) IN CM.'
      READ(3,*)CL
C
      WRITE(5,*)'ENTER YMIN(COORDINATE OF BOTTOM OF SLIT)IN CM.'
      READ(3,*)YMIN
C
      WRITE(5,*)'ENTER YMAX(COORDINATE OF TOP OF SLIT)IN CM.'
      READ(3,*)YMAX
C
      WRITE(5,*)'ENTER DESIRED BRAGG ANGLE RANGE IN DEG.'
      READ(3,*)THETAMIN1,THETAMAX1
      THETAMIN=THETAMIN1*PI/180.0
      THETAMAX=THETAMAX1*PI/180.0
C
C ***********************************************************
C *    DESIRED BRAGG ANGLE RANGE DETERMINES THE BRAGG ANGLE TO *
C *    THE CRYSTAL CENTER, THETABC.  THIS IN TURN DETERMINES   *
C *    THE VALUE OF XC, THE X-COORDINATE OF THE CRYSTAL CENTER.*
C *    THE ACTUAL BRAGG ANGLE RANGE AND ENERGY RANGE CAN THEN  *
C *    BE CALCULATED.                                          *
C ***********************************************************
C
      THETABC=(THETAMIN+THETAMAX)/2.0
      THETABC1=THETABC*180.0/PI
C
      XC=RHO*COS(THETABC)/SIN(THETABC)
C
C
      THETA1=ATAN(RHO/(XC-(CL/2.0)))
      THETA2=ATAN(RHO/(XC+(CL/2.0)))
      DELTHE=THETA1-THETA2
C
      E1=12.396/(TWOD*SIN(THETA1))
      E2=12.396/(TWOD*SIN(THETA2))
      DELEN=E2-E1
```

```
C
C
    3  WRITE(5,*)'ENTER THETAB (BRAGG ANGLE) IN DEG.'
       READ(3,*)THETAB1
       THETAB=THETAB1*PI/180.0
C
       IF((THETAB.GE.THETA2).AND.(THETAB.LE.THETA1)) GO TO 4
       WRITE(5,*)'BRAGG ANGLE UNACCEPTABLE'
       GO TO 3
C
C ****FIRST OUTPUT PHASE****
C
    4  WRITE(6,5)RHO
    5  FORMAT(1H ,'CRYSTAL RADIUS OF CURVATURE = ',F6.2,2X,'CM'/)
C
       WRITE(6,6)THETAB1
    6  FORMAT(1H ,'BRAGG ANGLE = ',F6.2,2X,'DEG'/)
C
       WRITE(6,7)XC
    7  FORMAT(1H ,'COORDINATE OF CRYSTAL CENTER = ',F6.2,2X,'CM'/)
C
       WRITE(6,8)PSIMAX1
    8  FORMAT(1H ,'HALF-SECTOR ANGLE OF CRYSTAL = ',F6.2,2X,'DEG'/)
C
       WRITE(6,9)H
    9  FORMAT(1H ,'HALF-SLIT LENGTH = ', F6.2,2X,'CM'/)
C
       WRITE(6,10)TWOD
   10  FORMAT(1H ,'2*LATTICE SPACING = ',F8.4,2X,'ANGSTROMS'/)
C
       WRITE(6,11)CL
   11  FORMAT(1H ,'CRYSTAL LENGTH = ',F8.2,2X,'CM'/)
C
       WRITE(6,12)THETA1*180.0/PI
   12  FORMAT(1H ,'MAXIMUM BRAGG ANGLE = ',F6.2,2X,'DEG'/)
       WRITE(6,13)THETA2*180.0/PI
   13  FORMAT(1H ,'MINIMUM BRAGG ANGLE = ',F6.2,2X,'DEG'/)
C
       WRITE(6,14)DELTHE*180.0/PI
   14  FORMAT(1H ,'BRAGG ANGLE RANGE = ',F6.2,2X,'DEG'/)
C
       WRITE(6,15)E1
   15  FORMAT(1H ,'MINIMUM X-RAY ENERGY = ',F8.4,2X,'KEV'/)
       WRITE(6,16)E2
   16  FORMAT(1H ,'MAXIMUM X-RAY ENERGY = ',F8.4,2X,'KEV'/)
C
       WRITE(6,17)DELEN
   17  FORMAT(1H ,'ENERGY RANGE = ',F8.4,2X,'KEV'/)
C
       WRITE(6,18)YMIN,YMAX
   18  FORMAT(1H ,'SLIT COORDINATES ALONG Y-AXIS = ',F8.4,'CM, ',
     &        F8.4,'CM'/)
C
C ****INITIALIZE ARRAY X****
C
       DO 29 I=1,9
C
       DO 27 K=1,21
C
       DO 25 L=1,21
C
       X(I,K,L)=0.0
C
   25  CONTINUE
C
   27  CONTINUE
C
   29  CONTINUE
C
```

```
C ************************************************************
C *   MAIN DO LOOP OF PROGRAM.  THE FINITE RECTANGULAR SLIT IS *
C *   DIVIDED INTO 9 EVENLY SPACE LINE SLIT SOURCES PARALLEL TO*
C *   THE Z-AXIS.  THE Y-COORDINATES OF THE SLITS ARE CALCUL-  *
C *   ATED AND STORED IN THE ARRAY YS.  THE SUBROUTINE IMDSTRB *
C *   IS CALLED, WHICH CALCULATES THE X-COORDINATES OF THE LINE*
C *   SLIT SOURCES; THESE VALUES ARE STORED IN THE ARRAY X.    *
C ************************************************************
C
      DO 31 I=1,9
C
      YS(I)=YMIN+(YMAX-YMIN)*FLOAT(I-1)/8.0
C
C
      CALL IMDSTRB(THETAB,PSIMAX,RHO,THETABO,I,H,X,YS)
C
   31 CONTINUE
C
C ************************************************************
C *   INITIALIZE XMIN AND XMAX; THEN PROCEED TO SET XMIN TO    *
C *   MINIMUM X-VALUE OF IMAGE POINTS FROM TOP SLIT, AND XMAX TO*
C *   MAXIMUM X-VALUE OF IMAGE POINTS FROM BOTTOM SLIT.  DELX  *
C *   IS THE ACTUAL IMAGE EXTENSION ON THE DETECTOR, RATIO IS  *
C *   THE RATIO OF ACTUAL IMAGE EXTENSION TO ACTUAL SOURCE EX- *
C *   SOURCE EXTENSION.                                        *
C ************************************************************
C
      XMIN=100.0
      XMAX=-100.0
C
      DO 38 K=1,21
      DO 37 L=1,21
C
      XMAX=AMAX1(XMAX,X(1,K,L))
      XMIN=AMIN1(XMIN,X(9,K,L))
C
   37 CONTINUE
   38 CONTINUE
C
      DELX=XMAX-XMIN
      WRITE(6,39)XMIN,XMAX
   39 FORMAT(1H ,'IMAGE RANGE ON DETECTOR IS ',F8.4,2X,' CM TO',
     3        F8.4,2X,'CM'/)
C
      WRITE(6,40)DELX
   40 FORMAT(1H ,'EFFECTIVE SOURCE HEIGTH = ',F8.4,' CM'//)
C
C ************************************************************
C *   CHANGE VALUES OF XMIN AND XMAX FOR PLOTTING PURPOSES,    *
C *   TO BE USED IN THE PLOT OF INTENSITY OF COLLECTED X-RAYS  *
C *   VS. X ON DETECTOR.                                       *
C ************************************************************
C
      XMAX=XMAX+(ABS(XMAX-XMIN))/2.0
      XMIN=XMIN-(ABS(XMAX-XMIN))/2.0
C
C ************************************************************
C *   DIVIDE THE RANGE XMIN TO XMAX INTO 21 EQUAL INCREMENTS,  *
C *   STORING THESE VALUES IN THE ARRAY XB.  FOR EACH IMAGE POINT *
C *   IN THE ARRAY X, DETERMINE FOR WHICH M XB(M)<X<XB(M+1), FOR  *
C *   M BETWEEN 1 AND 20.  FOR THIS M, ADVANCE THE COUNTER N(M)   *
C *   BY ONE.  CONTINUE FOR ALL IMAGE POINTS.                  *
C ************************************************************
C
      DO 41 M=1,21
C
      XB(M)=XMIN+(XMAX-XMIN)*FLOAT(M-1)/20.0
C
   41 CONTINUE
C
      DO 50 M=1,20
```

```
C
      N(M)=0
C
   50 CONTINUE
C
C
C
      DO 90 I=1,9
C
      DO 80 K=1,21
C
      DO 70 L=1,21
C
      DO 60 M=1,20
C
      IF((X(I,K,L).LT.XB(M)).OR.(X(I,K,L).GT.XB(M+1))) GO TO 60
C
      N(M)=N(M)+1
      GO TO 70
C
   60 CONTINUE
C
   70 CONTINUE
C
   80 CONTINUE
C
   90 CONTINUE
C
C ****SECOND OUTPUT PHASE****
C
      WRITE(6,100)
  100 FORMAT(1H ,5X,'XB(I)',9X,'N(I)'/)
C
C
      DO 120 I=1,20
      WRITE(6,110)XB(I),N(I)
  110 FORMAT(1H ,F10.4,2X,I10/)
C
  120 CONTINUE
      WRITE(6,130)XB(21)
  130 FORMAT(1H ,F10.4)
C
C
      DO 140 I=1,100
      NCD(I)=1H-
      NCH(I)=1H
  140 CONTINUE
C
      CALL BAR(N,XB,NCD)
C
      GO TO 1
C
      END

      SUBROUTINE IMDSTRB(THETAB,PSIMAX,RHO,THETABC,I,H,X,YS)
C
C ************************************************************
C *   THIS SUBROUTINE TAKES THE ABOVE INPUT PARAMETERS AND CAL- *
C *   CULATES THE X-COORDINATES OF THE IMAGE POINTS, STORING THE*
C *   VALUES IN THE ARRAY X.                                    *
C ************************************************************
C
      DIMENSION YS(9),X(9,21,21)
C
      DO 50 K=1,21
C
      PSIVAR=PSIMAX*(1.0-2.0*(FLOAT(K-1))/20.0)
C
      DO 40 L=1,21
C
      ZS=2.0*H*FLOAT(L-1)/20.0-H
```

```
C
      T1=SIN(PSIVAR)
      T2=COS(PSIVAR)
      T5=SIN(THETAB)
      T6=COS(THETAB)
      T7=T6/T5
      T8=T1/T2
C
      S1=SIN(THETABC)
      S2=COS(THETABC)
      S3=S2/S1
C
      IF(PSIVAR.EQ.0.0) GO TO 20
C
      T9=T2/T1
      ZB=(ZS*T8-YS(I))/(T8+T9)
      AB=SQRT((YS(I)+T9*ZB)**2+(ZS-ZB)**2)
      BS=SQRT((RHO*T2-ZB*T9)**2+(ZB-RHO*T1)**2)
      GO TO 25
C
   20 AB=ZS
      BS=RHO+YS(I)
C
   25 XS=SQRT(T7**2*BS**2-AB**2)
      DD=YS(I)-(2*BS*T2)
      EE=((RHO*T2+DD)/(-XS))+S3
C
      XD=(S3**2*RHO*2-DD)/EE
C
      X(I,K,L)=(XD-2*RHO*S3)/(-S1)
C
   40 CONTINUE
C
   50 CONTINUE
C
      END
      SUBROUTINE BAR(N,XB,NCD)
C
C ****THIS IS THE PLOTTING SUBROUTINE****
C
      DIMENSION XB(21),N(20),NCD(100),NCH(100)
C
C
      WRITE(6,8)
    8 FORMAT(1H1,45X,'INTENSITY')
C
C
      WRITE(6,10)NCD
   10 FORMAT(1H ,13X,100A1/)
C
      DO 100 J=1,20
C
      DO 20 I=1,100
      NCH(I)=4H
   20 CONTINUE
C
      DO 30 I=1,N(J)/10
      NCH(I)=4H*
   30 CONTINUE
C
      WRITE(6,40)XB(J),NCH,NCH
   40 FORMAT(1H ,F10.4,2X,'!',100A1,'!'/13X,'!',100A1,'!'/)
C
C
  100 CONTINUE
C
C
      WRITE(6,110)NCD
  110 FORMAT(1H ,13X,100A1/)
C
C
      END
```

CRYSTAL RADIUS OF CURVATURE = 25.40 CM

BRAGG ANGLE = 29.40 DEG

COORDINATE OF CRYSTAL CENTER = 40.00 CM

HALF-SECTOR ANGLE OF CRYSTAL = 12.00 DEG

HALF-SLIT LENGTH = 0.50 CM

2*LATTICE SPACING = 6.6870 ANGSTROMS

CRYSTAL LENGTH = 10.16 CM

MAXIMUM BRAGG ANGLE = 36.03 DEG

MINIMUM BRAGG ANGLE = 29.40 DEG

BRAGG ANGLE RANGE = 6.63 DEG

MINIMUM X-RAY ENERGY = 3.1517 KEV

MAXIMUM X-RAY ENERGY = 3.7762 KEV

ENERGY RANGE = 0.6249 KEV

SLIT COORDINATES ALONG Y-AXIS = -0.0150CM, 0.0150CM

IMAGE RANGE ON DETECTOR IS -5.0068 CM TO -4.8833 CM

EFFECTIVE SOURCE HEIGTH = 0.1235 CM

XB(I)	N(I)
-5.0994	0
-5.0855	0
-5.0716	0
-5.0577	0
-5.0438	0
-5.0299	0
-5.0160	126
-5.0021	694
-4.9882	951
-4.9744	612
-4.9605	472
-4.9466	406
-4.9327	352
-4.9188	236
-4.9049	102
-4.8910	18
-4.8771	0
-4.8632	0
-4.8493	0
-4.8354	0
-4.8215	

```
                                   INTENSITY
 ------------------------------------------------------------------------------------------------------------------------
-5.0994  !                                                                                                                !
         !                                                                                                                !
-5.0855  !                                                                                                                !
         !                                                                                                                !
-5.0716  !                                                                                                                !
         !                                                                                                                !
-5.0577  !                                                                                                                !
         !                                                                                                                !
-5.0438  !                                                                                                                !
         !                                                                                                                !
-5.0299  !                                                                                                                !
         !                                                                                                                !
-5.0160  !************                                                                                                    !
         !************                                                                                                    !
-5.0021  !*********************************************************************                                          !
         !*********************************************************************                                          !
-4.9882  !*************************************************************************************************************  !
         !*************************************************************************************************************  !
-4.9744  !*************************************************************                                                  !
         !*************************************************************                                                  !
-4.9605  !************************************************                                                                !
         !************************************************                                                                !
-4.9466  !****************************************                                                                      !
         !****************************************                                                                      !
-4.9327  !************************************                                                                          !
         !************************************                                                                          !
-4.9188  !************************                                                                                      !
         !************************                                                                                      !
-4.9049  !***********                                                                                                     !
         !***********                                                                                                     !
-4.8910  !*                                                                                                               !
         !*                                                                                                               !
-4.8771  !                                                                                                                !
         !                                                                                                                !
-4.8632  !                                                                                                                !
         !                                                                                                                !
-4.8493  !                                                                                                                !
         !                                                                                                                !
-4.8354  !                                                                                                                !
         !                                                                                                                !
 ------------------------------------------------------------------------------------------------------------------------
```

FILE : FISHROT.FTN 11:31 20 MAR 85

```
C
C                          FISHROT.FTN
C
C  ************************************************************
C     PROGRAM TO CALCULATE SPECTROMETER PERFORMANCE
C     BY FINDING THE INTENSITY OF THE IMAGE OF A
C     FINITE EXTENDED SLIT AS A FUNCTION OF POSITION
C     ALONG THE DETECTOR. THE PROGRAM UTILIZES GEOMETRY 3:
C     ROTATION OF THE CRYSTAL ALTERS THE BRAGG ANGLE RANGE.
C  ***************************************************************
C
      DIMENSION YS(9),X(9,21,21),XB(21),N(20),NCH(100),NCD(100)
      DIMENSION YSR(9)
C
      PI=2.0*ASIN(1.0)
C
C ****INTERACTIVELY ENTER INPUT PARAMETERS****
C
    1 WRITE(5,*)'TYPE "END" TO END, OTHERWISE RETURN'
      READ(3,2)IPLOF
    2 FORMAT(A4)
      IF(IPLOF.EQ.'END')CALL EXIT(0)
C
      WRITE(5,*)'ENTER RHO (CRYSTAL RADIUS OF CURVATURE) IN CM.'
      READ(3,*)RHO
C
      WRITE(5,*)'ENTER XC (COORDINATE OF CRYSTAL CENTER) IN CM.'
      READ(3,*)XC
C
      WRITE(5,*)'ENTER PSIMAX (HALF-SECTOR ANGLE OF CRYSTAL) IN DEG.'
      READ(3,*)PSIMAX1
      PSIMAX=PSIMAX1*PI/180.0
C
      WRITE(5,*)'ENTER HALF-SLIT LENGTH H IN CM.'
      READ(3,*)H
C
      WRITE(5,*)'ENTER TWOD (LATTICE SPACING) IN ANGSTROMS'
      READ(3,*)TWOD
C
      WRITE(5,*)'ENTER CL (CRYSTAL LENGTH) IN CM.'
      READ(3,*)CL
C
      WRITE(5,*)'ENTER YMIN(COORDINATE OF BOTTOM OF SLIT)IN CM.'
      READ(3,*)YMIN
C
      WRITE(5,*)'ENTER YMAX(COORDINATE OF TOP OF SLIT)IN CM.'
      READ(3,*)YMAX
C
C ***********************************************************
C *   DESIRED BRAGG ANGLE RANGE DETERMINES THE BRAGG ANGLE    *
C *   TO THE CRYSTAL CENTER, THETABC; THIS AND XC DETER-      *
C *   MINE THE ANGLE OF ROTATION OF THE CRYSTAL ALPHA         *
C ***********************************************************
C
C
C
      WRITE(5,*)'ENTER DESIRED BRAGG ANGLE RANGE IN DEG.'
      READ(3,*)THETAMIN1,THETAMAX1
      THETAMIN=THETAMIN1*PI/180.0
      THETAMAX=THETAMAX1*PI/180.0
C
C ************************************************************
C *   THETABC, ALPHA, DETECTOR POSITION, AND SLIT COORDINATES*
C *   ARE NOW CALCULATED.                                    *
C ************************************************************
C
      YSO=(YMIN+YMAX)/2.0
      THETABC=(THETAMAX+THETAMIN)/2.0
      THETABC1=THETABC*180.0/PI
C
      ALPHA=ATAN((RHO+YSO)/XC)-THETABC
C
      GAMMA=THETABC-ALPHA
C
      DEN=((YSO+RHO-RHO*COS(ALPHA))/(XC+RHO*SIN(ALPHA)))+TAN(GAMMA)
```

```
C
      XD=(YSO+RHO+XC*TAN(GAMMA))/DEN
      YD=TAN(GAMMA)*(XD-XC)-RHO
C
C
C
      WRITE(5,*)'ENTER THETAB (BRAGG ANGLE) IN DEG.'
      READ(3,*)THETAB1
      THETAB=THETAB1*PI/180.0
C
C ****END OF INPUT PHASE; START FIRST OUTPUT PHASE****
C
      WRITE(6,3)RHO
    3 FORMAT(1H ,'CRYSTAL RADIUS OF CURVATURE = ',F6.2,2X,'CM'/)
C
      WRITE(6,4)THETAB1
    4 FORMAT(1H ,'BRAGG ANGLE = ',F6.2,2X,'DEG'/)
C
      WRITE(6,5)XC
    5 FORMAT(1H ,'COORDINATE OF CRYSTAL CENTER = ',F6.2,2X,'CM'/)
C
      WRITE(6,6)PSIMAX1
    6 FORMAT(1H ,'HALF-SECTOR ANGLE OF CRYSTAL = ',F6.2,2X,'DEG'/)
C
      WRITE(6,7)H
    7 FORMAT(1H ,'HALF-SLIT LENGTH = ', F6.2,2X,'CM'/)
C
      WRITE(6,8)TWOD
    8 FORMAT(1H ,'2*LATTICE SPACING = ',F8.4,2X,'ANGSTROMS'/)
C
      WRITE(6,9)CL
    9 FORMAT(1H ,'CRYSTAL LENGTH = ',F8.2,2X,'CM'/)
C
C
      WRITE(6,18)YMIN,YMAX
   18 FORMAT(1H ,'SLIT COORDINATES ALONG Y-AXIS = ',F8.4,'CM, ',
     &        F8.4,'CM'/)
C
      WRITE(6,20)ALPHA*180.0/PI
   20 FORMAT(1H ,'ANGLE OF ROTATION OF CRYSTAL = ',F8.4,' DEG'/)
C
      WRITE(6,22)XD,YD
   22 FORMAT(1H ,'DETECTOR LOCATION = (',F9.4,', ',F8.4,',0.0000)'/)
C
C
C ****INITIALIZE ARRAY X****
C
      DO 29 I=1,9
C
      DO 27 K=1,21
C
      DO 25 L=1,21
C
      X(I,K,L)=0.0
C
   25 CONTINUE
C
   27 CONTINUE
C
   29 CONTINUE
C
C ***********************************************************
C *   MAIN DO LOOP OF PROGRAM. THE FINITE RECTANGULAR SLIT IS *
C *   DIVIDED INTO 9 EVENLY SPACED LINE SLIT SOURCES PARALLEL *
C *   TO THE Z-AXIS.  THE Y-COORDINATES YS ARE CALCULATED AND *
C *   STORED IN AN ARRAY; THE POSITIONS OF THE DETECTOR AND   *
C *   CRYSTAL CENTER ARE THEN FOUND, AS WELL AS THE ACTUAL    *
C *   BRAGG ANGLE RANGE AND ENERGY RANGE, AFTER THE COORDINATE*
C *   TRANSFORMATION IS PERFORMED. SUBROUTINE IMDSTR IS THEN *
C *   CALLED, AND THE X-COORDINATES OF THE IMAGE POINTS ARE   *
C *   CALCULATED FOR THE LINE SLIT SOURCE; THESE VALUES ARE   *
C *   STORED IN THE ARRAY X.                                  *
C ***********************************************************
C
C
```

```
      DO 31 I=1,9
C
      YS(I)=YMIN+(YMAX-YMIN)*FLOAT(I-1)/8.0
C
      XCR=XC*COS(ALPHA)+(RHO+YS(I))*SIN(ALPHA)
C
      YSR(I)=(YS(I)+RHO)*COS(ALPHA)-XC*SIN(ALPHA)-RHO
C
      THETA1=ATAN((RHO+YSR(I))/(XCR-0.5*CL))
      THETA2=ATAN((RHO+YSR(I))/(XCR+0.5*CL))
      DELTHE=THETA1-THETA2
C
      E1=12.396/(TWOD*SIN(THETA1))
      E2=12.396/(TWOD*SIN(THETA2))
      DELEN=E2-E1
C
      XDR=XD*COS(ALPHA)+(YS(I)-YD)*SIN(ALPHA)
      YDR=(XD-XC)*SIN(ALPHA)+(RHO+YD)*COS(ALPHA)-RHO
C
C
C
      CALL IMDSTRB(THETAB,PSIMAX,RHO,THETABC,I,H,X,YS,YSR,XDR,YDR)
C
   31 CONTINUE
C
C ***********************************************************
C *   INITIALIZE XMIN AND XMAX; THEN PROCEED TO SET XMIN     *
C *   TO MINIMUM X-VALUE OF IMAGE POINTS FROM TOP SLIT, AND  *
C *   XMAX TO MAXIMUM X-VALUE OF IMAGE POINTS FROM BOTTOM    *
C *   SLIT.  DELX IS THE ACTUAL IMAGE EXTENSION ON THE DETEC-*
C *   TOR, RATIO IS THE RATIO OF ACTUAL IMAGE EXTENSION TO   *
C *   ACTUAL SOURCE EXTENSION.                               *
C ***********************************************************
C
      XMIN=100.0
      XMAX=-100.0
C
      DO 38 K=1,21
      DO 37 L=1,21
C
      XMAX=AMAX1(XMAX,X(1,K,L))
      XMIN=AMIN1(XMIN,X(9,K,L))
C
   37 CONTINUE
   38 CONTINUE
C
      DELX=XMAX-XMIN
      WRITE(6,39)XMIN,XMAX
   39 FORMAT(1H ,'IMAGE RANGE ON DETECTOR IS ',F8.4,2X,' CM TO',
     &        F8.4,2X,'CM'/)
C
      WRITE(6,40)DELX
   40 FORMAT(1H ,'EFFECTIVE SOURCE HEIGTH = ',F8.4,' CM'//)
C
C ****************************************************************
C *   CHANGE THE VALUES OF XMIN AND XMAX FOR PLOTTING PURPOSES, TO *
C *   BE USED IN THE PLOTS OF INTENSITY OF COLLECTED X-RAYS VS. X  *
C ****************************************************************
C
      XMAX=XMAX+(ABS(XMAX-XMIN))/2.0
      XMIN=XMIN-(ABS(XMAX-XMIN))/2.0
C
C ****************************************************************
C *   DIVIDE THE RANGE XMIN TO XMAX INTO 21 EQUAL INCREMENTS, STORE*
C *   THESE VALUES IN THE ARRAY XB.  FOR EACH IMAGE POINT IN THE   *
C *   ARRAY X FOR A GIVEN SLIT HEIGTH YS, CHECK IF THE IMAGE POINT *
C *   LIES IN THE REGION XB(M) TO XB(M+1), AS M VARIES FROM 1 TO 20*
C *   IF X IS IN THIS REGION,ADVANCE THE COUNTER N(M) BY 1; IF NOT,*
C *   ADVANCE M AND TEST THE IMAGE POINT X AGAIN.                  *
C ****************************************************************
      DO 41 M=1,21
C
      XB(M)=XMIN+(XMAX-XMIN)*FLOAT(M-1)/20.0
C
   41 CONTINUE
```

```
C
      DO 50 M=1,20
C
      N(M)=0
C
   50 CONTINUE
C
C
C
      DO 90 I=1,9
C
      DO 80 K=1,21
C
      DO 70 L=1,21
C
      DO 60 M=1,20
C
      IF((X(I,K,L).LT.XB(M)).OR.(X(I,K,L).GT.XB(M+1))) GO TO 60
C
      N(M)=N(M)+1
      GO TO 70
C
   60 CONTINUE
C
   70 CONTINUE
C
   80 CONTINUE
C
   90 CONTINUE
C
C ****SECOND OUTPUT PHASE****
C
      WRITE(6,100)
  100 FORMAT(1H ,5X,'XB(I)',9X,'N(I)'/)
C
C
      DO 120 I=1,20
      WRITE(6,110)XB(I),N(I)
  110 FORMAT(1H ,F10.4,2X,I10/)
C
  120 CONTINUE
      WRITE(6,130)XB(21)
  130 FORMAT(1H ,F10.4)
C
C
      DO 140 I=1,100
      NCD(I)=1H-
      NCH(I)=1H
  140 CONTINUE
C
C ****CALL PLOTTING SUBROUTINE****
C
      CALL BAR(N,XB,NCD)
C
      GO TO 1
C
      END

      SUBROUTINE IMDSTRE(THETAB,PSIMAX,RHO,THETABC,I,H,X,YS,YSR,XDR,YDR)
C
C ***************************************************************
C * THIS SUBROUTINE TAKES THE ABOVE INPUT PARAMETERS AND CALCULATES*
C * THE X-COORDINATES OF THE IMAGE POINTS, STORING THE VALUES IN   *
C * THE ARRAY X.                                                   *
C ***************************************************************
C
      DIMENSION YS(9),X(9,21,21),YSR(9)
C
      DO 50 K=1,21
C
      PSIVAR=PSIMAX*(1.0-2.0*(FLOAT(K-1))/20.0)
C
      DO 40 L=1,21
C
      ZS=2.0*H*FLOAT(L-1)/20.0-H
C
```

```
      T1=SIN(PSIVAR)
      T2=COS(PSIVAR)
      T5=SIN(THETAB)
      T6=COS(THETAB)
      T7=T6/T5
      T8=T1/T2
C
      S1=SIN(THETABC)
      S2=COS(THETABC)
      S3=S2/S1
C
      IF(PSIVAR.EQ.0.0) GO TO 20
C
      T9=T2/T1
      ZB=(ZS*T8-YSR(I))/(T5+T9)
      AB=SQRT((YSR(I)+T9*ZB)**2+(ZS-ZB)**2)
      BS=SQRT((RHO*T2-ZB*T9)**2+(ZB-RHO*T1)**2)
      GO TO 25
C
   20 AB=ZS
      BS=RHO+YSR(I)
C
   25 XS=SQRT(T7**2*BS**2-AB**2)
      DD=YSR(I)-(2*BS*T2)
      EE=((RHO*T2+DD)/(-XS))+S3
C
      XINT=(XDR*S3+YDR-DD)/EE
C
      X(I,K,L)=(XDR-XINT)/S1
C
   40 CONTINUE
C
   50 CONTINUE
C
      END
      SUBROUTINE BAR(N,XB,NCD)
C
C ****THIS IS THE PLOTTING SUBROUTINE****
C
      DIMENSION XB(21),N(20),NCD(100),NCH(100)
C
C
      WRITE(6,8)
    8 FORMAT(1H1,45X,'INTENSITY')
C
C
      WRITE(6,10)NCD
   10 FORMAT(1H ,13X,100A1/)
C
      DO 100 J=1,20
C
      DO 20 I=1,100
      NCH(I)=4H
   20 CONTINUE
C
      MIN=MIN0(1000,N(J))
C
      DO 30 I=1,MIN/10
      NCH(I)=4H*
   30 CONTINUE
C
      WRITE(6,40)XB(J),NCH,NCH
   40 FORMAT(1H ,F10.4,2X,'!',100A1,'!'/13X,'!',100A1,'!'/)
C
C
  100 CONTINUE
C
C
      WRITE(6,110)NCD
  110 FORMAT(1H ,13X,100A1/)
C
C
      END
```

CRYSTAL RADIUS OF CURVATURE = 25.40 CM

BRAGG ANGLE = 35.00 DEG

COORDINATE OF CRYSTAL CENTER = 40.00 CM

HALF-SECTOR ANGLE OF CRYSTAL = 12.00 DEG

HALF-SLIT LENGTH = 0.50 CM

2*LATTICE SPACING = 6.6870 ANGSTROMS

CRYSTAL LENGTH = 10.16 CM

SLIT COORDINATES ALONG Y-AXIS = -0.0150CM, 0.0150CM

ANGLE OF ROTATION OF CRYSTAL = -2.5845 DEG

DETECTOR LOCATION = (72.9381, -0.0485,0.0000)

IMAGE RANGE ON DETECTOR IS -0.0190 CM TO 0.0354 CM

EFFECTIVE SOURCE HEIGTH = 0.0544 CM

XB(I)	N(I)
-0.0599	0
-0.0537	0
-0.0476	0
-0.0415	0
-0.0354	0
-0.0293	0
-0.0231	16
-0.0170	309
-0.0109	644
-0.0048	776
0.0014	338
0.0075	796
0.0136	368
0.0197	158
0.0259	56
0.0320	9
0.0381	0
0.0442	0
0.0504	0
0.0565	0
0.0626	

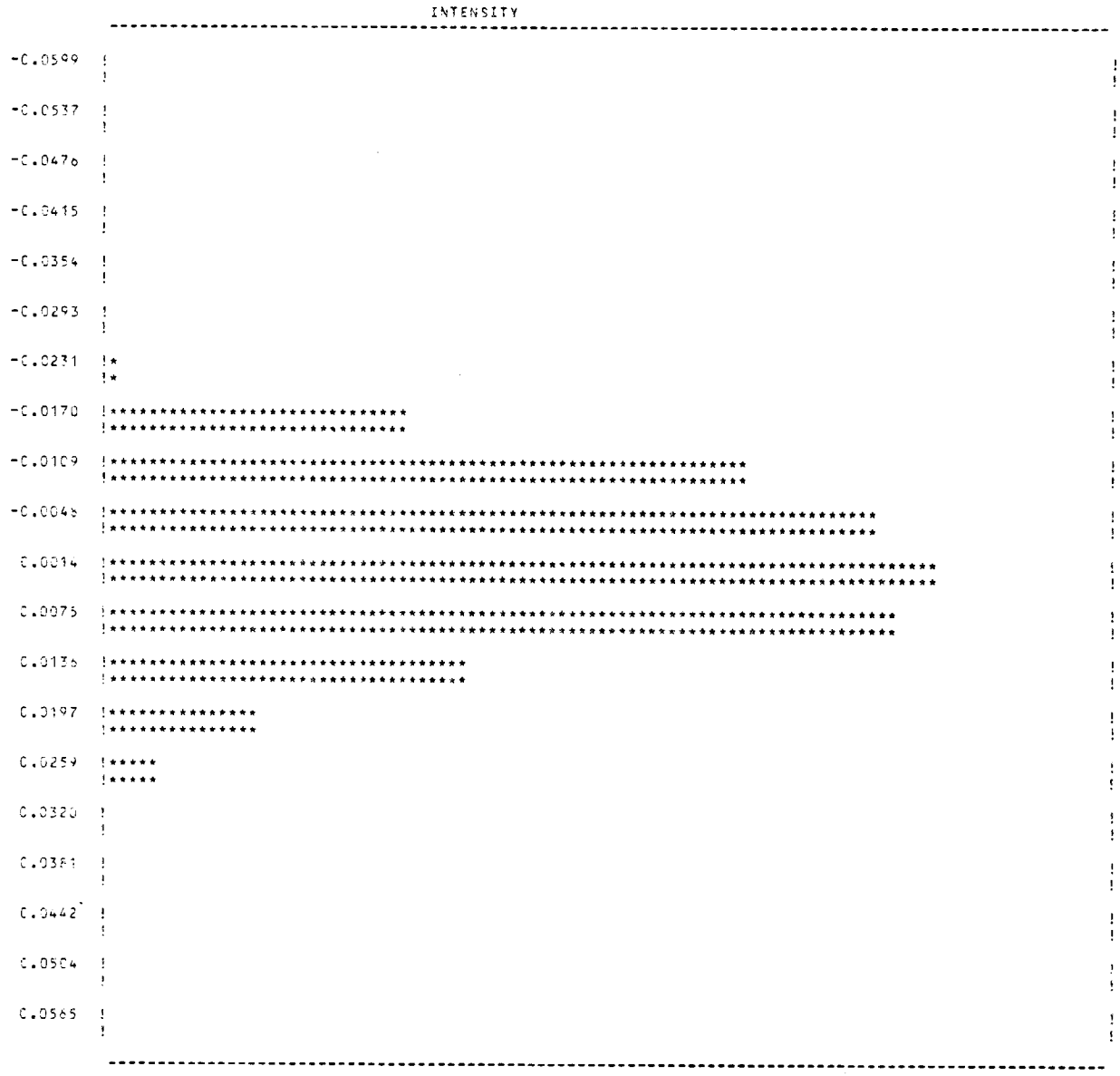
INTENSITY
-0.0599
-0.0537
-0.0476
-0.0415
-0.0354
-0.0293
-0.0231
-0.0170
-0.0109
-0.0048
0.0014
0.0075
0.0136
0.0197
0.0259
0.0320
0.0381
0.0442
0.0504
0.0565

Appendix F. Computer Program for Spectrometer Operation

VHHELP.FOR an interactive program for calculation of optimum operating conditions of von Hamos spectrometer, energy scaling, and expected resolution and collection efficiency. The program is written in FORTRAN on a VAX 11/785 system. A sample output file is also appended where standard source and detector parameters are defined in the program and the following parameters are input:

X-ray region of interest = 2.089 to 2.325 keV.

Projectile energy/amu = 2.6 MeV/u.

Crystal half-height in degrees = 7.8°.

Crystal and 2d(Å) = Quartz($10\bar{1}1$), 2d = 6.687Å.

Specific line energy and channel number = 2.1387 keV @ channel 1180

requested channel number energies = 1180, 1156, and 2820.

Energy scaling using two known energies = 2.1369 keV @ channel 1156 and 2.1387 keV @ channel 1180.

Requested channel number energies = 828, 874, 910, 978, 1099, 1156, and 1180.

Est. efficiency at lab energies 2.1368 and 2.1164 keV.

Expected count rates for 50 nA, Si^{11+} on 5 $\mu g/cm^2$ of target with x-ray production cross-section of 1×10^{-20} cm^2.

The results are pertinent to data of figs. 29 and 30.

```
c               VHHELP- VON HAMOS SPECTROMETER HELP PGM.
C       PROGRAM FOR CALCULATION OF OPERATING PARAMETERS OF VON
C       HAMOS SPECTROMETER.
C
c       Negative energy input means rest-frame energy, i.e. source
c       moving with beam velocity wrt detection system.
        DIMENSION El(3),Er(3),theta(3),Fn(2),twod(5),axtl(10),E(2),Ecal(2),
        1Resolp(5),Refl(5)
        DOUBLE PRECISION YN, axtl
C
c       Standard operating parameter list
c       crystal parameters
        Itag=0
        twod(1)=10.648
        twod(2)=6.687
        twod(3)=4.027
        twod(4)=2.715
        twod(5)=9999.
c       resolving powers and integrated reflectivities
        Resolp(1)=8200.
        Resolp(2)=7700.
        Resolp(3)=27000.
        Resolp(4)=99999999.
        Resolp(5)=99999999.
c
        Refl(1)=9.0E-5
        Refl(2)=1.23E-4
        Refl(3)=1.5E-4
        Refl(4)=0.0
        Refl(5)=0.0
c
c       crystal names
        axtl(1)='ADP'
        axtl(2)='(101)'
        axtl(3)='QTZ'
        axtl(4)='(1011)'
        axtl(5)='LiF'
        axtl(6)='(200)'
        axtl(7)='Si'
        axtl(8)='(100)'
        axtl(9)='NONE'
        axtl(10)='(----)'
c       special notes for the various available crystals.
c
c
c       geomteric and mechanical parameters
        wresS=0.010
        lx=4.0
        hx=4.0
        rhox=10.0
        xoffset=-76.24
c       detector parameters
        fld=4.26
        dxoffst=-125.6
        droffst=100.0
        drfac=19.1
c       det dispersion in inches per channel. measured for det "B" 5/1/86.
        ddisp=0.0014672
c       det "A" had a disp. of 0.001386 in/chnl, measured 3/16/85.
c       det "B" measured electronic (pulser) resol. of 4.5 chnls*ddisp.
```

```
      wresD=0.0066
c     det"B"signal midpt=low chnl+hi chnl/2, chnls are where cts start&stop
      idxo=1874
      idstrt=400
      idstp=3300
      type 300
300   format(' OUTPUT WRITTEN ON FILE -- FOR091.DAT;#, in this SUBDIR.')
c
10    continue
c
c     INPUT OF X-RAY REGION OF INTEREST AND PROJECTILE ENERGY.
      TYPE 100
100   FORMAT(' Enter rest-frame x-ray energies and projectile energy/u.')
      accept 101, Erl,Erh,Epro
101   format(3f)
      Erl=abs(Erl)
      Erh=abs(Erh)
c     branch to "specific dial settings calcs" if Erl=0.0
c     If Epro N.E. 0.0, enter psimax, height of crystal in degrees.
      fpsimax=0.0
      if(Epro.EQ.0.0) go to 1013
      type 1011
1011  format(' enter crystal acceptance half-height (degrees)')
      accept 1012, fpsimax
1012  format(1F)
      dpsimax=fpsimax
      rpsimax=fpsimax/57.296
      if(fpsimax.LE.0.0) rpsimax=0.1972
      if(fpsimax.LE.0.0) dpsimax=11.3
c     doppler factor calc--shift in line enrgy due to crystal opening angle
      Dopfac=(1.0+cos(rpsimax))/2.0
1013  continue
c
c     1st calc.  gamma, and beta
      gamma=1.0+abs(Epro/931.50)
      beta=(sqrt(gamma**2.0-1.0))/gamma
      if(Erl.LE.0.0) go to 105
      if(Epro.EQ.0.0) go to 102
      beta=beta*(Epro/(abs(Epro)))
102   continue
      Er(2)=(Erl+Erh)/2.0
      if(Itag.GT.0) go to 200
105   continue
      type 110
110   format(' Enter crystal 2d(angs), hit "return" if unknown.')
      accept 111, twodx,norder
111   format(1F,1I)
      fordbest=float(norder)
      if(norder.LE.0) fordbest=1.0
      ctwod=twodx
      if(twodx.LE.0.0) go to 120
      ibest=99
      do 112 I=1,5
      if(ctwod.EQ.twod(I)) ibest=I
112   continue
      if(ibest.NE.99) go to 113
      type 114
114   format(' crystal not found in stock list.')
      go to 105
113   continue
```

```
        ixt1=2*ibest-1
        ixt2=ixt1+1
        type 115, axtl(ixt1),axtl(ixt2),ctwod
115     format(' crystal chosen is '2A6' with 2d(A)= '1F7.4)
        ccb=fordbest*12.3981/ctwod
        ibest=1
        if(twodx .GT. 0.0) go to 200
120     continue
c       auto selection of "best" crystal based on angle to reach Er(2).
        lstheta=0.4999
c       branch for "specific dial settings calcs." where twodx must be set;
c       if xray energies given in projectile frame, for example.
        if(Erl.LE.0.0) go to 105
        fordbest=1.0
        do 150 n=1,2
        forder=float(n)
        do 150 I=1,5
        cb=forder*12.3981/twod(I)
        El(2)=(Er(2)/gamma)+beta*cb*Dopfac
        stheta=cb/El(2)
        if(stheta.GT.0.940) go to 150
        if(stheta.LT.0.4999) go to 150
        if(stheta.GT.lstheta) ibest=I
        if(stheta.GT.lstheta) fordbest=forder
c       if the diff. order (norder) was input explicitly, set it here.
        if(norder.GT. 0) fordbest=float(norder)
        lstheta=stheta
150     continue
        ccb=fordbest*12.3981/twod(ibest)
        ixt1=2*ibest-1
        ixt2=ixt1+1
        type 155, axtl(ixt1),axtl(ixt2),twod(ibest)
155     format(' The best crystal for this energy region is '2A6' ,2d='F6.3)
        if(fordbest.GT.1.0) type 156,fordbest
156     format(' Note that this requires order='1f2.0' diffraction.')
        ctwod=twod(ibest)
200     continue
c       SPECIFIC DIAL SETTINGS CALCS. ROUTINE
        if(Erl.GT.0.0) go to 555
        type 500
500     format(' Enter specific xtal and detector dial settings:'/
        1' xtal dial, detector linear dial, and detector rotational dial.')
        accept 501, cxctr, cdxctr, cdrctr
501     format(3F)
c       calc of xo and dxo using these settings.
        xcntr=cxctr
        dxcntr=cdxctr
        drcntr=cdrctr
        xo=(xcntr-xoffst)/40.
        dxo=(dxcntr-dxoffst)/40.
        theta(2)=atan(rhox*2.0/dxo)
        El(2)=ccb/(sin(theta(2)))
        Er(2)=gamma*(El(2)-(ccb*Dopfac*beta))
c       ck. drcntr to make certain detector is reasonably perpendicular to
c       central ray.
        pdrctr=droffst-drfac*theta(2)
        type 1111, pdrctr
1111    format(' best det. rot. dial setting is '1f5.2)
        cdrthe=(droffst-drcntr)/drfac
        mxrctr=pdrctr+0.75
```

```
      mnrctr=pdrctr-0.75
      if(drcntr.GT.mxrctr) type 520, pdrctr,drcntr
      if(drcntr.LT.mnrctr) type 520, pdrctr, drcntr
520   format(' Chosen rotational setting will not yield high resolution.'/
      1' At this det. linear position, the rotation dial should be set
      1to '1F8.3,/' Calcs. will proceed using dial setting '1F8.3)
c     make 1st order correction for off-normal det. rotation
      deldr=(drcntr-pdrctr)/drfac
      ddisp=ddisp/(cos(deldr))
      go to 560
555   continue
c     calc of Bragg angle for mid ray.
      El(2)=(Er(2)/gamma) + beta*ccb*Dopfac
      theta(2)=asin(ccb/El(2))
c     calc of xo" to place El(2) at xtal center.
      xo=rhox/(tan(theta(2)))
      dxo=2.0*xo
      xcntr=40.0*xo+xoffst
      dxcntr=40.0*dxo+dxoffst
      drcntr=droffst-drfac*(theta(2))
560   continue
c     calc energies intercepted by the detector, assuming normal to mid ray.
      fL=sqrt(rhox**2. + (dxo/2.)**2.)
      delthe=atan(fld/(4.*fL))
      themin=(theta(2) - delthe)
      themax=(theta(2) + delthe)
      El(1)=ccb/(sin(themax))
      El(3)=ccb/(sin(themin))
      Er(1)=gamma*(El(1)-beta*ccb*Dopfac)
      Er(3)=gamma*(El(3)-beta*ccb*Dopfac)
c     Resolution estimate assuming 10mil wide source slit and 6mil det res.
c     Doppler width, due to psimax crystal opening height, also included
      Dopwdth= 1000.*(1.0 - cos(rpsimax))*beta*ccb
      if(Epro.GT.0.0) type 3091,Dopwdth
      if(Epro.GT.0.0) write(91,3091) Dopwdth
3091  format(' Doppler line width estd = '1f7.2' eV')
c
      weff=sqrt(wresS**2.0+wresD**2.0)
      resol=500.*weff*El(2)*(cos(theta(2)))/rhox
      resol=sqrt(Dopwdth**2. + resol**2.)
c     output written to for091.dat
      write(91,310)
310   format(//,' OUTPUT FROM VHHELP.CRV',//)
      if(Erl.GT.0.0) write(91,311) Erl,Erh
311   format(' x-ray rest-frame region of interest is '1F7.4
      1' to '1F7.4' keV')
      if(Epro.EQ.0.0) go to 313
      write(91,312) Epro,gamma,beta,dpsimax
312   format(' Emitting projectile energy is '1F4.1' MeV/u, gamma=
      1'1F6.4' , beta= '1f7.5,/'   crystal psimax= '1f5.2' degrees.')
313   continue
      write(91,315) axtl(ixt1),axtl(ixt2),ctwod,fordbest
315   format(/' Crystal of choice is '2A6' ,2d(A)='1f7.4' ,order='1f2.0)
      write(91,316) El(1),El(3)
316   format(' Lab frame energy range of det. = '1F7.4' to'1F7.4' keV')
      if(Epro.EQ.0.0) write(91,317) Er(1),Er(3)
317   format(' This corresponds to '1F7.4' to' 1F7.4' keV at rest.')
c     output positioning information for xtal and detector.
      if(Erl.GT.0.0) write(91,323)
      if(Erl.LE.0.0) write(91,324)
```

```
323     format(//,' Calculated optimum operating conditions: ')
324     format(//,' You chose operating conditions: ')
        type 325,xcntr
        type 326,dxcntr
        type 327,drcntr
        type 328, El(2), resol
        write(91,325) xcntr
        write(91,326) dxcntr
        write(91,327) drcntr
        write(91,328) El(2),resol
325     format(' crystal dial setting = '1F8.2)
326     format(' detector linear dial setting = '1F8.2)
327     format(' detector rotation dial setting = '1F8.3)
328     format(/' Expected energy resolution at '1F7.4' keV is '1F5.2' eV.')
        write (91,8888)
8888    format(/' ******************************************************
        1********************'/)
c
c       tabulation of chnl #,lab energy,dispersion,rest energy, & wavelength
c       using standard values for idxo, idstrt, etc.
        istep=200
        write(91,442)
442     format(//,' Approx. calcs. done using default channel values. ')
        write(91,440)
440     format(' CHNL#  LAB ENERGY(keV) DISP(eV/chnl)  REST ENERGY(keV)
        1WAVELENGTH(angstroms)',/)
488     continue
        do 450 k=idstrt,idstp,istep
        z=(float(k-idxo))*ddisp
        dtheta=-atan(z/(2.*fL))
        ttheta=theta(2)+dtheta
        tEl=ccb/(sin(ttheta))
        tEr=gamma*(tEl-beta*ccb*Dopfac)
c       calc energy/chnl = dispersion using measured det. disp.-ddisp
        disfac=(ddisp*tEl**2.)/(ccb*2.0*fL)
        cosfac=(cos(ttheta))*((cos(dtheta))**2.)
        tdelEl=1000.*cosfac*disfac
        tlmbda=12.3981/tEr
        if(istep.EQ.1) type 440
        if(istep.EQ.1) type 441, k,tEl,tdelEl,tEr,tlmbda
        write(91,441) k,tEl,TdelEl,tEr,tlmbda
441     format(1I5,5x,1F9.4,5x,1F9.4,10x,1F9.4,5x,1F9.4)
450     continue
c       getting est. energy at specific chnl #.
        type 455
455     format(//,' Enter chnl # for est. of energy there, return to stop.')
        accept 456, iun, Exkun
456     format(1I,1F)
        if(iun.EQ.0)go to 489
c       correction approximation using a known energy line at chnl iun.
c       if Exkun LT 0.0 it means that it was given in the proj. rest frame.
        if(Exkun.EQ.0.0) go to 460
        if(Exkun.LT.0.0) Exkun=((abs(Exkun))/gamma)+beta*ccb*Dopfac
        thekun=asin(ccb/Exkun)
        dthekun=theta(2)-thekun
        zkun=2.0*fL*(tan(dthekun))
        kidxo=iun-(int(zkun/ddisp))
        idxo=kidxo
        if(Exkun.GT.0.0) type 459, Exkun,iun,idxo
        if(Exkun.GT.0.0) write(91,459) Exkun,iun,idxo
```

```
459     format(/,' *** Input of '1F7.4' keV at chnl' I5' forces idxo= 'I5,/
        1' Further calcs. are done using this value.')
460     continue
c       loop for specific chnl conversions to energy
        idstrt=iun
        idstp=iun
        istep=1
        go to 488
489     continue
c       getting energies from scaling using two known lines as input.
        type 470
470     format(' Do you want energy scaling using known lines?(Y/N)')
        accept 471, YN
471     format(A4)
        if(YN.EQ.'y') go to 808
        if(YN.EQ.'Y') go to 808
600     continue
c       System efficiency estimates.  SYSEFF related to Kallne luminosity
c       but not exactly the same. SYSEFF=I/I0 ie. detected/emitted rate.
c       Assume P10 gas @ 1 atmos. and 1/2 mil mylar window.
c       SYSEFF=I/I0=Effdet*Reflavg(Ex)*dOmega(Ex)/4*pi.
c       Detection efficiency approximation, assumes 1/2 mil mylar window,
c       1 atmos of P10 gas, nearly constant det eff over limited energy
c       regions. See pg. 87, von Hamos logbook I.
c       For 2nd and 3rd order diffraction, it is assumed that the efficiency
c       decreases like (order)**-1.5 .
        Reflavg=0.0
        type 8888
        write(91,8888)
665     continue
        Exeff=0.0
        type 666
666     format(' Enter x-ray energy to get sys. efficiency estimate.')
        accept 667, Exeff
667     format(1F)
        if(Exeff.EQ.0.0) go to 689
        Exlast=Exeff
        if(Exeff.LT.0.0) Exeff=(abs(Exeff))/gamma + beta*ccb*Dopfac
        theeff=asin(ccb/Exeff)
c       these ests. are only good for P10
        if(Exeff.GT.1.5) Effdet=0.25
        if(Exeff.GT.7.0) Effdet=0.15
        if(Exeff.LT.1.5) Effdet=0.10
c       crystal reflectivity avg'd over a resolution width.
        if(Refl(ibest).EQ.0.0) type 670
        if(Resolp(ibest).EQ.99999.) type 670
670     format(' crystal parameters unknown.')
        Reflavg= (Refl(ibest)*Resolp(ibest))/(2.0*tan(theeff))
        if(Reflavg.LE.0.0) go to 689
c       solid angle intercepted by crystal in one resolution width.
        fL=rhox/(sin(theeff))
        dthec= (tan(theeff))/(Resolp(ibest))
        dthesys= sqrt(dthec**2.0 +(wresS**2.0 + wresD**2.0)/(4.*fL**2.0))
        dOmega= dthesys*hx*(sin(theeff))/rhox
c
        SYSEFF=Effdet*Reflavg*dOmega/((fordbest**1.5)*12.56)
        type 675, Exeff, SYSEFF
675     format(/,' estd system effic./resol width at 'F7.4' keV = '1E9.3)
        write(91,675) Exeff, SYSEFF
        go to 665
```

```
689     continue
        if(Reflavg.LE.0.0) go to 789
c       count rate estimates for ions on solids
c
        type 750,Exlast
750     format(/' For ct. rate estimate at 'F7.4' keV, enter: Qbeam,'/
        1' Ibeam(nA),sigma(cm2),targ. thickness(ugm/cm2),& targ. mass(u).')
        accept 751, IQb,fIb,sigma,fNt,A2
751     format(1I,1F,1E,2F)
        if(IQb.LE.0) go to 789
c       count rate est. using SYSEFF.
        crconst=0.376E28
        CRX=crconst*sigma*fIb*fNt*SYSEFF/(A2*float(IQb))
        type 755, CRX
        write(91,754)fIb,Epro,IQb,fNt,A2,Exlast
754     format(/' For 'F7.2' nA of'F4.1' MeV/u,Q='I2' + on 'F7.2' ug/cm2'/
        1' of target A = '1F6.2' amu, at 'F7.4' keV the ')
        write(91,755) CRX
755     format(' expected ct. rate intg. over resol. width = 'E9.2' /sec'/)
        go to 689
789     continue
c
c       output note that crystal doesn't span the region of interest.
        if(Erl.LE.0.0) go to 699
        if(Er(1).GT.Erl) type 400
        if(Er(3).LT.Erh) type 400
        if(Er(1).GT.Erl) write(91,400)
        if(Er(3).LT.Erh) write(91,400)
        write(91,8888)
400     FORMAT(' NOTE: CHOSEN CRYSTAL DOES NOT SPAN REGION SPECIFIED.',//)
699     continue
C
        TYPE 700
700     FORMAT(' DO YOU WANT ANOTHER ENERGY REGION, SAME CRYSTAL?(Y/N)')
        ACCEPT 701, YN
701     FORMAT(A4)
        Itag=1
        IF(YN.EQ.'y') go to 10
        IF(YN.EQ.'Y') GO TO 10
        GO TO 888
808     CONTINUE
        write(91,8888)
        write(91,857)
857     format(///,2x,' SPECIFIC CHANNEL CONVERSIONS USING
        1ENERGY SCALING BASED ON TWO KNOWN LINES :',/)
C       ENERGY SCALING ROUTINE
C       E(N)=E0+A(N-N0)+B(N-N0)**2
        DO 830 I=1,2
        TYPE 828, I
828     FORMAT(' ENTER KNOWN ENERGY(KEV) AND CHNL# FOR PEAK '1I2)
        read(5,*)Ecal(I), FN(I)
c       if Ecal(I) LT. 0.0, it means energy was given in the proj. rest frame
c       convert to lab frame.
        if(Ecal(I).LT.0.0) Ecal(I)=((abs(Ecal(I)))/gamma)+beta*ccb*Dopfac
830     CONTINUE
        if(Ecal(1).LT.0.0) type 829
        if(Ecal(1).LT.0.0) write(91,829)
829     format(' neg #s means energies given in the projectile frame.')
c       write calibration line data to for091
        write(91,858) Ecal(1),FN(1),Ecal(2),FN(2)
```

```
858     format(5x,1F7.4' keV at chl '1F6.1' & '1F7.4' keV at chl '1F6.1,//)
        write(91,440)
C       CALCS OF E0, A, B, AND N0P
        C2=ccb**2.0
        EO=(Ecal(1)+Ecal(2))/2.0
        A=(Ecal(2)-Ecal(1))/(FN(2)-FN(1))
        BN=(A**2.0)*((2.0*(EO**2.))-C2)
        BD=2.0*EO*((EO**2.0)-C2)
        B=BN/BD
        FNB=(FN(1)+FN(2))/2.0
        FN0P=FNB+(B/(4.*A))*((FN(2)-FN(1))**2.0)
C       CORRECTION FOR A
        ECAL1=EO+A*(FN(1)-FN0P)+B*((FN(1)-FN0P)**2.)
        ECAL2=EO+A*(FN(2)-FN0P)+B*((FN(2)-FN0P)**2.)
        DELER=(ECAL1-Ecal(1)+Ecal(2)-ECAL2)/2.
        DELA=2.*DELER/(FN(2)-FN(1))
        A=A+DELA
C       calculation of coeffs. aaa, bbb, and ccc for quadratic scaling.
        aaa=EO-A*FN0P+B*(FN0P**2.0)
        bbb=A-2.*B*FN0P
        ccc=B
C       change to eV units.
        aaa=1000.*aaa
        bbb=1000.*bbb
        ccc=1000.*ccc
c
        type 835, aaa,bbb,ccc
        write(91,835) aaa,bbb,ccc
c       n is chnl number, aaa,bbb,ccc are in terms of eV.
835     format(' Energy scaling-  E(n)(in eV)=a+bn+cn**2:a,b,c='/,3F,/)
C
C       E(N) AND DISPE(N) CALCS
840     CONTINUE
        TYPE 848
848     FORMAT(//' ENTER CHNL# TO GET ENERGIES AND DISPERSION.')
        accept 849, iun
849     format(1I)
        un=float(iun)
        IF(UN .LE. 0.0) GO TO 860
        ElCALC=EO+A*(UN-FN0P)+B*((UN-FN0P)**2.0)
        Ercalc=gamma*(Elcalc-beta*ccb*Dopfac)
        flmbda=12.3981/Ercalc
        dElcal=A+2.0*B*(UN-FN0P)
        dElcal=1000.*dElcal
        type 440
        type 441, iun,Elcalc,delcal,Ercalc,flmbda
        write(91,441) iun,Elcalc,delcal,Ercalc,flmbda
        GO TO 840
860     type 861
861     format(' Do you want to try another set of calibration lines?(Y/N)')
        accept 471, YN
        if(YN.EQ.'y') go to 808
        if(YN.EQ.'Y') go to 808
        go to 600
888     CONTINUE
        STOP
        END
```

INTERNAL DISTRIBUTION

1 R. L. Auble
2 J. B. Ball
3 R. L. Becker
4 J. M. Dale
5 S. Datz
6 P. Dittner
7 L. D. Hulett, Jr.
8 G. E. Ice
9 S. Kahane
10 H. J. Kim
11 H. F. Krause
12 M. O. Krause
13 M. T. Milner
14 C. W. Nestor
15 G. D. O'Kelley
16 H. Postma
17 S. Raman
18 T. Rosseel
19 C. J. Sparks, Jr.
20 P. H. Stelson
21 J. K. Swenson
22 C. R. Vane
23 T. A. Walkiewicz
24 A. Zucker
25-73 Physics Division Library
74-75 Central Research Library
76 Document Reference Section
77-78 Laboratory Records Dept.
79 Laboratory Records-RC
80 ORNL Patent Office

EXTERNAL DISTRIBUTION

81 T. Åberg, Helsinki University of Technology, SF-02150 Espoo, FINLAND

82 P. Armbruster, GSI, P.O. Box 110541, D-6100 Darmstadt, W. GERMANY

83 Y. Awaya, Inst. of Physical and Chemical Research, Wako-Shi, Saitama, 351 JAPAN

84 K. M. Barfoot, Department of Electronic and Electrical Engineering, University of Surrey, Guildford, Surrey, GU25XH, ENGLAND

85 D. Berenyi, Institute for Nuclear Research, ATOMKI, Debrecen, HUNGARY

86 C. P. Bhalla, Department of Physics, University of Kansas, Manhattan, KS 66506

87 P. K. Bhattacharya, Van de Graaff Laboratory, Bhabha Atomic Research Centre, Trombay, Bombay, 400-085 INDIA

88 J. P. Briand, Institut Curie and University Pierre et Marie Curie, 11, rue Pierre et Marie Curie, 75231 Paris Cedex 05, FRANCE

89 T. A. Callcott, Department of Physics, University of Tennessee, Knoxville, TN 37996

90 J. L. Campbell, Dean, College of Physical Science, Guelph, Ontario, CANADA, NIG2W1

91 Chau Chinwei, Institute of Physics, National Tsing Hua University, Kuang Fu Rd., Hsinchu, Taiwan, REPUBLIC OF CHINA

92 C. L. Cocke, Department of Physics, Kansas State University, Manhattan, KS 66506

93 G. Deconninck, Laboratoire d'Analyses, par Reachons Nucleaires, 22 Rue Muzet, B-5000 Namur, BELGIUM

94 J. L. Debrun, CNRS/Cyclotron Laboratory, 34 rue de la Fegullerie, U5 045 Orleans, FRANCE

95 J. A. Demarest, Advanced Tech. Division, Air Force Weapons Laboratory, Kirkland AFB, NM 87117

96 R. D. Deslattes, Physics Bldg., Room A141, National Bureau of Standards, Washington, DC 20234

97 D. D. Dietrich, Physics E-Division, Lawrence Livermore National Laboratory, P.O. Box 808, L-401, Livermore, CA 94550

98 J. L. Duggan, Department of Physics, North Texas State University, Denton, TX 76203

99 E. Förster, Department of Physics, Freidrich-Schiller-Universität Jena, Max-Wien-Platz 1, DDR-6900, JENA, GERMAN DEMOCRATIC REPUBLIC

100 R. J. Fortner, Physics E-Division, Lawrence Livermore National Laboratory, P.O. Box 808, L-401, Livermore, CA 94550

101 F. L. Freire, Jr., Pontifica Universidade Catolica, Institute of Physics, R. Marques de S. Vicente, 209-Gavea-7C-20, Rio de Janeiro, BRAZIL

102 R. Garten, Institute für Spectrochemie and Angewandte Spektroskopie, D-46 Dortmund, Postfach-778, W. GERMANY

103 R. Gowda, Department of Physics, Baylor University, Waco, TX 76798

104 K-O. Groeneveld, Institute für Kernphysik, J-W-Goethe University, A-Euler Str. 6, D-7000 Frankfurt am, Main 900, W. GERMANY

105 D. L. Hendrie, U.S. Department of Energy, Division of High Energy and Nuclear Physics, Washington DC 20545

106 L. M. Howe, Chalk River Nuclear Laboratories, Chalk River, Ontario, CANADA KOJ 1JO

107 S. Ito, Radioisotope Research Center, Kyoto University, Kyoto 606, JAPAN

108 Elizabeth Källne, JET Undertaking, Abingdon, Oxford, OX143EA, ENGLAND

109 Jan Källne, JET Undertaking, Abingdon, Oxford, OX143EA, ENGLAND

110 T. Kitahara, Yamanashi, Medical University, Department of Physics, Tamaho, Nakakoma-gun, Yamanashi, 409-38, JAPAN

111 A. Kucrymov, University of Maria Curie, Sklodowska, Institute of Chemistry, Lubin, POLAND

112 G. Lapicki, Department of Physics, East Carolina State University, Greenville, NC 27834

113 R. Mann, Gesellschaft für Schwerionenforschung mbH (GSI), D-6100 Darmstadt 11, P.O. Box 110541, W. GERMANY

114 D. Maor, Israel Institute of Technology, Department of Physics, Technion City, 32000 Haifa, ISRAEL

115 J. V. Martinez, U. S. Department of Energy, DOE-ER-141, GTN, Washington, DC 20545

116 Y. Matsuda, Radiation Center of Osaka Prefecture Shinke-cho, Sakai, Osaka 583, JAPAN

117 F. D. McDaniel, Department of Physics, North Texas State University, Denton, TX 76203

118 G. K. Mehta, Nuclear Science Centre, Jawaharlal Nehru University, P.O. Box 10502, New Delhi 110067, INDIA

119 E. Merzbacher, Department of Physics and Astronomy, University of North Carolina, Chapel Hill, NC 27514

120 J. R. Mowat, Department of Physics, North Carolina State University, Raleigh, NC 27607

121 L. G. Multhauf, L- Division, Lawrence Livermore National Laboratory, P.O. Box 808, Livermore, CA 94550

122 D. J. Nagel, Naval Research Lab., 4555 Overlook Ave., S.W., Washington, DC 20375

123 S. O. Olabanji, CERD, University of IFE, ILE-IFE, NIGERIA

124 M. Payek, Laboratory of Neutron Physics, Joint Institute for Nuclear Research, Head Post Office Box 79, Moscow, USSR

125 J. R. Pope, Dow Chemical USA, P. O. Box 9002, Walnut Creek, CA 945980

126 M. A. Popescu, Institute of Physics and Technology of Materials, P.O. Box 5207, Magurele, Bucharest, ROMANIA

127 R. Prakash, Department of Physics, University of Manitoba, Winnipeg, Manitoba, R3T 2N2, CANADA

128 J. L. Price, Jr., Department of Physics, North Texas State University, Denton, TX 76203

129 B. Raith, Institute of Exper.-Physik, Ruhr-Universitaet Bochum, Postfach 102148, D4630 Bochum 1, WEST GERMANY

130 P. V. Rao, Department of Physics, Emory University, Atlanta, GA 30322

131 K. Rashid, Nuclear Physics Division, Pakistan Inst. of Nuclear Science, P.O. Nilore, Islamabad, PAKISTAN

132 M. Th. Rekveldt, Interuniversitair Reactor Instituut, 2629 JB Delft, THE NETHERLANDS

133 P. Richard, Department of Physics, University of Kansas, Manhattan, KS 66506

134 E. Rieger, Hungarian Academy of Sciences Research Laboratory of Inorganic Chemistry, P.O. Box 132, Budapest 112, HUNGARY 1502

135 P. Rymuza, Institute for Nuclear Physics, 05-400 Otwock-Świerk, POLAND

136 H. Schmidt-Böcking, Department of Physics, Kansas State University, Manhattan, KS 66506

137 R. Schuch, Research Institute of Physics, Frescativ 50, 10405 Stockholm 50, SWEDEN

138 S. M. Shafroth, Department of Physics and Astronomy, University of North Carolina, Chapel Hill, NC 27514

139 J. D. Silver, University of Oxford, Clarendon Laboratory, Parks Rd., Oxford, OX1 3PU, ENGLAND

140 M. S. Smith, A. W. Wright Nuclear Structure Laboratory, Yale University, P.O. Box 6666, New Haven, CT 06511

141 N. Stolterfoht, Hahn-Meitner-Institut, Berlin, Glienickerstr. 100, D-1000 Berlin 39, WEST GERMANY

142 J. A. Tanis, Department of Physics, Western Michigan University, Kalamazoo, MI 49008

143 I. Török, Institute of Nuclear Research of the Hungarian Academy of Sciences, Atommag, Kutato Intezete, Debrecen, Pf51, H-4001, HUNGARY

144 M. Uda, Institute of Physical and Chemical Research, Wako-Shi, Saitama, 351 JAPAN

145 P. Van Assche, SCK/CEN, B-2400 MOL, BELGIUM

146 S. L. Varghese, Department of Physics, East Carolina State University, Greenville, NC 27834

147 H. R. Verma, Department of Physics, Punjabi University, Patiala, 147002, INDIA

148 R. D. Vis, Department of Physics, Free University, de Boeletaan 1081, Amsterdam, THE NETHERLANDS

149 R. L. Watson, Department of Chemistry, Texas A&M University, College Station, TX 77843

150 A. Witzmann, Friedrich-Schiller-University, Jena, Physics Department, DDR-6900 Jena, Max-Wien-Platz 1, WEST GERMANY

151 B. Yaakobi, Laboratory for Laser Energetics, University of Rochester, 250 East River Road, Rochester, NY 14623

152. Office of Assistant Manager for Energy Research and Development, DOE-ORO, P.O. Box E, Oak Ridge, TN 37831

153-162. Office of Scientific and Technical Information, Oak Ridge, TN 37831

☆U.S. GOVERNMENT PRINTING OFFICE: 1 9 8 8-5 4 8-2 1 8/5 0 1 6 3